Protection Strategies for Catalytic Conversion of Biomass-derived Furanics to Monomers for Polyamides

(保護基活用戦略に基づくバイオマス由来フラン化合物からポリアミド原料への触媒変換)

Tat Boonyakarn

Hokkaido University

北海道大学

2022

Table of Contents

Chapter 1

General Introduction

1.1 Background

Recently, the fuel cost has been rising enormously owing to the increasing world population and energy demand for industry and transportation. As a result, the development of new technologies to utilize nonpetroleum feedstocks for sustainable production of renewable chemicals has gained much attention worldwide. Lignocellulosic biomass mainly consists of cellulose, hemicellulose, and lignin (Figure 1.1), and is generally the most abundant organic compound derived from agricultural residues and industrial food wastes no longer fit for consumption.

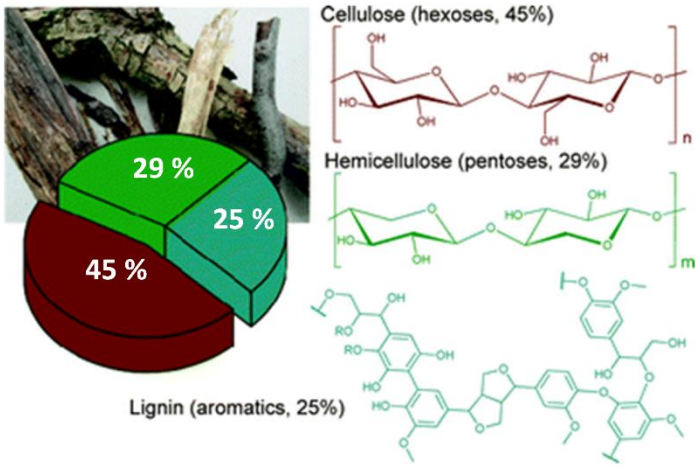

Figure 1.1 Representation of woody biomass composition.[1,2]

A number of cascaded reactions such as hydrolysis, dehydration, aldol condensation, hydrogenation, and reductive amination are required to convert lignocellulose biomass into valuable chemicals such as transport fuels, monomers, and

solvents. Thus, the biggest challenge of biomass utilization curtails its selective conversion into a handful of chemicals, so-called platform molecules,[3] which can be used in the same way as petroleum-sourced intermediates.

Holocellulose moiety is depolymerized by the acid-catalyzed hydrolysis to yield simple hexose and pentose sugars, which can then be dehydrated to 5-(hydroxymethyl)furfural (HMF)[4] and furfural.[5] HMF and furfural are both very versatile molecules, comprising an aromatic 5-membered furan ring and an aldehyde, as well as a hydroxymethyl moiety in the case of HMF (Scheme 1.1). Both can be transformed into transport fuels, but especially HMF lends itself exceptionally well to the production of fine chemicals and monomers due to its hydroxymethyl and aldehyde functionalities.

1.2 5-Hydroxymethylfurfural (HMF)

HMF is a versatile intermediate for the production of a wide range of chemicals and fuel.[6–12] Scheme 1.1 presents reaction paths for the conversion of HMF to key intermediates, which can be used as transport fuels and monomers of biobased polymers with a reduced carbon footprint. For example, HMF can be hydrogenated to 2,5-bis(hydroxymethyl)furan (BHMF)[13–16] and 2,5-(bis(hydroxymethyl)tetrahydrofuran (BHMTHF).[17–21] BHMTHF can be further transformed to aliphatic alcohols such as 1,6-hexanediol and 1,2,6-hexanetriol, and 1,6-hexanediol is a source of adipic acid.[17,22–24] HMF can also be hydrodeoxygenated to yield 2,5-dimethylfuran, which has a high octane number than bio-ethanol and is then suitable for transportation fuels.[25] HMF can be rehydrated to levulinic acid,[26] which is a valuable compound applied as a plasticizer, coating, fuel additive and antifreeze, as well as processing of resins, textiles, and even used as animal feed.[27] HMF can be fully oxidized to 2,5-furandicarbocylic acid

(FDCA),[28–32] which is considered a valuable compound for uses as potentially biobased monomer of polyester in plastic and textile industries. Partial oxidation of HMF produces 2,5-diformylfuran (DFF), which can be further converted to 2,5-bis(aminomethyl)furan (AMF).[33–37] Although AMF has substantial potential as a building block for polyamides,[38,39]efficient synthetic procedures have not been yet developed.

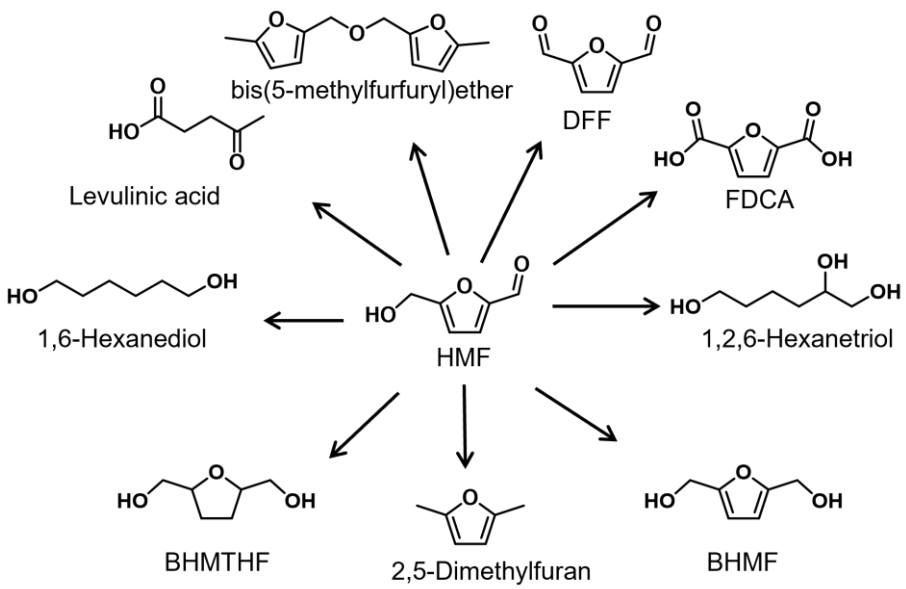

Scheme 1.1 Reaction pathways to several valuable compound obtainable from HMF.

1.3 Aerobic oxidation of HMF

Recently, aerobic oxidation of HMF has been conducted in water using heterogeneous catalysts was well studied.[40–42] In the first step, oxidation of the hydroxyl group of HMF affords DFF, whereas oxidation of the aldehyde group of HMF affords HMFCA. Further oxidation of DFF or HMFCA produces to FFCA, which subsequently converts into FDCA in Scheme 1.2.

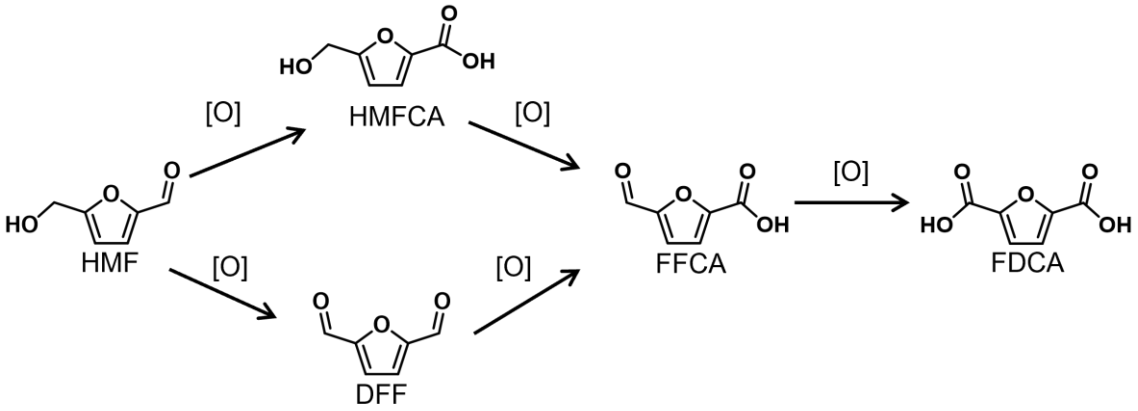

Scheme 1.2 Reaction pathway for aerobic oxidation of HMF to FDCA in water.

Previously, it has been reported that the oxidation pathway of HMF depends on the catalyst used and the reaction conditions. For example, oxidation of HMF through HMFCA formation has been observed with Au supported on hydrotalcite catalysts,[30] Fe_2O_3 or CeO_2,[43] and Cu supported on TiO_2,[44] in water. On the other hand, oxidation of HMF through DFF formation observed with Au supported on TiO_2 or CeO_2 and Pt supported on Al_2O_3 or SiO_2.[45] Although oxidation of HMF through DFF formation can be selected by type of catalyst, it is difficult to prevent further oxidation of DFF to FFCA due to geminal diol formation promoted by water in Scheme 1.3

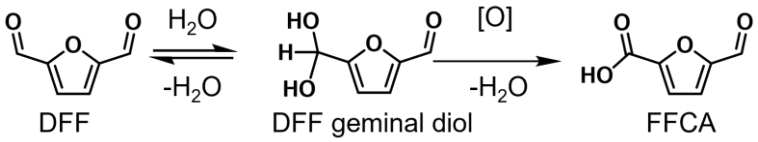

Scheme 1.3 Reaction pathway for aerobic oxidation of DFF to FFCA in water.

Inhibiting further oxidation of the aldehyde of DFF is a big challenge as DFF is easily converted to its geminal diol form in a basic aqueous solution and subsequently oxidized

to yield FDCA.[46,47] The aldehyde group of DFF is oxidized to the corresponding carboxylic acid, yielding FFCA, and finally to FDCA through the formation of an additional geminal diol and its oxidation in Scheme 1.3. The selective oxidation of HMF has been developed in anhydrous and non-protic organic solvents such as N,N'-dimethylformamide (DMF) and N-methyl pyrrolidone (NMP) with basic salts such as K_2CO_3[48] and Cs_2CO_3[49]. However, DFF yield was low, as the presence of base promoted the formation of FFCA instead. When HMF is oxidized in anhydrous, non-protic solvents in absence of base, HMF can be selectively oxidized to DFF, using a suitable catalyst (Table 1.1).[50–59] Table 1.1 summarizes previous reports on aerobic oxidation of HMF to DFF in anhydrous and non-protic solvents. Supported noble metal (Ru, Pd, Au) catalysts show excellent selectivity for DFF. Other active catalysts include metal oxides containing Mn, V, Cu, Co, and Fe,[60–64] and also a metal-free and nitrogen-doped carbon catalyst showing significant potential for this reaction.[65] Despite high DFF yields, all reactions in the previous works were only studied using dilute HMF solutions (<10 wt% HMF) as shown in Table 1.1.

Studies involving HMF are often limited to dilute solutions as concentrated solutions are often met with severe byproduct formation as exemplified in the aerobic oxidation of HMF in water and methanol over a CeO_2-supported Au catalyst.[66,67] The tendency of HMF to form byproducts is caused by its very reactive formyl group, which cannot be controlled by merely optimization of the reaction conditions (temperatures, substrate concentrations, type of catalysts, etc) alone.

Table 1.1 Representative reports on selective HMF conversion to DFF using heterogeneous catalysts

#	Catalyst	HMF (wt%	Solvent	T (K)	t (h)	Conv. (%)	Selec. (%)	Ref.
1	Ru/HT	4.4	DMF	393	6	94	97	[55]
2	Ru/C	1.4	Toluene	383	1	30	96	[50]
3	Ru/γ-Al_2O_3	2	Toluene	393	4	99	97	[56]
4	Ru/NiO	0.7	Toluene	283	2	91	81	[59]
5	Ru/mPMF	3	Toluene	378	12	99	85	[57]
6	Ru/PVP-CNT	1.3	DMF	393	12	100	94	[58]
7	Pt/C	1.4	Toluene	383	0.5	30	73	[50]
8	Pd/C	1.4	Toluene	383	0.5	30	53	[50]
9	Cs/MnO_x	0.67	DMF	373	10	76.8	98.1	[64]
10	Nitrogen-Doped Carbon	0.8	Acetonitrile	373	14	92.9	84.8	[65]
11	FeCo/Carbon	7	Toluene	373	6	100	99	[62]
12	VPO/P-Carbon	1	DMSO	393	10	100	97	[61]
13	Au/MnO_2	4	DMF	393	6	82	99	[52]

Protection strategies, a common phenomenon in organic chemistry, are now being investigated for biomass valorization.[68–72] In the case of HMF, severe byproduct formation can be greatly repressed by protecting this formyl function as its acetal with 1,3-propanediol.[66,67] Acetalization of the formyl group with 1,3-propanediol forms a six-membered ring acetal, which shows high stability against side reactions during aerobic

oxidation and oxidative esterification to synthesize FDCA and its alkyl carboxylate derivatives. Oxidation of HMF acetalized with 1,3-propanediol in water has already reported that FFCA yield was obtained more than 90% at high concentrations (~20 wt%).[73] Such protection strategies are recently regarded to be effective for biomass conversion as biomass-derived intermediates usually have highly reactive functional groups that are easily involved in side-reactions.[66,73]

1.4 Reductive amination of biomass-derived furanics

Aerobic oxidation of the two functional groups in HMF affords three important compounds, 2,5-diformylfuran (DFF), 5-formyl-2-furancarboxylic acid (FFCA), and FDCA (Scheme 1.2).[28–32] DFF can be further converted to 2,5-bis(aminomethyl)furan (AMF).[33–37] AMF has substantial potential as a building block for polyamides.[38,39] FFCA can be also converted to 5-(aminomethyl)furan-2-carboxylic acid used potentially as a building block for polyamides.

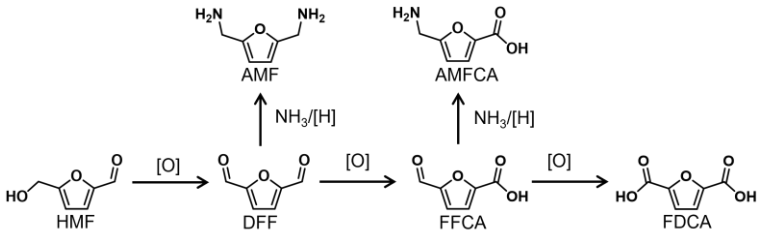

Scheme 1.4 Oxidation and reductive amination pathways of HMF to synthesize monomers for polyesters and polyamides.

FFCA, produced by partial oxidation of HMF, can be converted to its corresponding imine with ammonia and subsequently hydrogenated to AMFCA as laid out in Scheme 1.4. AMFCA is a biobased monomer for polyamide production. Polymerization of

AMFCA alone produces a semi-aromatic polyamide, while hydrogenation, and hydrodeoxygenation (HDO) affords an aliphatic polyamide similar to Nylon-6.[74] AMFCA can be potentially utilized to synthesize another attractive polyamide, poly(iminomethylene(cis-tetrahydro-2,5-furandiyl)carbonyl) (PITC)[75] via the formation of 8-oxa-3-azabicyclo[3.2.1]octan-2-one.[76] Applications of AMFCA possibly extend in biochemical products, which include oligopeptides[77] such as G-quadruplex used for the development of anticancer drugs.[78]

Besides FFCA, other aldehydes such as HMF, DFF, benzaldehyde, glyceraldehyde and so on, can be valorized via reductive amination. Precious metal-based catalysts such as ruthenium, rhodium, and gold are active for reductive amination to synthesize functional amines.[36,79–87] Liang et al. reported reductive amination of several important biomass-derived Aldehydes or ketones to their primary amines in high selectivities (> 90%) by using Ru/ZrO_2.[36] In contrast, non-noble metal catalysts typically studied in the reductive amination are Raney Ni or Co catalysts.[88–90] Despite their high activities, the use of these Raney catalysts accompanies several drawbacks typically represented by pyrophoricity, which results in the difficulty of catalyst handling and its reuse.[91] Recently, several non-noble metal catalysts were developed through precise control of their physicochemical properties (particle size, crystal phase, additional dopants, etc.) and studied in the reductive amination of benzaldehyde and biomass-derived furanics such as glyceraldehyde, HMF, and DFF to their respective primary amines with high selectivities (>80%) as shown in entries 3-6 and 8-14 of Table 1.2.[84,89,92–98] Yuan et al. synthesized primary amines in excellent yields, ranging from 82% to 100%, from several carbonyl compounds using a nitrogen-doped carbon-supported Co catalyst.[98]

Table 1.2. Representative reports on reductive amination of aldehydes to amines using heterogeneous catalysts

#	Catalyst	Raw material	Solvent	P_{H2} (MPa)	NH_3 (mmol)	T (K)	t (h)	Conv. (%)	Selec. (%)	Ref.
1	Ru/ZrO_2	Glyceral	Water	3	35	348	12	100	93	[36]
2	Rh/Al_2O_3	Furfural	Water	2	70	353	5	100	82	[82]
3	Ni/SBA-15	HMF	MeOH -water	1.5	74	373	4	100	90	[84]
4	Raney Ni	HMF	MeOH -water	1.5	74	373	4	100	90	[84]
5	Raney Ni	HMF	THF	1	0.35 MPa	433	2	100	80	[89]
6	Raney Co	HMF	THF	1	0.35 MPa	433	2	100	99.5	[89]
7	Raney Ni	DFF	THF -Water	2	140	393	6	100	42	[94]
8*	Ni/ZrO_2	DFF	MeOH	2	2 MPa	383	10	100	75	[37]
9*	Co/ZrO_2	DFF	MeOH	2	2 MPa	383	10	100	95	[37]
10	Co/Nb_2O_5	DFF	MeOH	2	2 MPa	383	10	100	85	[37]
11	Co/SiO_2	DFF	MeOH	2	2 MPa	383	10	100	73	[37]
12	Co_2P/HT	Nitriles	2-propanol	4	18	373	3	89	84	[97]
13	Co/NC-800	C_7H_6O	Ethanol	1	28	363	12	100	95	[98]
14	Co_2P NRs	C_7H_6O	Water	0.1	44	373	10	100	94	[100]

Condition of entries 8*-11* were adding additive amine for protection group (butylamine 0.75 mmol).

C_7H_6O is referred to benzaldehyde.

However, reductive amination of DFF was difficult due to two reactive aldehyde

groups leading to byproduct formation such as polyimine, polyamine or humin. For example, the amine product (AMF) was obtained in approximately 40% of the selectivity from DFF using Ni-Raney catalyst in THF-water mixture (Table 1.2, entry 7).[94] To suppress byproduct formation from DFF, Qi et. have developed a protection strategy of the formyl group in DFF by imine-protection in Scheme 1.5. Imine formation from DFF reacted with butylamine and imine was subsequently converted to AMF in 70%-90% of selectivities (Table 1.2, entries 8*-11*).[99]

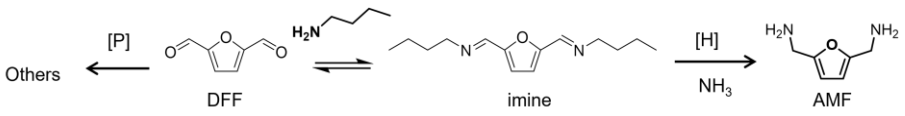

Scheme 1.5 Reductive amination pathways of DFF to AMF by imine-protection.

Moreover, Co_2P NRs catalyst exhibited high yield and selectivity (>90%) from several furan-based aldehydes by reductive amination with aqueous ammonia (NH_3) (Scheme 1.6).[96]

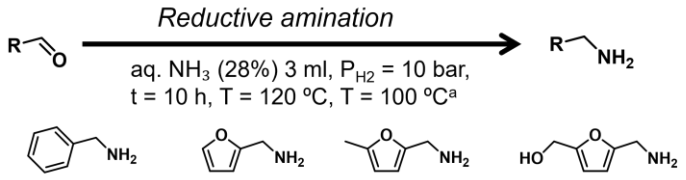

Conv. (%)	99	93	93	95
Sel. (%)	94	97	98	92
Yield (%)	94 [a]	90	91	87

Scheme 1.6 Co_2P NRs-catalyzed reductive amination of furan-based aldehydes with aq. NH_3.

The high performance of Co_2P NRs is related to its high hydrogenation activity. For

example, in reductive amination of benzaldehyde, hydrogenation of the primary and secondary imines (Scheme 1.7) proceeded rapidly to yield benzylamine due to the rod-like morphology of the catalyst, which provides a number of coordinatively unsaturated Co-Co surface site as compared to bulk cobalt phosphide (bulk Co_2P).[96]

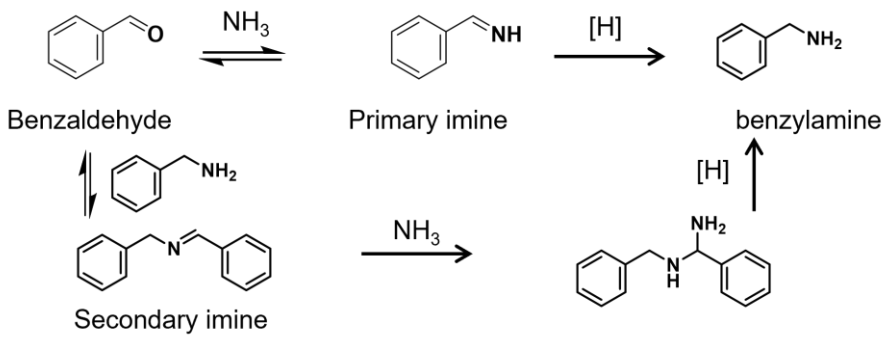

Scheme 1.7 Reductive amination of benzaldehyde.[96]

The difference between the Co_2P NRs and bulk Co_2P is the coordination number (CN) ratio, CN_{Co-Co}/CN_{Co-P}. The CN ratio (1.6) of the Co_2P NRs is smaller than that of bulk Co_2P (2.0), with the ideal value (1.8) calculated from the crystal structure of orthorhombic Co_2P.[96] The small CN ratio of the Co_2P NRs indicates that a number of coordinatively unsaturated Co−Co sites are present on the nanorod surfaces, which is induced by the formation of the rod-shape morphology with a high content of Co, as shown in Scheme 1.7. Such undercoordinated metals are known to enhance hydrogenation activity, as compared to their saturated counterparts.[101–105]

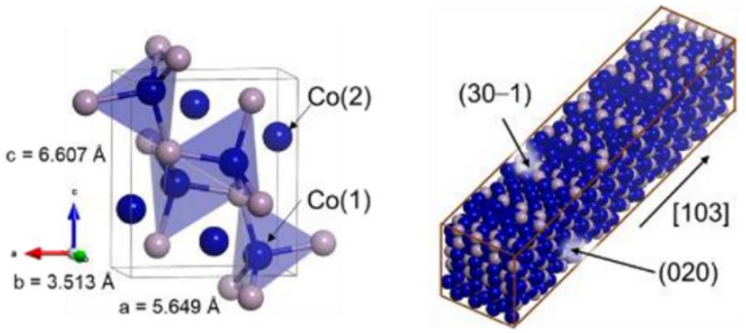

Scheme 1.7 Structure of Co_2P NRs[96]

1.5 Arrangement of the thesis

This thesis starts with the oxidation of a HMF to DFF in Chapter 2. In this chapter, HMF and HMF-acetal in various concentrations (10−70 wt%) were oxidized to clarify the effect of the acetal protection on the product distribution. Kinetic studies were used to evaluate the electron-donating effect of the acetal functionality toward the -CH_2OH oxidation rate by the comparison with other reference hydroxymethylfuran compounds bearing different electron donating and withdrawing groups. Furthermore, a regeneration strategy was developed for the used Ru catalyst.

Chapter 3 deals with reductive amination of FFCA, which is obtained from partial oxidation of HMF. In this chapter, reductive amination of FFCA using Co_2P NRs catalyst was optimized by exploring different factors such as type of nitrogen source, reaction solvent, and so on. Interestingly, we found that FFCA was partially acetalized to the dimethyl acetal of FFCA (FFCA-acetal) when using methanol as a solvent, which possibly improved selectivity of AMFCA by suppressing side reaction.

The benefits of using FFCA-acetal in AMFCA synthesis was explored in Chapter 4. FFCA-acetal was reductively aminated in methanol-water mixtures at different ratios

to clarify the effect of the acetal functionality on the product distribution. Kinetic studies were used to evaluate the effect of the acetal functionality toward the reductive amination rate.

Chapter 5 covers reductive amination of DFF-acetal, which is obtained from oxidation from HMF-acetal in chapter 2. In this chapter, the insights obtained from Chapters 3 and 4 were used to design a two-step reaction route to AMF. The first step is reductive amination of DFF-acetal, which is hydrolyzed in-situ and reductively aminated to yield AMF.

1.6 References

(1) Herbst, A.; Janiak, C. MOF Catalysts in Biomass Upgrading towards Value-Added Fine Chemicals. *CrystEngComm* **2017**, *19* (29), 4092–4117. https://doi.org/10.1039/C6CE01782G.

(2) Esposito, D.; Antonietti, M. Redefining Biorefinery: The Search for Unconventional Building Blocks for Materials. *Chem. Soc. Rev.* **2015**, *44* (16), 5821–5835. https://doi.org/10.1039/C4CS00368C.

(3) Bozell, J. J.; Petersen, G. R. Technology Development for the Production of Biobased Products from Biorefinery Carbohydrates—the US Department of Energy's "Top 10" Revisited. *Green Chem.* **2010**, *12* (4), 539–555. https://doi.org/10.1039/b922014c.

(4) Van Putten, R. J.; Van Der Waal, J. C.; De Jong, E.; Rasrendra, C. B.; Heeres, H. J.; De Vries, J. G. Hydroxymethylfurfural, a Versatile Platform Chemical Made from Renewable Resources. *Chem. Rev.* **2013**, *113* (3), 1499–1597. https://doi.org/10.1021/cr300182k.

(5) Li, X.; Jia, P.; Wang, T. Furfural: A Promising Platform Compound for Sustainable Production of C4 and C5 Chemicals. *ACS Catal.* **2016**, *6* (11), 7621–7640. https://doi.org/10.1021/acscatal.6b01838.

(6) Zhao, H.; Holladay, J. E.; Brown, H.; Zhang, Z. C. Metal Chlorides in Ionic Liquid Solvents Convert Sugars to 5-Hydroxymethylfurfural. *Science.* **2007**, *316* (5831), 1597–1600. https://doi.org/10.1126/science.1141199.

(7) Pidko, E. A.; Degirmenci, V.; Van Santen, R. A.; Hensen, E. J. M. Glucose Activation by Transient Cr^{2+} Dimers. *Angew. Chem. Int. Ed.* **2010**, *49* (14), 2530–2534. https://doi.org/10.1002/anie.201000250.

(8) Nikolla, E.; Román-Leshkov, Y.; Moliner, M.; Davis, M. E. "One-Pot" Synthesis of 5-(Hydroxymethyl)Furfural from Carbohydrates Using Tin-Beta Zeolite. *ACS Catal.* **2011**, *1* (4), 408–410. https://doi.org/10.1021/cs2000544.

(9) Nakajima, K.; Baba, Y.; Noma, R.; Kitano, M.; N. Kondo, J.; Hayashi, S.; Hara, M. Nb_2O_5•nH_2O as a Heterogeneous Catalyst with Water-Tolerant Lewis Acid Sites. *J. Am. Chem. Soc.* **2011**, *133* (12), 4224–4227. https://doi.org/10.1021/ja110482r.

(10) Noma, R.; Nakajima, K.; Kamata, K.; Kitano, M.; Hayashi, S.; Hara, M. Formation of 5-(Hydroxymethyl)Furfural by Stepwise Dehydration over TiO_2 with Water-Tolerant Lewis Acid Sites. *J. Phys. Chem. C* **2015**, *119* (30), 17117–17125. https://doi.org/10.1021/acs.jpcc.5b03290.

(11) Yue, C.; Li, G.; Pidko, E. A.; Wiesfeld, J. J.; Rigutto, M.; Hensen, E. J. M. Dehydration of Glucose to 5-Hydroxymethylfurfural Using Nb-Doped Tungstite. *ChemSusChem* **2016**, *9* (17), 2421–2429. https://doi.org/10.1002/cssc.201600649.

(12) Li, G.; Pidko, E. A.; Hensen, E. J. M.; Nakajima, K. A Density Functional Theory Study of the Mechanism of Direct Glucose Dehydration to 5-Hydroxymethylfurfural on Anatase Titania. *ChemCatChem* **2018**, *10* (18), 4084–4089. https://doi.org/10.1002/cctc.201800900.

(13) Takeda, Y.; Tamura, M.; Nakagawa, Y.; Okumura, K.; Tomishige, K. Hydrogenation of Dicarboxylic Acids to Diols over Re-Pd Catalysts. *Catal. Sci. Technol.* **2016**, *6* (14), 5668–5683. https://doi.org/10.1039/c6cy00335d.

(14) Tamura, M.; Tokonami, K.; Nakagawa, Y.; Tomishige, K. Rapid Synthesis of Unsaturated Alcohols under Mild Conditions by Highly Selective Hydrogenation. *Chem. Commun.* **2013**, *49* (63), 7034–7036. https://doi.org/10.1039/c3cc41526k.

(15) Thompson, S. T.; Lamb, H. H. Palladium-Rhenium Catalysts for Selective Hydrogenation of Furfural: Evidence for an Optimum Surface Composition. *ACS Catal.* **2016**, *6* (11), 7438–7447. https://doi.org/10.1021/acscatal.6b01398.

(16) Wiesfeld, J. J.; Kim, M.; Nakajima, K.; Hensen, E. J. M. Selective Hydrogenation of 5-Hydroxymethylfurfural and Its Acetal with 1,3-Propanediol to 2,5-Bis(Hydroxymethyl)Furan Using Supported Rhenium-Promoted Nickel Catalysts in Water. *Green Chem.* **2020**, *22* (4), 1229–1238. https://doi.org/10.1039/c9gc03856f.

(17) Buntara, T.; Noel, S.; Phua, P. H.; Melián-Cabrera, I.; De Vries, J. G.; Heeres, H. J. Caprolactam from Renewable Resources: Catalytic Conversion of 5-Hydroxymethylfurfural into Caprolactone. *Angew. Chem. Int. Ed.* **2011**, *50* (31), 7083–7087. https://doi.org/10.1002/anie.201102156.

(18) Kong, X.; Zheng, R.; Zhu, Y.; Ding, G.; Zhu, Y.; Li, Y. W. Rational Design of Ni-Based Catalysts Derived from Hydrotalcite for Selective Hydrogenation of 5-

Hydroxymethylfurfural. *Green Chem.* **2015**, *17* (4), 2504–2514. https://doi.org/10.1039/c5gc00062a.

(19) Chen, J.; Liu, R.; Guo, Y.; Chen, L.; Gao, H. Selective Hydrogenation of Biomass-Based 5-Hydroxymethylfurfural over Catalyst of Palladium Immobilized on Amine-Functionalized Metal-Organic Frameworks. *ACS Catal.* **2015**, *5* (2), 722–733. https://doi.org/10.1021/cs5012926.

(20) Nakagawa, Y.; Takada, K.; Tamura, M.; Tomishige, K. Total Hydrogenation of Furfural and 5-Hydroxymethylfurfural over Supported Pd-Ir Alloy Catalyst. *ACS Catal.* **2014**, *4* (8), 2718–2726. https://doi.org/10.1021/cs500620b.

(21) Nakagawa, Y.; Tomishige, K. Total Hydrogenation of Furan Derivatives over Silica-Supported Ni-Pd Alloy Catalyst. *Catal. Commun.* **2010**, *12* (3), 154–156. https://doi.org/10.1016/j.catcom.2010.09.003.

(22) Yao, S.; Wang, X.; Jiang, Y.; Wu, F.; Chen, X.; Mu, X. One-Step Conversion of Biomass-Derived 5-Hydroxymethylfurfural to 1,2,6-Hexanetriol over Ni-Co-Al Mixed Oxide Catalysts under Mild Conditions. *ACS Sustain. Chem. Eng.* **2014**, *2* (2), 173–180. https://doi.org/10.1021/sc4003714.

(23) Buntara, T.; Melián-Cabrera, I.; Tan, Q.; Fierro, J. L. G.; Neurock, M.; De Vries, J. G.; Heeres, H. J. Catalyst Studies on the Ring Opening of Tetrahydrofuran-Dimethanol to 1,2,6-Hexanetriol. *Catal. Today* **2013**, *210*, 106–116. https://doi.org/10.1016/j.cattod.2013.04.012.

(24) Gilkey, M. J.; Mironenko, A. V.; Yang, L.; Vlachos, D. G.; Xu, B. Insights into the Ring-Opening of Biomass-Derived Furanics over Carbon-Supported Ruthenium. *ChemSusChem* **2016**, *9* (21), 3113–3121. https://doi.org/10.1002/cssc.201600681.

(25) Hoang, A. T.; Nižetić, S.; Ölçer, A. I. 2,5-Dimethylfuran (DMF) as a Promising Biofuel for the Spark Ignition Engine Application: A Comparative Analysis and Review. *Fuel* **2021**, *285*, 119140. https://doi.org/10.1016/J.FUEL.2020.119140.

(26) Boonyakarn, T.; Wataniyakul, P.; Boonnoun, P.; Quitain, A. T.; Kida, T.; Sasaki, M.; Laosiripojana, N.; Jongsomjit, B.; Shotipruk, A. Enhanced Levulinic Acid Production from Cellulose by Combined Brønsted Hydrothermal Carbon and Lewis Acid Catalysts. *Ind. Eng. Chem. Res.* **2019**, *58* (8), 2697–2703. https://doi.org/10.1021/acs.iecr.8b05332.

(27) Ghorpade, V.; Hanna, M. Industrial Applications for Levulinic Acid. *Cereals* **1997**, 49–55. https://doi.org/10.1007/978-1-4757-2675-6_7.

(28) Casanova, O.; Iborra, S.; Corma, A. Biomass into Chemicals: Aerobic Oxidation of 5-Hydroxymethyl-2-Furfural into 2,5-Furandicarboxylic Acid with Gold Nanoparticle Catalysts. *ChemSusChem* **2009**, *2* (12), 1138–1144. https://doi.org/10.1002/cssc.200900137.

(29) Casanova, O.; Iborra, S.; Corma, A. Biomass into Chemicals: One Pot-Base Free Oxidative Esterification of 5-Hydroxymethyl-2-Furfural into 2,5-Dimethylfuroate with Gold on Nanoparticulated Ceria. *J. Catal.* **2009**, *265* (1), 109–116. https://doi.org/10.1016/j.jcat.2009.04.019.

(30) Gupta, N. K.; Nishimura, S.; Takagaki, A.; Ebitani, K. Hydrotalcite-Supported Gold-Nanoparticle-Catalyzed Highly Efficient Base-Free Aqueous Oxidation of 5-Hydroxymethylfurfural into 2,5-Furandicarboxylic Acid under Atmospheric Oxygen Pressure. *Green Chem.* **2011**, *13* (4), 824–827. https://doi.org/10.1039/c0gc00911c.

(31) Sajid, M.; Zhao, X.; Liu, D. Production of 2,5-Furandicarboxylic Acid (FDCA)

from 5-Hydroxymethylfurfural (HMF): Recent Progress Focusing on the Chemical-Catalytic Routes. *Green Chem.* **2018**, *20* (24), 5427–5453. https://doi.org/10.1039/c8gc02680g.

(32) Hayashi, E.; Yamaguchi, Y.; Kamata, K.; Tsunoda, N.; Kumagai, Y.; Oba, F.; Hara, M. Effect of MnO_2 Crystal Structure on Aerobic Oxidation of 5-Hydroxymethylfurfural to 2,5-Furandicarboxylic Acid. *J. Am. Chem. Soc.* **2019**, *141* (2), 899–900. https://doi.org/10.1021/jacs.8b09917.

(33) Pingen, D.; Schwaderer, J. B.; Walter, J.; Wen, J.; Murray, G.; Vogt, D.; Mecking, S. Diamines for Polymer Materials via Direct Amination of Lipid- and Lignocellulose-Based Alcohols with NH_3. *ChemCatChem* **2018**, *10* (14), 3027–3033. https://doi.org/10.1002/cctc.201800365.

(34) Xu, Y.; Jia, X.; Ma, J.; Gao, J.; Xia, F.; Li, X.; Xu, J. Selective Synthesis of 2,5-Bis(Aminomethyl)Furan: Via Enhancing the Catalytic Dehydration-Hydrogenation of 2,5-Diformylfuran Dioxime. *Green Chem.* **2018**, *20* (12), 2697–2701. https://doi.org/10.1039/c8gc00947c.

(35) Zhou, K.; Liu, H.; Shu, H.; Xiao, S.; Guo, D.; Liu, Y.; Wei, Z.; Li, X. A Comprehensive Study on the Reductive Amination of 5-Hydroxymethylfurfural into 2,5-Bisaminomethylfuran over Raney Ni Through DFT Calculations. *ChemCatChem* **2019**, *11* (11), 2649–2656. https://doi.org/10.1002/cctc.201900304.

(36) Liang, G.; Wang, A.; Li, L.; Xu, G.; Yan, N.; Zhang, T. Production of Primary Amines by Reductive Amination of Biomass-Derived Aldehydes/Ketones. *Angew. Chem. Int. Ed.* **2017**, *56* (11), 3050–3054. https://doi.org/10.1002/anie.201610964.

(37) Qi, H.; Liu, F.; Zhang, L.; Li, L.; Su, Y.; Yang, J.; Hao, R.; Wang, A.; Zhang, T. Modulating: Trans -Imination and Hydrogenation towards the Highly Selective Production of Primary Diamines from Dialdehydes. *Green Chem.* **2020**, *22* (20), 6897–6901. https://doi.org/10.1039/d0gc02280b.

(38) Winnacker, M.; Rieger, B. Biobased Polyamides: Recent Advances in Basic and Applied Research. *Macromol. Rapid Commun.* **2016**, *37* (17), 1391–1413. https://doi.org/10.1002/marc.201600181.

(39) García, J. M.; García, F. C.; Serna, F.; de la Peña, J. L. High-Performance Aromatic Polyamides. *Prog. Polym. Sci.* **2010**, *35* (5), 623–686. https://doi.org/10.1016/J.PROGPOLYMSCI.2009.09.002.

(40) Han, X.; Li, C.; Liu, X.; Xia, Q.; Wang, Y. Selective Oxidation of 5-Hydroxymethylfurfural to 2,5-Furandicarboxylic Acid over MnOx–CeO2 Composite Catalysts. *Green Chem.* **2017**, *19* (4), 996–1004. https://doi.org/10.1039/C6GC03304K.

(41) Ban, H.; Chen, S.; Zhang, Y.; Cheng, Y.; Wang, L.; Li, X. Kinetics and Mechanism of Catalytic Oxidation of 5-Methylfurfural to 2,5-Furandicarboxylic Acid with Co/Mn/Br Catalyst. *Ind. Eng. Chem. Res.* **2019**, *58* (41), 19009–19021. https://doi.org/10.1021/acs.iecr.9b03573.

(42) Corma Canos, A.; Iborra, S.; Velty, A. Chemical Routes for the Transformation of Biomass into Chemicals. *Chem. Rev.* **2007**, *107* (6), 2411–2502. https://doi.org/10.1021/cr050989d.

(43) Casanova, O.; Iborra, S.; Corma, A. Biomass into Chemicals: Aerobic Oxidation of 5-Hydroxymethyl-2-Furfural into 2,5-Furandicarboxylic Acid with Gold Nanoparticle Catalysts. *ChemSusChem* **2009**, *2* (12), 1138–1144.

https://doi.org/10.1002/CSSC.200900137.

(44) Ribeiro, M. L.; Schuchardt, U. Cooperative Effect of Cobalt Acetylacetonate and Silica in the Catalytic Cyclization and Oxidation of Fructose to 2,5-Furandicarboxylic Acid. *Catal. Commun.* **2003**, *4* (2), 83–86. https://doi.org/10.1016/S1566-7367(02)00261-3.

(45) Lilga, M. A.; Hallen, R. T.; Gray, M. Production of Oxidized Derivatives of 5-Hydroxymethylfurfural (HMF). *Top. Catal.* **2010**, *53* (15–18), 1264–1269. https://doi.org/10.1007/s11244-010-9579-4.

(46) Ardemani, L.; Cibin, G.; Dent, A. J.; Isaacs, M. A.; Kyriakou, G.; Lee, A. F.; Parlett, C. M. A.; Parry, S. A.; Wilson, K. Solid Base Catalysed 5-HMF Oxidation to 2,5-FDCA over Au/Hydrotalcites: Fact or Fiction? *Chem. Sci.* **2015**, *6* (8), 4940–4945. https://doi.org/10.1039/C5SC00854A.

(47) Schade, O. R.; Gaur, A.; Zimina, A.; Saraçi, E.; Grunwaldt, J. D. Mechanistic Insights into the Selective Oxidation of 5-(Hydroxymethyl)Furfural over Silver-Based Catalysts. *Catal. Sci. Technol.* **2020**, *10* (15), 5036–5047. https://doi.org/10.1039/D0CY00878H.

(48) Xu, J.; Zhu, Z.; Yuan, Z.; Su, T.; Zhao, Y.; Ren, W.; Zhang, Z.; Lü, H. Selective Oxidation of 5-Hydroxymethylfurfural to 5-Formyl-2-Furancarboxylic Acid over a Fe-Anderson Type Catalyst. *J. Taiwan Inst. Chem. Eng.* **2019**, *104*, 8–15. https://doi.org/10.1016/J.JTICE.2019.08.006.

(49) Buonerba, A.; Impemba, S.; Litta, A. D.; Capacchione, C.; Milione, S.; Grassi, A. Aerobic Oxidation and Oxidative Esterification of 5-Hydroxymethylfurfural by Gold Nanoparticles Supported on Nanoporous Polymer Host Matrix. *ChemSusChem* **2018**, *11* (18), 3139–3149.

https://doi.org/10.1002/CSSC.201801560.

(50) Nie, J.; Xie, J.; Liu, H. Efficient Aerobic Oxidation of 5-Hydroxymethylfurfural to 2,5-Diformylfuran on Supported Ru Catalysts. *J. Catal.* **2013**, *301*, 83–91. https://doi.org/10.1016/j.jcat.2013.01.007.

(51) Davis, S. E.; Houk, L. R.; Tamargo, E. C.; Datye, A. K.; Davis, R. J. Oxidation of 5-Hydroxymethylfurfural over Supported Pt, Pd and Au Catalysts. *Catal. Today* **2011**, *160* (1), 55–60. https://doi.org/10.1016/j.cattod.2010.06.004.

(52) Zhu, Y.; Shen, M.; Xia, Y.; Lu, M. Au/MnO_2 Nanostructured Catalysts and Their Catalytic Performance for the Oxidation of 5-(Hydroxymethyl)Furfural. *Catal. Commun.* **2015**, *64*, 37–43. https://doi.org/10.1016/j.catcom.2015.01.031.

(53) Zhang, Z.; Yuan, Z.; Tang, D.; Ren, Y.; Lv, K.; Liu, B. Iron Oxide Encapsulated by Ruthenium Hydroxyapatite as Heterogeneous Catalyst for the Synthesis of 2,5-Diformylfuran. *ChemSusChem* **2014**, *7* (12), 3496–3504. https://doi.org/10.1002/cssc.201402402.

(54) Mishra, D. K.; Cho, J. K.; Kim, Y. J. Facile Production of 2,5-Diformylfuran from Base-Free Oxidation of 5-Hydroxymethyl Furfural over Manganese–Cobalt Spinels Supported Ruthenium Nanoparticles. *J. Ind. Eng. Chem.* **2018**, *60*, 513–519. https://doi.org/10.1016/j.jiec.2017.11.040.

(55) Takagaki, A.; Takahashi, M.; Nishimura, S.; Ebitani, K. One-Pot Synthesis of 2,5-Diformylfuran from Carbohydrate Derivatives by Sulfonated Resin and Hydrotalcite-Supported Ruthenium Catalysts. *ACS Catal.* **2011**, *1* (11), 1562–1565. https://doi.org/10.1021/cs200456t.

(56) Antonyraj, C. A.; Jeong, J.; Kim, B.; Shin, S.; Kim, S.; Lee, K. Y.; Cho, J. K. Selective Oxidation of HMF to DFF Using Ru/γ-Alumina Catalyst in Moderate

Boiling Solvents toward Industrial Production. *J. Ind. Eng. Chem.* **2013**, *19* (3), 1056–1059. https://doi.org/10.1016/j.jiec.2012.12.002.

(57) Ghosh, K.; Molla, R. A.; Iqubal, M. A.; Islam, S. S.; Islam, S. M. Ruthenium Nanoparticles Supported on N-Containing Mesoporous Polymer Catalyzed Aerobic Oxidation of Biomass-Derived 5-Hydroxymethylfurfural (HMF) to 2,5-Diformylfuran (DFF). *Appl. Catal. A Gen.* **2016**, *520*, 44–52. https://doi.org/10.1016/j.apcata.2016.03.035.

(58) Chen, J.; Zhong, J.; Guo, Y.; Chen, L. Ruthenium Complex Immobilized on Poly(4-Vinylpyridine)-Functionalized Carbon-Nanotube for Selective Aerobic Oxidation of 5-Hydroxymethylfurfural to 2,5-Diformylfuran. *RSC Adv.* **2015**, *5* (8), 5933–5940. https://doi.org/10.1039/c4ra14592e.

(59) Liu, Y.; Gan, T.; He, Q.; Zhang, H.; He, X.; Ji, H. Catalytic Oxidation of 5-Hydroxymethylfurfural to 2,5-Diformylfuran over Atomically Dispersed Ruthenium Catalysts. *Ind. Eng. Chem. Res.* **2020**, *59* (10), 4333–4337. https://doi.org/10.1021/acs.iecr.9b06470.

(60) Biswas, S.; Dutta, B.; Mannodi-Kanakkithodi, A.; Clarke, R.; Song, W.; Ramprasad, R.; Suib, S. L. Heterogeneous Mesoporous Manganese/Cobalt Oxide Catalysts for Selective Oxidation of 5-Hydroxymethylfurfural to 2,5-Diformylfuran. *Chem. Commun.* **2017**, *53* (86), 11751–11754. https://doi.org/10.1039/c7cc06097a.

(61) Wen, S.; Liu, K.; Tian, Y.; Xiang, Y.; Liu, X.; Yin, D. Phosphorus-Doped Carbon Supported Vanadium Phosphate Oxides for Catalytic Oxidation of 5-Hydroxymethylfurfural to 2,5-Diformylfuran. *Processes* **2020**, *8* (10), 1–8. https://doi.org/10.3390/pr8101273.

(62) Fang, R.; Luque, R.; Li, Y. Selective Aerobic Oxidation of Biomass-Derived HMF to 2,5-Diformylfuran Using a MOF-Derived Magnetic Hollow Fe-Co Nanocatalyst. *Green Chem.* **2016**, *18* (10), 3152–3157. https://doi.org/10.1039/c5gc03051j.

(63) Nocito, F.; Ventura, M.; Aresta, M.; Dibenedetto, A. Selective Oxidation of 5-(Hydroxymethyl)Furfural to DFF Using Water as Solvent and Oxygen as Oxidant with Earth-Crust-Abundant Mixed Oxides. *ACS Omega* **2018**, *3* (12), 18724–18729. https://doi.org/10.1021/acsomega.8b02839.

(64) Yuan, Z.; Liu, B.; Zhou, P.; Zhang, Z.; Chi, Q. Aerobic Oxidation of Biomass-Derived 5-Hydroxymethylfurfural to 2,5-Diformylfuran with Cesium-Doped Manganese Dioxide. *Catal. Sci. Technol.* **2018**, *8* (17), 4430–4439. https://doi.org/10.1039/c8cy01246f.

(65) Ren, Y.; Yuan, Z.; Lv, K.; Sun, J.; Zhang, Z.; Chi, Q. Selective and Metal-Free Oxidation of Biomass-Derived 5-Hydroxymethylfurfural to 2,5-Diformylfuran over Nitrogen-Doped Carbon Materials. *Green Chem.* **2018**, *20* (21), 4946–4956. https://doi.org/10.1039/c8gc02286k.

(66) Kim, M.; Su, Y.; Fukuoka, A.; Hensen, E. J. M.; Nakajima, K. Aerobic Oxidation of 5-(Hydroxymethyl)Furfural Cyclic Acetal Enables Selective Furan-2,5-Dicarboxylic Acid Formation with CeO_2-Supported Gold Catalyst. *Angew. Chem. Int. Ed.* **2018**, *57* (27), 8235–8239. https://doi.org/10.1002/anie.201805457.

(67) Kim, M.; Su, Y.; Aoshima, T.; Fukuoka, A.; Hensen, E. J. M.; Nakajima, K. Effective Strategy for High-Yield Furan Dicarboxylate Production for Biobased Polyester Applications. *ACS Catal.* **2019**, *9* (5), 4277–4285.

https://doi.org/10.1021/acscatal.9b00450.

(68) Shuai, L.; Amiri, M. T.; Questell-Santiago, Y. M.; Héroguel, F.; Li, Y.; Kim, H.; Meilan, R.; Chapple, C.; Ralph, J.; Luterbacher, J. S. Formaldehyde Stabilization Facilitates Lignin Monomer Production during Biomass Depolymerization. *Science (80-.).* **2016**, *354* (6310), 329–333. https://doi.org/10.1126/science.aaf7810.

(69) Lan, W.; Amiri, M. T.; Hunston, C. M.; Luterbacher, J. S. Protection Group Effects During α,γ-Diol Lignin Stabilization Promote High-Selectivity Monomer Production. *Angew. Chem. Int. Ed.* **2018**, *57* (5), 1356–1360. https://doi.org/10.1002/anie.201710838.

(70) Questell-Santiago, Y. M.; Zambrano-Varela, R.; Talebi Amiri, M.; Luterbacher, J. S. Carbohydrate Stabilization Extends the Kinetic Limits of Chemical Polysaccharide Depolymerization. *Nat. Chem.* **2018**, *10* (12), 1222–1228. https://doi.org/10.1038/s41557-018-0134-4.

(71) Questell-Santiago, Y. M.; Yeap, J. H.; Talebi Amiri, M.; Le Monnier, B. P.; Luterbacher, J. S. Catalyst Evolution Enhances Production of Xylitol from Acetal-Stabilized Xylose. *ACS Sustain. Chem. Eng.* **2020**, *8* (4), 1709–1714. https://doi.org/10.1021/acssuschemeng.9b06456.

(72) Luo, X.; Li, Y.; Gupta, N. K.; Sels, B.; Ralph, J.; Shuai, L. Protection Strategies Enable Selective Conversion of Biomass. *Angew. Chem. Int. Ed.* **2020**, *59* (29), 11704–11716. https://doi.org/10.1002/anie.201914703.

(73) Wiesfeld, J. J.; Asakawa, M.; Aoshima, T.; Fukuoka, A.; Emiel,]; Hensen, J. M.; Nakajima, K. A Catalytic Strategy for Selective Production of 5-Formylfuran-2-Carboxylic Acid and Furan-2,5-Dicarboxylic Acid. *ChemCatChem* **2022**,

e202200191. https://doi.org/10.1002/CCTC.202200191.

(74) CN105658700A - Compounds and Methods for Producing Nylon 6 - Google Patents.

(75) Woroch, C. P.; Lankenau, A. W.; Kanan, M. W. A High-T g Polyamide Derived from Lignocellulose and CO_2. https://doi.org/10.1021/acs.macromol.1c01547.

(76) Lankenau, A. W.; Kanan, M. W. Polyamide Monomers via Carbonate-Promoted C–H Carboxylation of Furfurylamine. *Chem. Sci.* **2019**, *11* (1), 248–252. https://doi.org/10.1039/C9SC04460D.

(77) Singh, H.; Arora, K.; Tapadar, S.; Chakraborty, T. K. Preferential Polymerization of 5-(Aminomethyl)-2-Furancarboxylic Acid (AMFC) into a Cyclic Tripeptide. *J. Theor. Comput. Chem.* **2004**, *3* (4), 555–566. https://doi.org/10.1142/S0219633604001203.

(78) Chakraborty, T. K.; Arora, A.; Roy, S.; Kumar, N.; Maiti, S. Furan Based Cyclic Oligopeptides Selectively Target G-Quadruplex. *J. Med. Chem* **2007**, *50*, 5539–5542. https://doi.org/10.1021/jm070619c.

(79) Beydoun, K.; Ghattas, G.; Thenert, K.; Klankermayer, J.; Leitner, W. Ruthenium-Catalyzed Reductive Methylation of Imines Using Carbon Dioxide and Molecular Hydrogen. *Angew. Chem. Int. Ed. Engl.* **2014**, *53* (41), 11010–11014. https://doi.org/10.1002/ANIE.201403711.

(80) Zhu, S.; Lu, X.; Luo, Y.; Zhang, W.; Jiang, H.; Yan, M.; Zeng, W. Ruthenium(II)-Catalyzed Regioselective Reductive Coupling of α-Imino Esters with Dienes. *Org. Lett.* **2013**, *15* (7), 1440–1443. https://doi.org/10.1021/OL4006079.

(81) Zhu, M. Ruthenium-Catalyzed Direct Reductive Amination in HCOOH/NEt_3

Mixture. *Catal. Lett. 2014 1449* **2014**, *144* (9), 1568–1572. https://doi.org/10.1007/S10562-014-1314-5.

(82) Chatterjee, M.; Ishizaka, T.; Kawanami, H. Reductive Amination of Furfural to Furfurylamine Using Aqueous Ammonia Solution and Molecular Hydrogen: An Environmentally Friendly Approach. *Green Chem.* **2016**, *18* (2), 487–496. https://doi.org/10.1039/c5gc01352f.

(83) Kolobova, E.; Mäki-Arvela, P.; Pestryakov, A.; Pakrieva, E.; Pascual, L.; Smeds, A.; Rahkila, J.; Sandberg, T.; Peltonen, J.; Murzin, D. Y. Reductive Amination of Ketones with Benzylamine Over Gold Supported on Different Oxides. *Catal. Lett. 2019 14912* **2019**, *149* (12), 3432–3446. https://doi.org/10.1007/S10562-019-02917-1.

(84) Chen, W.; Sun, Y.; Du, J.; Si, Z.; Tang, X.; Zeng, X.; Lin, L.; Liu, S.; Lei, T. Preparation of 5-(Aminomethyl)-2-Furanmethanol by Direct Reductive Amination of 5-Hydroxymethylfurfural with Aqueous Ammonia over the Ni/SBA-15 Catalyst. *J. Chem. Technol. Biotechnol.* **2018**, *93* (10), 3028–3034. https://doi.org/10.1002/JCTB.5661.

(85) Bódis, J.; Lefferts, L.; Müller, T. E.; Pestman, R.; Lercher, J. A. Activity and Selectivity Control in Reductive Amination of Butyraldehyde over Noble Metal Catalysts. *Catal. Lett. 2005 1041* **2005**, *104* (1), 23–28. https://doi.org/10.1007/S10562-005-7431-4.

(86) Sha, J.; Kusema, B. T.; Zhou, W.-J.; Yan, Z.; Streiff, S.; Pera-Titus, M. Single-Reactor Tandem Oxidation–Amination Process for the Synthesis of Furan Diamines from 5-Hydroxymethylfurfural. *Green Chem.* **2021**, *23* (18), 7093–7099. https://doi.org/10.1039/D1GC01621K.

(87) Komanoya, T.; Kinemura, T.; Kita, Y.; Kamata, K.; Hara, M. Electronic Effect of Ruthenium Nanoparticles on Efficient Reductive Amination of Carbonyl Compounds. *J. Am. Chem. Soc.* **2017**, *139* (33), 11493–11499. https://doi.org/10.1021/jacs.7b04481.

(88) Nugent, T. C.; Wakchaure, V. N.; Ghosh, A. K.; Mohanty, R. R. Evolution of Titanium(IV) Alkoxides and Raney Nickel for Asymmetric Reductive Amination of Prochiral Aliphatic Ketones. *Org. Lett.* **2005**, *7* (22), 4967–4970. https://doi.org/10.1021/OL051909V.

(89) Wei, Z.; Cheng, Y.; Zhou, K.; Zeng, Y.; Yao, E.; Li, Q.; Liu, Y.; Sun, Y. One-Step Reductive Amination of 5-Hydroxymethylfurfural into 2,5-Bis(Aminomethyl)Furan over Raney Ni. *ChemSusChem* **2021**. https://doi.org/10.1002/cssc.202100564.

(90) Zhou, K.; Chen, B.; Zhou, X.; Kang, S.; Xu, Y.; Wei, J. Selective Synthesis of Furfurylamine by Reductive Amination of Furfural over Raney Cobalt. *ChemCatChem* **2019**, *11* (22), 5562–5569. https://doi.org/10.1002/CCTC.201901269.

(91) Ertl, G.; Knozinger, H.; Weitkamp, J. Preparation of Solid Catalysts. *Prep. Solid Catal.* **2008**, 1–622. https://doi.org/10.1002/9783527619528.

(92) Hangkong Yuan; T. Kusema, B.; Zhen Yan; Stéphane Streiff; Feng Shi. Highly Selective Synthesis of 2,5-Bis(Aminomethyl)Furan via Catalytic Amination of 5-(Hydroxymethyl)Furfural with NH_3 over a Bifunctional Catalyst. *RSC Adv.* **2019**, *9* (66), 38877–38881. https://doi.org/10.1039/C9RA08560B.

(93) Chatterjee, M.; Ishizaka, T.; Kawanami, H. Reductive Amination of Furfural to Furfurylamine Using Aqueous Ammonia Solution and Molecular Hydrogen: An

Environmentally Friendly Approach. *Green Chem.* **2016**, *18* (2), 487–496. https://doi.org/10.1039/C5GC01352F.

(94) Le, N.-T.; Byun, A.; Han, Y.; Lee, K.-I.; Kim, H. Preparation of 2,5-Bis(Aminomethyl)Furan by Direct Reductive Amination of 2,5-Diformylfuran over Nickel-Raney Catalysts. *Green Sustain. Chem.* **2015**, *05* (03), 115–127. https://doi.org/10.4236/gsc.2015.53015.

(95) Qi, H.; Liu, F.; Zhang, L.; Li, L.; Su, Y.; Yang, J.; Hao, R.; Wang, A.; Zhang, T. Modulating: Trans -Imination and Hydrogenation towards the Highly Selective Production of Primary Diamines from Dialdehydes. *Green Chem.* **2020**, *22* (20), 6897–6901. https://doi.org/10.1039/d0gc02280b.

(96) Sheng, M.; Fujita, S.; Yamaguchi, S.; Yamasaki, J.; Nakajima, K.; Yamazoe, S.; Mizugaki, T.; Mitsudome, T. Single-Crystal Cobalt Phosphide Nanorods as a High-Performance Catalyst for Reductive Amination of Carbonyl Compounds. *JACS Au* **2021**, *1* (4), 501–507. https://doi.org/10.1021/jacsau.1c00125.

(97) Mitsudome, T.; Sheng, M.; Nakata, A.; Yamasaki, J.; Mizugaki, T.; Jitsukawa, K. A Cobalt Phosphide Catalyst for the Hydrogenation of Nitriles. *Chem. Sci.* **2020**, *11* (26), 6682–6689. https://doi.org/10.1039/d0sc00247j.

(98) Yuan, Z.; Liu, B.; Zhou, P.; Zhang, Z.; Chi, Q. Preparation of Nitrogen-Doped Carbon Supported Cobalt Catalysts and Its Application in the Reductive Amination. *J. Catal.* **2019**, *370*, 347–356. https://doi.org/10.1016/J.JCAT.2019.01.004.

(99) Qi, H.; Liu, F.; Zhang, L.; Li, L.; Su, Y.; Yang, J.; Hao, R.; Wang, A.; Zhang, T. Modulating: Trans -Imination and Hydrogenation towards the Highly Selective Production of Primary Diamines from Dialdehydes. *Green Chem.* **2020**, *22* (20),

6897–6901. https://doi.org/10.1039/d0gc02280b.

(100) Sheng, M.; Fujita, S.; Yamaguchi, S.; Yamasaki, J.; Nakajima, K.; Yamazoe, S.; Mizugaki, T.; Mitsudome, T. Single-Crystal Cobalt Phosphide Nanorods as a High-Performance Catalyst for Reductive Amination of Carbonyl Compounds. *JACS Au* **2021**, *1* (4), 501–507. https://doi.org/10.1021/jacsau.1c00125.

(101) Singh, J. A.; Yang, N.; Liu, X.; Tsai, C.; Stone, K. H.; Johnson, B.; Koh, A. L.; Bent, S. F. Understanding the Active Sites of CO Hydrogenation on Pt-Co Catalysts Prepared Using Atomic Layer Deposition. *J. Phys. Chem. C* **2018**, *122* (4), 2184–2194. https://doi.org/10.1021/ACS.JPCC.7B10541.

(102) Fujita, S.; Yamaguchi, S.; Yamasaki, J.; Nakajima, K.; Yamazoe, S.; Mizugaki, T.; Mitsudome, T. Ni_2P Nanoalloy as an Air-Stable and Versatile Hydrogenation Catalyst in Water: P-Alloying Strategy for Designing Smart Catalysts. *Chem. – A Eur. J.* **2021**, *27* (13), 4439–4446. https://doi.org/10.1002/CHEM.202005037.

(103) Wang, H.; Xu, K.; Yao, X.; Ye, D.; Pei, Y.; Hu, H.; Qiao, M.; Li, Z. H.; Zhang, X.; Zong, B. Undercoordinated Site-Abundant and Tensile-Strained Nickel for Low-Temperature CO_x Methanation. *ACS Catal.* **2018**, *8* (2), 1207–1211. https://doi.org/10.1021/ACSCATAL.7B02944.

(104) Hartfelder, U.; Kartusch, C.; Makosch, M.; Rovezzi, M.; Sá, J.; Van Bokhoven, J. A. Particle Size and Support Effects in Hydrogenation over Supported Gold Catalysts. *Catal. Sci. Technol.* **2013**, *3* (2), 454–461. https://doi.org/10.1039/C2CY20485A.

(105) Wang, M.; Feng, B.; Li, H.; Li, H. Controlled Assembly of Hierarchical Metal Catalysts with Enhanced Performances. *Chem* **2019**, *5* (4), 805–837. https://doi.org/10.1016/J.CHEMPR.2019.01.003.

Chapter 2

Oxidation of 5-Hydroxymethylfurfural to 2,5-Diformylfuran

Abstract

An acetal protection strategy for 5-hydroxymethylfurfural (HMF) was used to obtain 2,5-diformyfuran (DFF) using concentrated HMF solutions and a γ-Al_2O_3-supported Ru catalyst (Ru/γ-Al_2O_3). The HMF-acetal with 1,3-propanediol can be oxidized to DFF-acetal with a yield of 84.0% at an HMF conversion of 94.2% from a 50 wt% solution. In contrast, aerobic oxidation of nonprotected HMF using a 10 wt% solution afforded DFF only in a moderate yield (52.3%). Kinetic studies indicate that the six-membered ring acetal group not only prevents side reactions but also accelerates aerobic oxidation of the -CH_2OH moiety to -CHO under retention of the acetal functionality. Organic deposits formed during the reaction explained the significant decrease in the activity of the Ru/γ-Al_2O_3 catalyst, which could be recovered neither by washing in water or organic solvents, nor by a calcination-reduction treatment. Sonication of the used Ru/γ-Al_2O_3 catalyst in an aqueous NaOH solution successfully removed the deposits and allowed reuse of the catalyst for at least four times without activity loss.

2.1 Introduction

Lignocellulosic biomass is widely regarded as an abundant, easily accessible and

renewable carbon resource that can replace fossil fuels.[1,2] Catalytic valorization of its main constituents (cellulose, hemicellulose, and lignin) into platform molecules has been extensively studied to realize sustainable production of fuels and commodity chemicals.[3–7] Hydrolysis of cellulose into glucose and its subsequent dehydration lead to (5-hydroxymethyl)furfural (HMF),[8–14] which is a versatile intermediate for production of a wide range of chemicals and fuel additives. Scheme 2.1 presents reaction paths for the conversion of HMF to intermediates that can be used as monomers for manufacture of polymers with a reduced carbon footprint. Aerobic oxidation of the two functional groups in HMF affords 2,5-furandicarbocylic acid (FDCA),[15–19] while hydrogenation of HMF yields 2,5-bis(hydroxymethyl)furan (BHMF)[20–23] and 2,5-(bis(hydroxymethyl)tetrahydrofuran (BHMTHF).[24–28] BHMTHF can be further transformed to aliphatic alcohols such as 1,6-hexanediol and 1,2,6-hexanetriol, and 1,6-hexanediol is a source of adipic acid.[24,29–31] Partial oxidation of HMF can also lead to 2,5-diformylfuran (DFF), which can be further converted to 2,5-bis(aminomethyl)furan (AMF).[32–36] Although AMF has substantial potential as a building block for polyamides,[37,38] efficient synthetic procedures have not yet been developed. For the first step of AMF production, we have studied aerobic oxidation of the hydroxymethyl group in HMF to the corresponding formyl group using supported metal catalysts and concentrated solutions (Scheme 2.1).

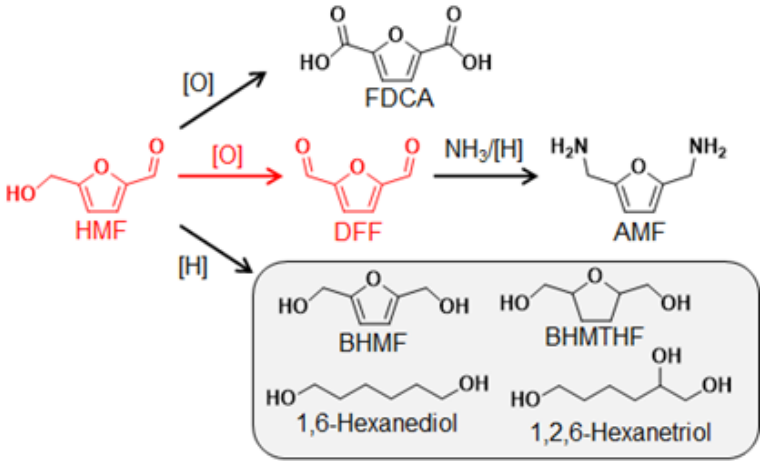

Scheme 2.1. Reaction pathways to several valuable monomers obtainable from HMF.

Reaction paths for the aerobic oxidation of HMF to FDCA in water are illustrated in Scheme 1.2. The formyl group is easily oxidized to the corresponding carboxylic acid in water via the formation of a geminal diol intermediate. HMF can be easily oxidized to FDCA through 5-(hydroxymethyl)furan-2-carboxylic acid (HMFCA) and 5-formylfuran-2-carboxylic acid (FFCA) as intermediates, while DFF is only obtained in very small amounts which can further oxidize to FFCA due to DFF geminal diol in Scheme 1.3.

The use of non-protic organic solvents such as toluene and N,N'-dimethylformamide (DMF) prevents the hydration of the formyl group of DFF to a geminal diol (Scheme 1.3) and its subsequent oxidative dehydrogenation to a carboxylic acid. This provides an opportunity to selectively oxidize HMF to DFF. Supported noble metal catalysts such as Pt, Pd, Au, or Ru have been extensively studied for the selective oxidation of HMF in toluene and DMF.[39–48] Other catalysts reported to be active for DFF formation include metal oxides containing Mn, V, Cu, Co, and Fe [49–53], while also metal-free and nitrogen-doped carbon catalysts show significant potential for this reaction.[54] Despite high DFF yields, all reactions in the previous works were only studied using

dilute HMF solutions (< 10 wt% HMF) in Table 1.1. This is most likely due to severe byproduct formation, which proceeds predominantly in concentrated solutions as exemplified in the aerobic oxidation of 10 wt% HMF in water and methanol over a CeO_2-supported Au catalyst.[55,56]

Byproduct formation is a serious issue for the catalytic valorization of lignocellulose biomass, which cannot be simply controlled by optimization of the reaction conditions (temperature, substrate concentration, type of catalyst, etc). To suppress byproduct formation in concentrated solutions, we have developed a protection strategy of the highly reactive formyl group in HMF with 1,3-propanediol.[55,56] Acetalization of the formyl group with 1,3-propanediol forms a six-membered ring acetal, which shows high stability against side reactions during aerobic oxidation and oxidative esterification to synthesize FDCA and its alkyl carboxylate derivatives. Such protection strategies are recently regarded to be effective for biomass conversion as biomass-derived intermediates usually have highly reactive functional groups that are easily involved in side reactions.[57–61]

Herein, we employed the acetal protection strategy for the selective production of DFF from HMF. We oxidized the acetal form of HMF with 1,3-propanediol (HMF-acetal) using carbon-, γ-Al_2O_3-, ZrO_2-, and hydrotalcite (HT)-supported Ru catalysts in DMF as a solvent, because the combination of supported Ru catalysts and DMF has been effective for selective DFF formation (> 90% selectivity) in dilute HMF solutions.[39,44,45] HMF and HMF-acetal in various concentrations (10 wt% to 70 wt%) were oxidized to clarify the effect of the acetal functionality on the product distribution. Kinetic studies were used to evaluate the electron-donating effect of the acetal functionality toward the oxidation rate for -CH_2OH by comparison with other reference furan compounds. Furthermore, a

regeneration strategy was developed for the used Ru catalyst.

2.2 Experimental

2.2.1 Materials

Ru/γ-Al_2O_3, DMF, hydrotalcite (HT), and ZrO_2 were purchased from FUJIFILM Wako Pure Chemical Corporation. HMF, 2-furoic acid, and furfural were procured from Sigma-Aldrich. DFF, FFCA, furfuryl alcohol, and FDCA were obtained from Tokyo Chemical Industry. HMFCA was purchased from Combi-Blocks Inc. Ruthenium (III) nitrosyl nitrate solution (1.5 wt% of Ru) was procured from Strem Chemicals. Aerosil-380 (SiO_2) and activated carbon (AC) were obtained from Evonik industries and Ajinomoto Fine-Techno Corporation, respectively.

2.2.2 Catalyst preparation

Ru/HT, Ru/C, Ru/SiO_2, and Ru/ZrO_2 catalysts with Ru loading of 5 wt% were prepared by incipient wetness impregnation using ruthenium (III) nitrosyl nitrate. HT, SiO_2, ZrO_2, or AC was added to an aqueous solution containing ruthenium (III) nitrosyl nitrate precursor. After stirring the mixture at room temperature and subsequent vacuum evaporation of water at 373 K, the solids recovered were dried at 393 K overnight in air and then reduced in H_2 at a flow of (10 mL min^{-1}) at 673 K for 2 h (10 K min^{-1}). Ru/γ-Al_2O_3 was used as received.

2.2.3 Synthetic procedure for HMF-acetal

In short, 5-acetoxymethyl-2-furaldehyde (2 g), indium triflate (100 mg), 1,3-

propanediol (3 mL), trimethyl orthoformate (3 mL) were added to dichloromethane (120 mL). The mixture was stirred at room temperature for 24 h and then filtrated through a short alumina plug. The residue after vacuum evaporation was mixed with an aqueous sodium carbonate (Na_2CO_3) solution (10 g Na_2CO_3 in 150 mL water and 50 mL ethanol), and the mixture was then stirred at room temperature for 6 h. Ethanol was removed by vacuum evaporation and the product in the mixture was extracted with ethyl acetate (50ml for 4 times). The crude product obtained after drying with magnesium sulfate and subsequent solvent evaporation was purified and dried overnight at room temperature under vacuum. The product was obtained as a pale-yellow oil in 92% yield with 90% purity. ^{1}H NMR spectra were recorded using an NMR spectrometer (ECX 400, JEOL Ltd.). Abbreviations used in the following represent s (singlet), d (doublet) and m (multiplet).^{1}H NMR assignment of HMF-acetal: ^{1}H NMR (400 MHz, $CDCl_3$) 6.39 (d, 1H), 6.28 (d, 1H), 5.57 (s, 1H), 4.61 (s, 2H), 4.25 (m, 2H), 3.94 (m, 2H), 2.23 (m, 1H), 1.44 (m, 1H)

2.2.4 Catalyst characterization

X-ray diffraction (XRD) patterns were obtained from an X-ray diffractometer (Rigaku, Ultima IV) using Cu Kα radiation (40 kV, 20 mA) over the 2θ range of 10°−90°. Adsorption isotherms were acquired from a Belsorp mini II (Microtrac MRB). The BET equation was used to estimate the specific surface areas (P/P_0 = 0.05−0.30). X-ray photoelectron spectroscopy (XPS) spectra were acquired using a JEOL JPC-9010MC instrument at pass energy of 20 eV using the Mg Kα line. Charge correction was based on the position of C 1s (284.6 eV). Transmission electron microscope (TEM) images were obtained using a microscope (JEM-2100F JEOL Ltd.) without metal deposition on the

sample. Possible metal leaching as a result of the alkaline washing procedure of spent catalysts was analyzed by inductively coupled plasma atomic emission spectroscopy (ICP-AES; ICPE-9000, Shimadzu). Thermogravimetric analyses (TGA) were performed on a Rigaku Thermo plus TG 8121 apparatus in the temperature range from room temperature to 1273 K at a heating rate of 10 K min^{-1} under flowing Air (50 mL min^{-1}).

2.2.5 Catalytic experiments

Catalytic activity was tested in a 10 ml SUS-316 stainless steel batch reactor equipped with a PTFE liner. 0.1-0.7 g of the substrate (HMF or HMF-acetal prepared according to a previous paper[55]), 0.3-0.9 g of DMF, and 0.1-0.7 g of the Ru catalyst were charged into the reactor, which was subsequently pressured with oxygen to 0.5 MPa and heated in an oil bath at 383 K, where substrate to catalyst (Ru) ratio on mass basis were kept constant at 20 in all reactions. After a specified reaction period, the reactor was cooled to room temperature, and products were analyzed by High-Performance Liquid Chromatography (HPLC). The quantification of HMF, DFF, FFCA, and FDCA was conducted by HPLC (SHIMADZU, Japan) consisting of a RID-10A detector, a UV-SPD-20A detector, and an Aminex HPX-87H ion column (column temp., 308 K). A diluted H_2SO_4 solution (5 mM) was used as the eluent at a flow rate of 0.5 mL min^{-1}. The retention times for furaldehyde, HMF, furoic acid, DFF, FFCA, HMFCA, FDCA, and furfuryl alcohol were 67.0, 43.3, 42.5, 54.4, 30.0, 27.0, 21.0, and 15.6 min, respectively. As reported in previous papers, HMF-acetal, DFF-acetal, or FFCA-acetal were quantitatively converted to HMF, DFF, or FFCA, respectively, during HPLC measurement.[55]

2.3 Results and discussion

2.3.1 XRD characterization

A previous study[39] reported that inert or weakly amphoteric supports are well-suited for HMF oxidation to DFF as HMF degrades rapidly in contact with strongly acidic or basic supports, and Ru/C is found to be the most optimal catalyst. In this paper, we also prepared supported Ru catalysts with inert (C and SiO_2) and amphoteric oxide (γ-Al_2O_3, HT, and ZrO_2) supports and examined them in aerobic oxidation of HMF-acetal. All supported Ru catalysts were characterized by XRD (Figure 2.1). No distinct diffraction features related to Ru were observed for Ru/γ-Al_2O_3 and Ru/C (Figures 2.1 (B), and (E)), while Ru/SiO_2, Ru/HT, and Ru/ZrO_2 exhibited broad features assignable to metallic Ru (Figures 2.1 (A), (C), and (D)).

The former samples likely contain highly dispersed and metallic Ru nanoparticles, which cannot be detected by XRD due to their small size. The average size of the metallic Ru nanoparticles in Ru/SiO_2, Ru/HT, and Ru/ZrO_2, estimated by use of the Scherrer equation (using the Ru (101) reflection), was 3.8 nm, 6.3 nm, and 12.3 nm, respectively. The original layered structure of the HT support was completely lost during the reduction step (Figure 2.1 (C)).[62] The XRD pattern of the resulting Ru/HT catalyst did not contain features associated with the original HT support, which means that the Ru nanoparticles are situated on a mixed oxide of MgO and Al_2O_3.

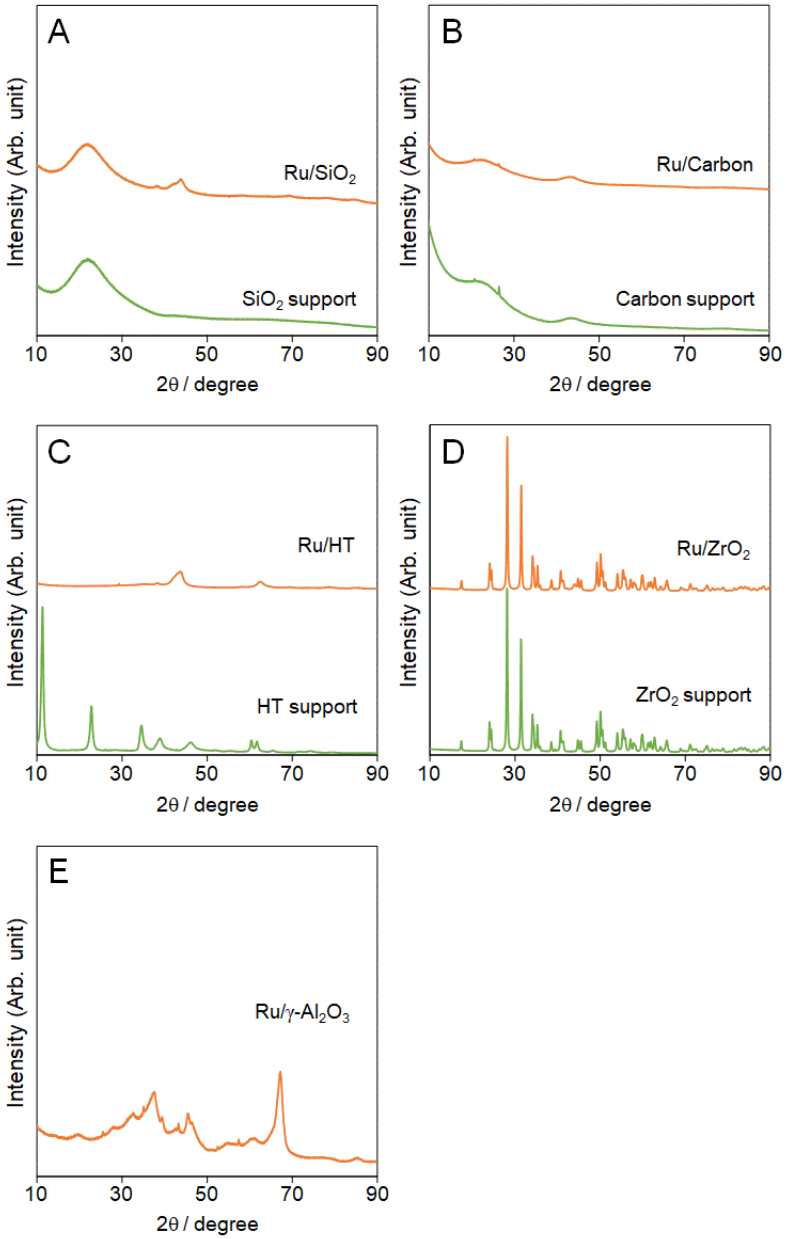

Figure 2.1. XRD patterns of supported Ru catalysts and their respective bare supports: (A) Ru/SiO_2, (B) Ru/C, (C) Ru/HT, (D) Ru/ZrO_2, and (E) commercial $Ru/\gamma\text{-}Al_2O_3$

2.3.2 Aerobic oxidation of HMF-acetal with supported Ru catalysts

$Ru/\gamma\text{-}Al_2O_3$, Ru/C, Ru/SiO_2, Ru/HT, and Ru/ZrO_2 catalysts were preliminarily examined in aerobic oxidation of the HMF-acetal using a 10 wt% HMF-acetal solution

(Figure 2.2).

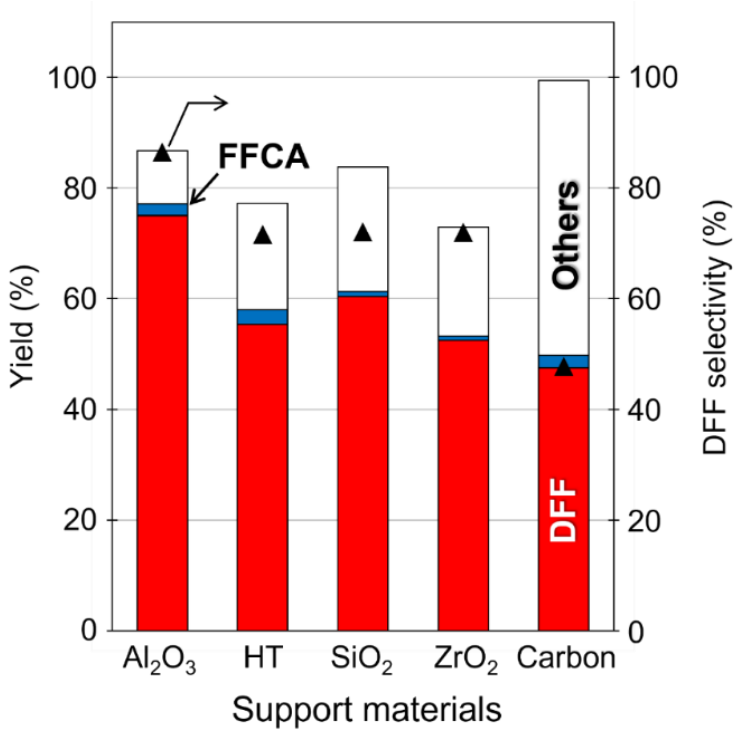

Figure 2.2. HMF-acetal oxidation with various supported Ru catalysts: HMF-acetal 0.1 g; DMF, 0.9 g; 5 wt%, Ru/support, 0.1 g (substrate to Ru ratio of 20 (wt./wt.)); oxygen pressure, 0.5 MPa; temp., 383 K; time, 300 min.

Here, Ru/γ-Al_2O_3 vastly outperformed Ru/C, which differs from the results reported by the previous study.[39] Ru/ZrO_2, Ru/SiO_2 and Ru/HT performed fairly equal in terms of DFF yield and selectivity but these three catalysts were also less active than Ru/γ-Al_2O_3. The lower activities of Ru/ZrO_2, Ru/SiO_2 and Ru/HT can instead be explained by the difference in Ru particle size. Average particle sizes of Ru/SiO_2, Ru/HT, and Ru/ZrO_2 were 3.8-12.3 nm, respectively, which were all significantly larger than that of Ru/γ-Al_2O_3. Ru/γ-Al_2O_3 was therefore selected for further optimization studies.

2.3.3 Aerobic oxidation of HMF and HMF-acetal with various concentrations

Ru/γ-Al_2O_3 was used to examine the performance in the aerobic oxidation of HMF and HMF-acetal as a function of the substrate concentration. The oxidation reaction was conducted at 383 K for 300 min in DMF under 0.5 MPa O_2 pressure with a substrate to Ru ratio of 20 wt/wt. Table 2.1 summarizes the catalytic performance data at various HMF-acetal concentrations (entries 1-4).

Table 2.1. Aerobic oxidation of HMF and HMF-acetal over supported Ru catalysts.[a]

Entry	Substrate	Concentration (wt%)	Conversion (%)	Product yield (%)			Carbon balance (%)
				DFF	FFCA	Byproducts	
1	HMF-acetal	10	90.4	77.6	2.7	10.1	89.9
2		30	95.0	79.3	2.6	13.1	86.9
3		50	94.2	84.0	2.6	7.6	92.4
4		70	96.7	53.3	1.9	41.5	58.5
5	HMF	10	96.4	52.3	15.1	29.0	71.0
6		30	93.1	53.3	14.5	25.3	74.7
7		50	91.2	21.2	6.7	63.3	36.7
8		70	99.4	4.6	0.4	94.4	5.6

[a]Reaction conditions: substrate, HMF-acetal or HMF (0.1-0.7 g); solvent, DMF (0.3-0.9 g); catalyst, Ru/γ-Al2O3 (substrate to Ru ratio of 20 (wt./wt.)); oxygen pressure, 0.5 MPa; temp., 383 K; time, 300 min.

All acetal moieties were completely removed from the reaction products (DFF-acetal and FFCA-acetal) and the substrate (HMF-acetal) during HPLC analysis involving the use of a diluted H_2SO_4 eluent.[55] However, kinetic studies in the following section, in which analysis relied on a combination of HPLC and ^{1}H NMR, revealed that deprotection of HMF-acetal under the given reaction conditions was negligible in Figure 2.3.

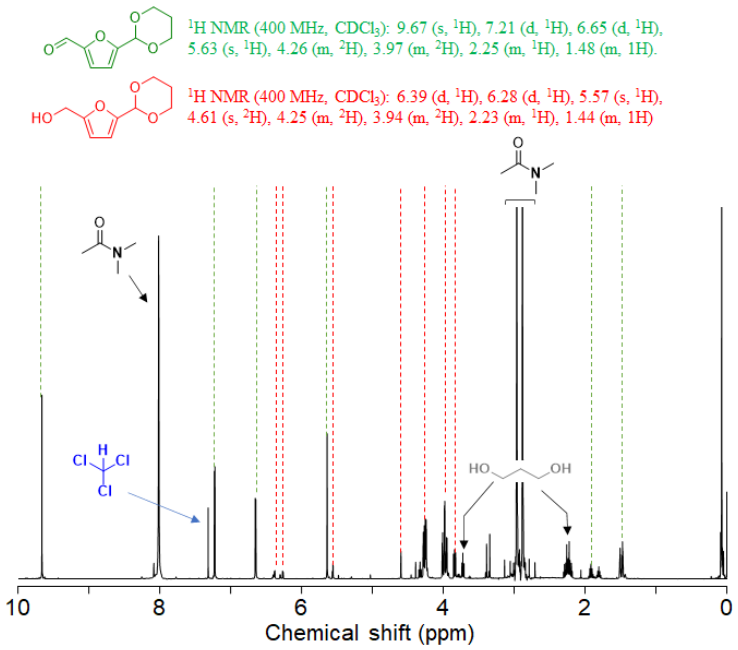

Figure 2.3. ^{1}H NMR profile of a reaction solution during HMF-acetal oxidation with Ru/γ-Al_2O_3.

This means that DFF and FFCA were only present in their acetal form during the reaction. For the sake of brevity, the yields of DFF-acetal and FFCA-acetal are nevertheless expressed as “DFF yield” and FFCA yield” in Table 2.1. The conversion values estimated by HPLC therefore reflect the HMF-acetal conversion. Ru/γ-Al_2O_3 afforded DFF in 77.6% yield at 90.4% conversion in a 10 wt% HMF-acetal solution (entry 1). FFCA was obtained as a minor product in a yield of only 2.7%, which means that the oxidation of the formyl group in DFF is effectively suppressed under the given reaction conditions, which is due to the absence of water in the reaction medium (Scheme 1.3). High DFF yields (~ 80%) could also be obtained in 30 wt% and 50 wt% solutions (entries 2 and 3). The difference between HMF-acetal conversion and the sum of identified products (DFF and FFCA) is very small in these experiments, indicating that the amount of oligomerized products that cannot be detected, was very low, even at an HMF-acetal

concentration as high as 50 wt%. However, a further increase in the HMF-acetal concentration to 70 wt% (entry 4) led to a lower DFF yield of 53.3% with a large increase in byproduct yield (41.5%). When HMF-acetal was replaced by HMF, the dependence of the product distribution on substrate concentration was very different. DFF yield was moderate (52.3%) at an HMF concentration of only 10 wt% (entry 5). The formation of FFCA in 15.1% yield and a large amount of undetectable byproducts in 29.0% yield point to substantial contributions of the over-oxidation of the formyl group in DFF and condensation reactions of HMF and DFF into oligomerized products. While similar results were obtained in a 30 wt% HMF solution (entry 6), the formation of byproducts became dominant upon a further increase of the HMF concentration, affording DFF yields of 21.2% at 50 wt% substate concentration (entry 7) and 4.6% at 70 wt% substrate concentration (entry 8). These results demonstrate that the protection of formyl moiety with 1,3-propanediol can facilitate the selective synthesis of DFF in concentrated solutions.[55] HMF-acetal provided significant advantage in DFF formation using concentrated solutions compared to HMF. However, the values of carbon balance are approximately 90% (entries 1-3), which is due to humin-type byproduct formation. Such byproducts are stabilized on the catalyst surface and influence the reusability of the Ru/Al_2O_3 catalyst.

2.3.4 Kinetic studies on aerobic oxidation of HMF and HMF-acetal

Reaction pathways for the oxidation of HMF and HMF-acetal were investigated at 383 K under 0.5 MPa O_2 atmosphere using $Ru/\gamma\text{-}Al_2O_3$ as the catalyst and a substrate concentration of 50 wt%. Figure 2.4 shows time courses for HMF conversion and product yields. Kinetic traces were fitted using pseudo-first order-reaction kinetics. HMF was

oxidized to DFF, while the further conversion of DFF to FFCA was small. The reaction rate constant for DFF formation (k_1 = 0.84 h^{-1}) is much larger than that for FFCA formation (k_2 = 0.05 h^{-1}). Oxidation of the formyl group to the carboxylic acid is largely suppressed under the given reaction conditions as evidenced by the absence of HMFCA and FDCA as well as by the very small amount of FFCA formed (see Scheme 1.3). The high selectivity to DFF can be explained by the aprotic nature of the DMF solvent, which prevents the hydration of the aldehyde moiety to the geminal diol intermediate prior to its oxidation to the corresponding carboxylic acid (Scheme 1.3).[63] The DFF yield reached a maximum after 60 min and then decreased gradually with time, accompanied by increasing levels of oligomerized byproducts. Fitting of the kinetic traces suggests that these byproducts are formed from both HMF and DFF with similar reaction rate constants, i.e., 0.30 h^{-1} (k_3) and 0.24 h^{-1} (k_4), respectively.

Byproduct formation in HMF oxidation was further evaluated by carrying out two control experiments (Table 2.2). The reactions were conducted at 383 K for 30 min in the presence of Ru/γ-Al_2O_3 in an inert atmosphere (0.5 MPa N_2) using either a 50 wt% HMF solution or a 50 wt% DFF solution. Approximately 60% of HMF was converted to undetectable byproduct through non-oxidative side reactions (Table 2.2, entry 1). In contrast, DFF loss under the same reaction conditions was limited to 18.8% (Table 2.2, entry 2), despite there being no large difference between the rate constants for byproduct formation from HMF and DFF (i.e., k_3 and k_4 in aerobic HMF oxidation, Figure 2.4).

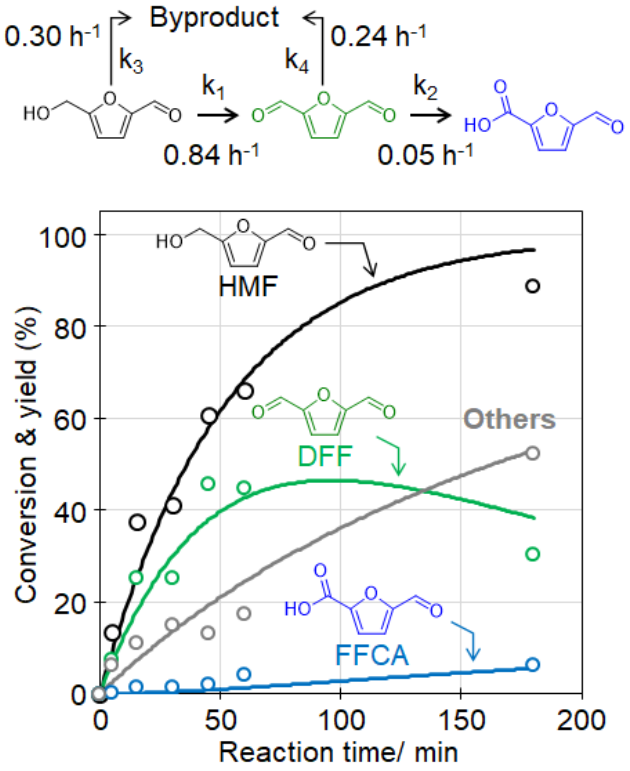

Figure 2.4. Time course for DFF formation from HMF: HMF 0.5 g; DMF, 0.5 g; Ru/γ-Al_2O_3 catalysts, 0.5 g (substrate to Ru ratio of 20 (wt./wt.)); oxygen pressure, 0.5 MPa; temp., 383 K.

Table 2.2. Non-catalytic degradation of HMF, HMF-acetal, DFF, and DFF-acetal in the absence of oxidant under the reaction conditions.[a]

Entry	Substrate	Conversion (%)	Byproduct yield (%)
1	HMF	60.3	60.1
2	DFF	18.8	18.5
3	HMF-acetal	1.9	1.5
4	DFF-acetal	1.2	0.8

[a]Reaction conditions: substrate, 0.5 g; DMF, 0.5 g; catalyst, Ru/γ-Al_2O_3 0.5 g (Substrate to Ru ratio of 20 (wt./wt.)); nitrogen pressure, 0.5 MPa; temp., 383 K; time, 30 min.

These results imply that DFF degradation is more pronounced under oxidative

reaction conditions or in the presence of HMF. Figure 2.5 shows time courses for HMF-acetal conversion and product yields, in which kinetic traces were also fitted using pseudo-first order-reaction kinetics. Quantitative analysis using ^{1}H NMR demonstrated that HMF and DFF are present in the acetal form in all reaction mixtures (Figure 2.3). HMF-acetal conversion and DFF-acetal yield continuously increased with time and reached 81.3% and 73.5% at 60 min and 93.0% and 84.2% at 180 min, respectively. Byproduct formation mainly took place in the initial stage of the reaction (8.8% yield at 30 min) and did not change much afterwards. Oxidation of the formyl group in DFF-acetal hardly proceeded as evident from the small reaction rate constant for FFCA-acetal formation (k_6 = 0.006 h^{-1}), which is an order of magnitude lower than that for FFCA formation in HMF oxidation (k_2 = 0.05 h^{-1}). The acetal moieties in HMF-acetal and DFF-acetal effectively prevent undesired side reactions that lead to condensed products. DFF-acetal was fully retained in the reaction mixture, whereas degradation of free DFF occurred in HMF oxidation (k_4 = 0.24 h^{-1} in Figure 2.4).

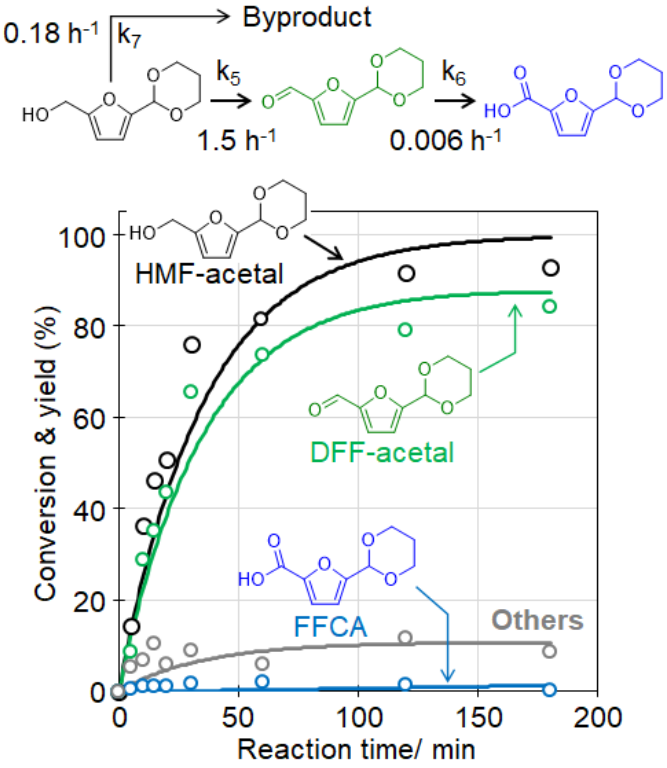

Figure 2.5. Time course for DFF-acetal formation from HMF-acetal: HMF-acetal 0.5 g; DMF, 0.5 g; Ru/γ-Al_2O_3 catalysts, 0.5 g (Substrate to Ru ratio of 20 (wt./wt.)); oxygen pressure, 0.5 MPa; temp., 383 K

Byproduct formation from HMF-acetal (k_7 = 0.18 h^{-1}) is approximately half that from HMF (k_3 = 0.30 h^{-1}). Thermal degradation of HMF-acetal and DFF-acetal was also evaluated under an inert atmosphere (Table 2.2). When the same reactions in entries 1 and 2 of Table 2.2 were conducted using HMF-acetal and DFF-acetal, both showed very low conversion (< 2%) and minor levels of degradation (entries 3 and 4). It should be noted that the rate constant for DFF-acetal formation (k_5 = 1.5 h^{-1}, Figure 2.5) is approximately two times higher than that of DFF formation (k_1 = 0.84 h^{-1}, Figure 2.4). Such a large difference can explain the efficient production of DFF-acetal in the aerobic oxidation of HMF-acetal. To understand the increase in the reaction rate constant for the

oxidation of -CH_2OH to -CHO in the presence of the acetal functional group, we selected two additional substrates, namely HMFCA and furfuryl alcohol. We compared the effect of the functional group (carboxylic acid in HMFCA, hydrogen in furfuryl alcohol, formyl group in HMF, and six-membered acetal group in HMF-acetal) against aerobic oxidation of the hydroxymethyl group over Ru/γ-Al_2O_3 (Figures 2.4, 2.5, 2.6, and 2.7).

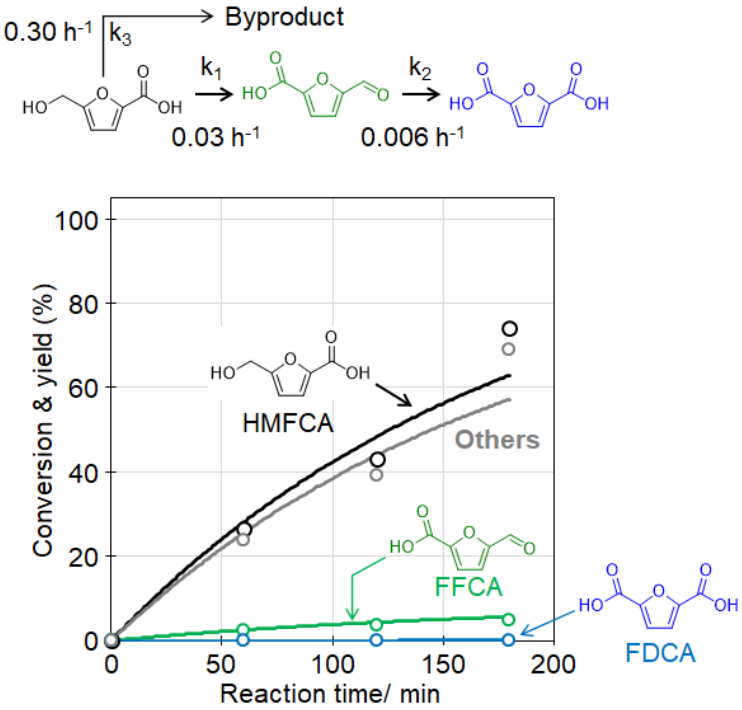

Figure 2.6. Time course for aerobic oxidation of HMFCA over Ru/γ-Al_2O_3: Reaction conditions: HMFCA 0.5 g; DMF, 0.5 g; Ru/γ-Al_2O_3 catalysts, 0.5 g (Substrate to Ru ratio of 20 (wt./wt.)); oxygen pressure, 0.5 MPa; temp., 383 K.

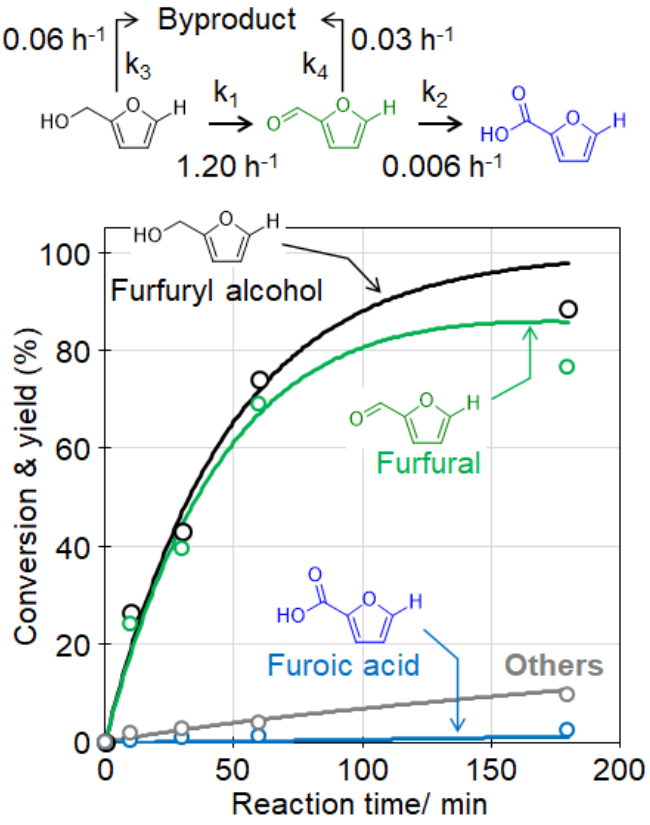

Figure 2.7. Time course for aerobic oxidation of furfuryl alcohol (FA) over Ru/γ-Al_2O_3: Reaction conditions: FA 0.5 g; DMF, 0.5 g; Ru/γ-Al_2O_3 catalysts, 0.5 g (Substrate to Ru ratio of 20 (wt./wt.)); oxygen pressure, 0.5 MPa; temp., 383 K.

Figure 2.8 summarizes rate constants for a series of substrates. The rate constant for HMF-acetal oxidation is larger (1.5 h^{-1}) compared to oxidation rate constants for furfuryl alcohol (1.2 h^{-1}), HMF (0.84 h^{-1}), and HMFCA (0.03 h^{-1}). There is a correlation between the rate constant and the electron-donating/-withdrawing nature of the functional group. The rate constants were relatively large for the electron-donating acetal functional group in the HMF-acetal. The rate constants decreased with increasing electron-withdrawing character of the functional group (electron-withdrawing property: -COOH in HMFCA > -CHO in HMF > -H in furfuryl alcohol). The presence of electron-donating

group most probably facilitated the dissociation of OH and/or CH bonds in -CH_2OH attached to furan ring and enhanced efficient aerobic oxidation to formyl group. A similar effect was observed for the photo-oxidation of substituted benzyl alcohols to benzaldehyde.[64] In sharp contrast to alcohol oxidation (-CH_2OH), similar reaction rate constants were obtained for aldehyde oxidation to carboxylic acid in three substrates (HMF-acetal, $k_6 = 0.006\ h^{-1}$ in Figure 2.5; HMFCA, $k_2 = 0.006\ h^{-1}$ in Figure 2.6; furfuryl alcohol, $k_2 = 0.006\ h^{-1}$ in Figure 2.7), suggesting no influence of the type of functional group on the reaction rate constant. The formation of carboxylic acid from aldehyde under the reaction conditions requires water to produce geminal diol intermediate as shown in Scheme 1.3.

All oxidation reactions were conducted in non-aqueous solutions, which successfully suppressed undesirable oxidation to the carboxylic acid. Aldehyde oxidation to carboxylic acid forming FFCA (Figure 2.4) is also nearly absent during HMF oxidation, but its rate constant ($k_2 = 0.05\ h^{-1}$) is an order of magnitude higher than for the other three substrates. Relatively large reaction rate constant in HMF oxidation is maybe attributed to water formation in pronounced side reactions leading to the formation of undesirable carboxylic acid by the oxidation of geminal diol intermediate as shown in Scheme 1.3.

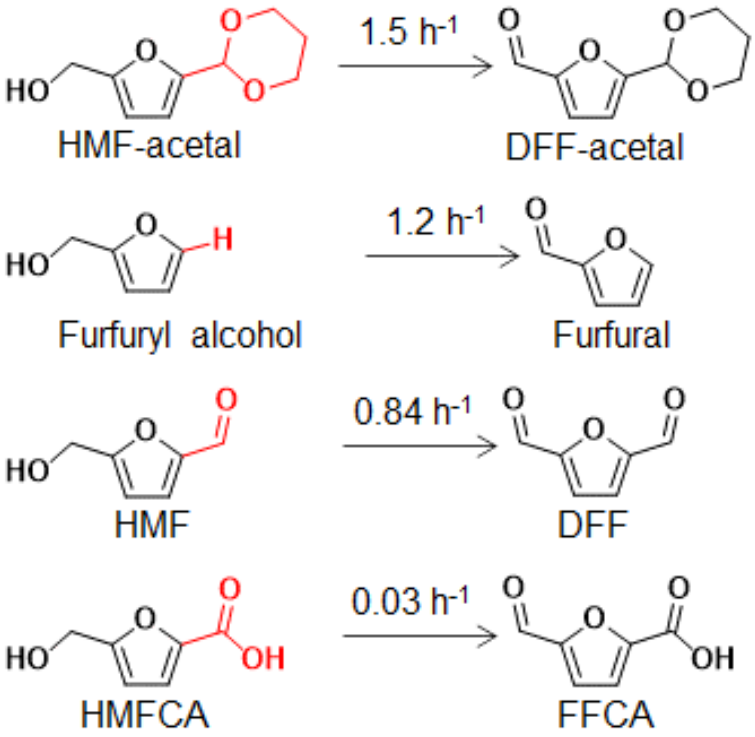

Figure 2.8. Rate constants for HMF-acetal and reference compounds (furfuryl alcohol, HMF, and HMFCA) in aerobic oxidation: substrate, 0.5 g; DMF, 0.5 g; Ru/γ-Al_2O_3 catalysts, 0.5 g (substrate to Ru ratio of 20 (wt./wt.)); oxygen pressure, 0.5 MPa; temp., 383 K.

2.3.5 Catalyst regeneration

The regeneration of Ru/γ-Al_2O_3 was investigated in the oxidation of HMF-acetal using concentrated solutions (50 wt%), where all reactions were conducted at 383 K for 60 min under 0.5 MPa O_2. After the reaction, the catalyst was recovered by filtration, washed with water (approximately 50 mL), dried at 373 K in air overnight, and then used again in the same reaction (Figure 2.9A).

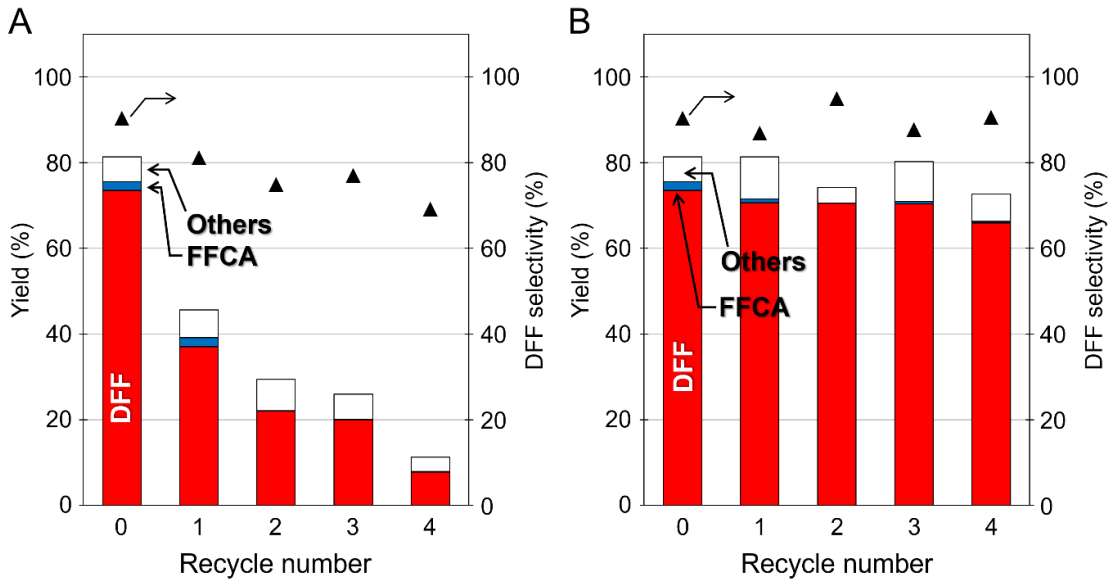

Figure 2.9. Recyclability of Ru/γ-Al_2O_3 catalyst in aerobic oxidation of HMF-acetal using 50 wt% solutions: (A) washing with water and (B) sonication in aqueous NaOH (pH = 12) solution. Reaction conditions: HMF-acetal 0.5 g; DMF, 0.5 g; Ru/γ-Al_2O_3 catalysts, 0.5 g (Substrate to Ru ratio of 20 (wt./wt.)); oxygen pressure, 0.5 MPa; temp., 383 K; time, 60 min.

The DFF- acetal yield decreased from 73.5% to 37.0% in the second run and further to 7.8% in the fifth run. The XRD patterns of fresh and used Ru/γ-Al_2O_3 were similar (Figure 2.10 (a) and (b)), implying that catalyst deactivation is not caused by Ru particle growth.

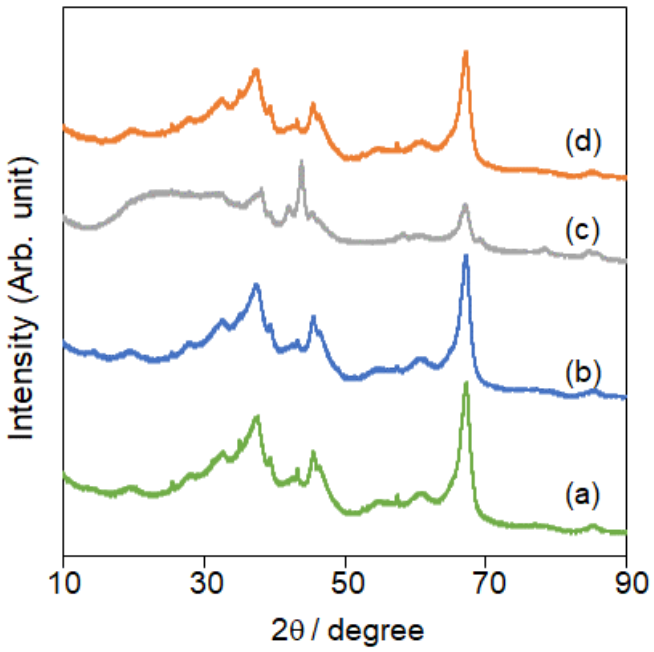

Figure 2.10. XRD patterns of (a) fresh Ru/γ-Al_2O_3 and (b, c, d) spent Ru/γ-Al_2O_3. (b) After every reaction, the spent catalyst was recovered by filtration, washed with water (50 mL), and used again for subsequent reactions. The profiles (b) and (c) are obtained from the spent catalyst after fifth run and subsequent water-washing treatment or calcination (773 K for 2 h in air) and subsequent reduction (673 K for 2 h in an H_2 flow with a flow rate of 10 mL min^{-1}) treatment, respectively. (d) After every reaction, the spent catalyst was recovered by filtration, sonicated in aqueous NaOH solution (pH=12, 50 mL), and used again for subsequent reactions. This profile is obtained from the spent catalyst after sonication with NaOH solutions.

It is more likely that deposition of humins blocks part of the surface [45,65] Humin build-up was confirmed by TG-DTA analysis of the used Ru/γ-Al_2O_3, which exhibits a weight loss of approximately 15% in the 423-673 K range (Figure 2.11(B)).

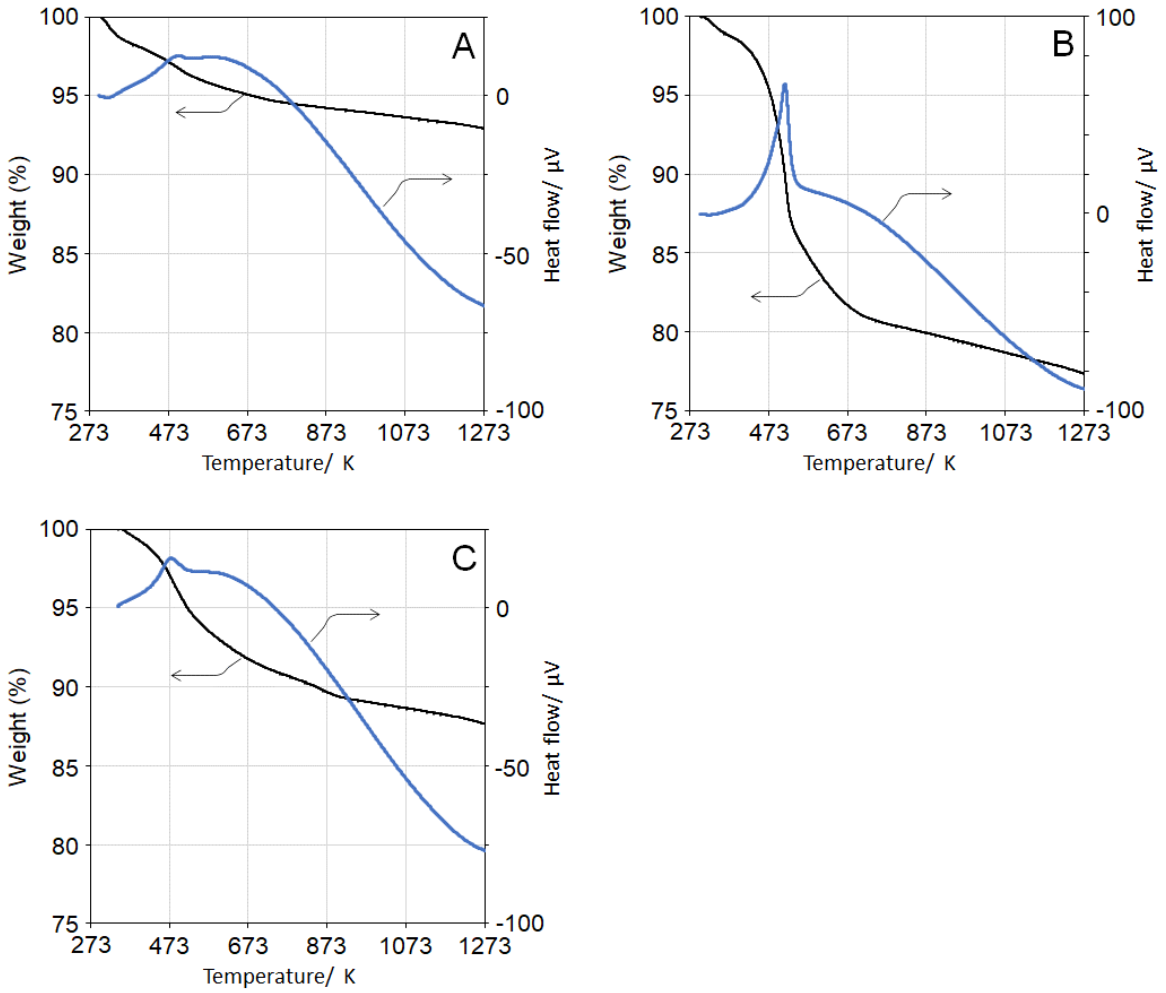

Figure 2.11. TG-DTA profiles of (A) fresh Ru/γ-Al_2O_3 catalyst, (B) spent Ru/γ-Al_2O_3 after simple water-washing treatment, and (C) spent Ru/γ-Al_2O_3 after sonication in aqueous NaOH solution. Post-treatments for the spent catalysts were conducted after every reaction.

The used catalyst after the fourth reuse was calcined at 773 K for 2 h in air to remove the deposits and reduced at 673 K for 2 h in an H_2 flow (10 mL min^{-1}). This treatment was not effective for the recovery of the original activity. The thus-regenerated catalyst gave a DFF yield of only 5.5% at a conversion of 23.8% in the sixth run under the same reaction conditions. XRD showed that the calcination-reduction treatment leads to growth

of Ru nanoparticles (Figure 2.10(c)), which results in the production of large amounts of undetectable byproduct (18.2%). Washing with organic solvent mixtures containing acetone, ethanol and toluene was equally ineffective in removing the humin depositions and recovering original activity (Table 2.3).

Table 2.3 Recyclability of Ru/γ-Al_2O_3 catalyst washing with different organic solvents

#	Washing solvent	Recycle	Con. (%)	Product yields (%)		
				DFF	FFCA	Byproducts
1	None	0	81.3	73.5	2.0	5.8
2	Acetone and toluene	1	77.7	31.0	0.0	46.7
3	Acetone, toluene, and ethanol	1	65.8	26.0	0.2	39.6

Reaction conditions**:** HMF-acetal 0.5 g; DMF, 0.5 g; Ru/γ-Al_2O_3 catalyst, 0.5 g (Substrate to Ru ratio of 20 (wt./wt.)); oxygen pressure, 0.5 MPa; temp., 383 K; time, 60 min.

Sonication in NaOH solution was therefore adopted to remove organic deposits from the surface of Ru nanoparticles.[45] The used catalyst was dispersed in an aqueous NaOH solution (pH = 12, 50 mL) and sonicated at room temperature for 10 min. This treatment was repeated three times with refreshing the solution at every cycle. After the final step, the catalyst was recovered by filtration, washed with water, dried in an oven overnight, and then used again in the DFF-acetal oxidation reaction. Figure 2.11B shows the catalytic activity of fresh and regenerated Ru/γ-Al_2O_3 catalysts. The HMF-acetal conversion of 70–80% and DFF-acetal selectivity of approximately 80% were maintained for five cycles. We also characterized the 4-times reused Ru/γ-Al_2O_3 catalyst after regeneration by TG-DTA, XRD, TEM, and XPS. The TG-DTA profile of the used catalyst in Figure 2.11(C) is similar to that of the fresh catalyst in Figure 2.11(A), showing that the NaOH treatment is effective in removing organic deposits. The XRD patterns of fresh and used-generated catalysts in Figure 2.10 (a) and (d) demonstrate that the NaOH

treatment did not lead to Ru nanoparticle growth. This finding is also corroborated by TEM analysis of fresh and used catalysts, showing a predominance of 1-2 nm sized Ru nanoparticles in both catalysts (Figure 2.12).

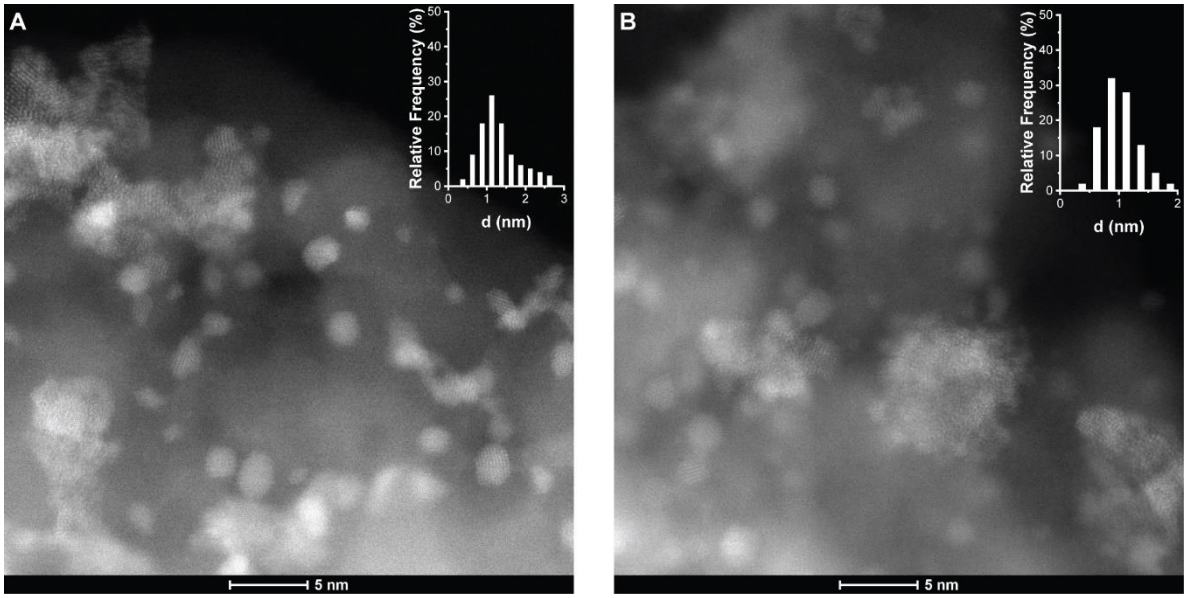

Figure 2.12. TEM images of (A) fresh Ru/γ-Al_2O_3 and (B) spent Ru/γ-Al_2O_3 after fourth reuse. The spent catalyst was recovered by filtration and regenerated after every reaction by the repeated sonication in NaOH solutions.

The oxidation state of Ru nanoparticle for fresh and used catalysts was investigated by XPS (Figure 2.13). There was no significant difference in the ratio of metallic Ru and oxidized Ru (Ru^{n+}) between fresh and used catalysts (Table 2.4).

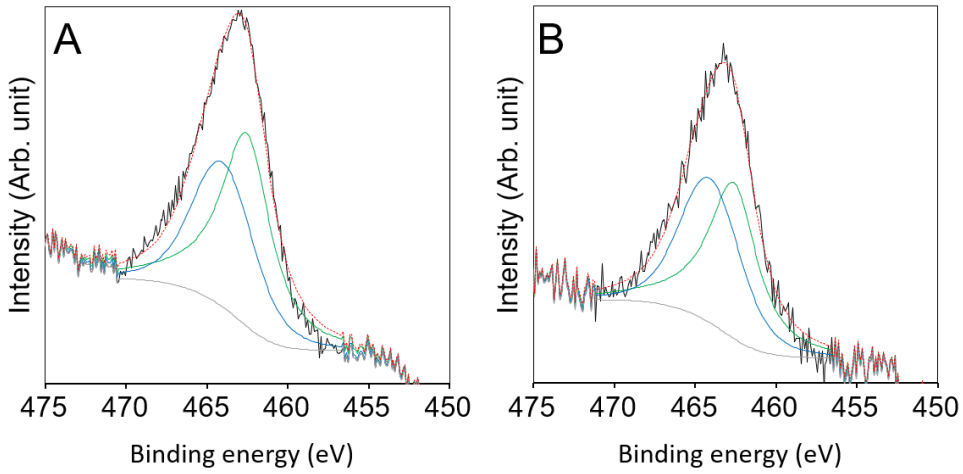

Figure 2.13. Ru 3p XPS spectra of (A) fresh Ru/γ-Al_2O_3 and (B) spent Ru/γ-Al_2O_3 after fourth reuse. The spent catalyst was recovered by filtration and regenerated after every reaction by the repeated sonication in NaOH solutions.

Table 2.4. Summary for Ru 3p XPS data of fresh and spent Ru/γ-Al_2O_3 catalysts

Catalyst	Reuse number	Regeneration conditions	Ru^0		Ru^{n+}	
			eV	at%	eV	at%
Fresh Ru/γ-Al_2O_3	-	Fresh (A)	462.5	56.32	464.0	43.68
Spent Ru/γ-Al_2O_3	5	Sonication (NaOH solutions)	462.5	51.02	464.0	48.98

Finally, leaching of oxidized Ru species during the regeneration treatment using NaOH solutions was evaluated by ICP-AES analysis. NaOH solutions after sonication with the used catalyst contained only trace level of Ru (~0.005%), demonstrating that leaching of the supported Ru nanoparticles is nearly negligible. All these results evidence that aerobic oxidation of HMF-acetal with 1,3-propanediol using Ru/γ-Al_2O_3 is a

promising strategy for the efficient and scalable production of DFF in excellent yields using concentrated solutions.

2.4 Conclusion

A facile reaction system to produce DFF from HMF was developed using concentrated HMF-acetal solutions and a Ru/γ-Al_2O_3 catalyst. Acetal protection of the formyl group in HMF prevents side reactions in concentrated solutions during aerobic oxidation. Under optimized conditions, HMF-acetal was oxidized at a concentration of 50 wt% in DMF using Ru/γ-Al_2O_3 at an HMF-acetal/Ru mass ratio of 20 at 383 K under 0.5 MPa O_2 pressure. After 5 h, a high DFF yield of 84.0% was obtained. Under comparable conditions, oxidation of HMF yielded only 21.2% of DFF. Deposition of humin-type organic compounds during the reactions resulted in a substantial decrease of the original activity of Ru/γ-Al_2O_3 in reuse experiments. Sonication of the used catalyst in NaOH solution removed the deposits and fully recovered the activity, allowing efficient regeneration for at least 4 times without significant loss of activity. DFF production using concentrated solutions in this study is significantly distinct from those in previous reports in terms of productivity as well as the energy consumption for the work-up process. The benefits of working with concentration substrate concentrations are a smaller reactor size and lower energy cost for recycling the organic solvent by evaporation and distillation. Thus, a novel chemocatalytic route to DFF, which is a precursor to building blocks for polyamides and polyesters, has been developed.

2.5 References

(1) Chheda, J. N.; Huber, G. W.; Dumesic, J. A. Liquid-Phase Catalytic Processing of Biomass-Derived Oxygenated Hydrocarbons to Fuels and Chemicals. *Angew. Chem. Int. Ed.* **2007**, *46* (38), 7164–7183. https://doi.org/10.1002/anie.200604274.

(2) Bozell, J. J.; Petersen, G. R. Technology Development for the Production of Biobased Products from Biorefinery Carbohydrates—the US Department of Energy's "Top 10" Revisited. *Green Chem.* **2010**, *12* (4), 539–555. https://doi.org/10.1039/b922014c.

(3) Huber, G. W.; Iborra, S.; Corma, A. Synthesis of Transportation Fuels from Biomass: Chemistry, Catalysts, and Engineering. *Chem. Rev.* **2006**, *106* (9), 4044–4098. https://doi.org/10.1021/cr068360d.

(4) Corma Canos, A.; Iborra, S.; Velty, A. Chemical Routes for the Transformation of Biomass into Chemicals. *Chem. Rev.* **2007**, *107* (6), 2411–2502. https://doi.org/10.1021/cr050989d.

(5) Delidovich, I.; Hausoul, P. J. C.; Deng, L.; Pfützenreuter, R.; Rose, M.; Palkovits, R. Alternative Monomers Based on Lignocellulose and Their Use for Polymer Production. *Chem. Rev.* **2016**, *116* (3), 1540–1599. https://doi.org/10.1021/acs.chemrev.5b00354.

(6) Li, C.; Zhao, X.; Wang, A.; Huber, G. W.; Zhang, T. Catalytic Transformation of Lignin for the Production of Chemicals and Fuels. *Chem. Rev.* **2015**, *115* (21), 11559–11624. https://doi.org/10.1021/acs.chemrev.5b00155.

(7) Isikgor, F. H.; Becer, C. R. Lignocellulosic Biomass: A Sustainable Platform for the Production of Bio-Based Chemicals and Polymers. *Polym. Chem.* **2015**, *6* (25), 4497–4559. https://doi.org/10.1039/c5py00263j.

(8) Zhao, H.; Holladay, J. E.; Brown, H.; Zhang, Z. C. Metal Chlorides in Ionic Liquid Solvents Convert Sugars to 5-Hydroxymethylfurfural. *Science.* **2007**, *316* (5831), 1597–1600. https://doi.org/10.1126/science.1141199.

(9) Pidko, E. A.; Degirmenci, V.; Van Santen, R. A.; Hensen, E. J. M. Glucose Activation by Transient Cr^{2+} Dimers. *Angew. Chem. Int. Ed.* **2010**, *49* (14), 2530–2534. https://doi.org/10.1002/anie.201000250.

(10) Nikolla, E.; Román-Leshkov, Y.; Moliner, M.; Davis, M. E. "One-Pot" Synthesis of 5-(Hydroxymethyl)Furfural from Carbohydrates Using Tin-Beta Zeolite. *ACS Catal.* **2011**, *1* (4), 408–410. https://doi.org/10.1021/cs2000544.

(11) Nakajima, K.; Baba, Y.; Noma, R.; Kitano, M.; N. Kondo, J.; Hayashi, S.; Hara, M. Nb_2O_5•nH_2O as a Heterogeneous Catalyst with Water-Tolerant Lewis Acid Sites. *J. Am. Chem. Soc.* **2011**, *133* (12), 4224–4227. https://doi.org/10.1021/ja110482r.

(12) Noma, R.; Nakajima, K.; Kamata, K.; Kitano, M.; Hayashi, S.; Hara, M. Formation of 5-(Hydroxymethyl)Furfural by Stepwise Dehydration over TiO_2 with Water-Tolerant Lewis Acid Sites. *J. Phys. Chem. C* **2015**, *119* (30), 17117–17125. https://doi.org/10.1021/acs.jpcc.5b03290.

(13) Yue, C.; Li, G.; Pidko, E. A.; Wiesfeld, J. J.; Rigutto, M.; Hensen, E. J. M. Dehydration of Glucose to 5-Hydroxymethylfurfural Using Nb-Doped Tungstite.

ChemSusChem **2016**, *9* (17), 2421–2429. https://doi.org/10.1002/cssc.201600649.

(14) Li, G.; Pidko, E. A.; Hensen, E. J. M.; Nakajima, K. A Density Functional Theory Study of the Mechanism of Direct Glucose Dehydration to 5-Hydroxymethylfurfural on Anatase Titania. *ChemCatChem* **2018**, *10* (18), 4084–4089. https://doi.org/10.1002/cctc.201800900.

(15) Casanova, O.; Iborra, S.; Corma, A. Biomass into Chemicals: Aerobic Oxidation of 5-Hydroxymethyl-2-Furfural into 2,5-Furandicarboxylic Acid with Gold Nanoparticle Catalysts. *ChemSusChem* **2009**, *2* (12), 1138–1144. https://doi.org/10.1002/cssc.200900137.

(16) Casanova, O.; Iborra, S.; Corma, A. Biomass into Chemicals: One Pot-Base Free Oxidative Esterification of 5-Hydroxymethyl-2-Furfural into 2,5-Dimethylfuroate with Gold on Nanoparticulated Ceria. *J. Catal.* **2009**, *265* (1), 109–116. https://doi.org/10.1016/j.jcat.2009.04.019.

(17) Gupta, N. K.; Nishimura, S.; Takagaki, A.; Ebitani, K. Hydrotalcite-Supported Gold-Nanoparticle-Catalyzed Highly Efficient Base-Free Aqueous Oxidation of 5-Hydroxymethylfurfural into 2,5-Furandicarboxylic Acid under Atmospheric Oxygen Pressure. *Green Chem.* **2011**, *13* (4), 824–827. https://doi.org/10.1039/c0gc00911c.

(18) Sajid, M.; Zhao, X.; Liu, D. Production of 2,5-Furandicarboxylic Acid (FDCA) from 5-Hydroxymethylfurfural (HMF): Recent Progress Focusing on the Chemical-Catalytic Routes. *Green Chem.* **2018**, *20* (24), 5427–5453.

https://doi.org/10.1039/c8gc02680g.

(19) Hayashi, E.; Yamaguchi, Y.; Kamata, K.; Tsunoda, N.; Kumagai, Y.; Oba, F.; Hara, M. Effect of MnO_2 Crystal Structure on Aerobic Oxidation of 5-Hydroxymethylfurfural to 2,5-Furandicarboxylic Acid. *J. Am. Chem. Soc.* **2019**, *141* (2), 899–900. https://doi.org/10.1021/jacs.8b09917.

(20) Takeda, Y.; Tamura, M.; Nakagawa, Y.; Okumura, K.; Tomishige, K. Hydrogenation of Dicarboxylic Acids to Diols over Re-Pd Catalysts. *Catal. Sci. Technol.* **2016**, *6* (14), 5668–5683. https://doi.org/10.1039/c6cy00335d.

(21) Tamura, M.; Tokonami, K.; Nakagawa, Y.; Tomishige, K. Rapid Synthesis of Unsaturated Alcohols under Mild Conditions by Highly Selective Hydrogenation. *Chem. Commun.* **2013**, *49* (63), 7034–7036. https://doi.org/10.1039/c3cc41526k.

(22) Thompson, S. T.; Lamb, H. H. Palladium-Rhenium Catalysts for Selective Hydrogenation of Furfural: Evidence for an Optimum Surface Composition. *ACS Catal.* **2016**, *6* (11), 7438–7447. https://doi.org/10.1021/acscatal.6b01398.

(23) Wiesfeld, J. J.; Kim, M.; Nakajima, K.; Hensen, E. J. M. Selective Hydrogenation of 5-Hydroxymethylfurfural and Its Acetal with 1,3-Propanediol to 2,5-Bis(Hydroxymethyl)Furan Using Supported Rhenium-Promoted Nickel Catalysts in Water. *Green Chem.* **2020**, *22* (4), 1229–1238. https://doi.org/10.1039/c9gc03856f.

(24) Buntara, T.; Noel, S.; Phua, P. H.; Melián-Cabrera, I.; De Vries, J. G.; Heeres, H. J. Caprolactam from Renewable Resources: Catalytic Conversion of 5-Hydroxymethylfurfural into Caprolactone. *Angew. Chem. Int. Ed.* **2011**, *50* (31),

7083–7087. https://doi.org/10.1002/anie.201102156.

(25) Kong, X.; Zheng, R.; Zhu, Y.; Ding, G.; Zhu, Y.; Li, Y. W. Rational Design of Ni-Based Catalysts Derived from Hydrotalcite for Selective Hydrogenation of 5-Hydroxymethylfurfural. *Green Chem.* **2015**, *17* (4), 2504–2514. https://doi.org/10.1039/c5gc00062a.

(26) Chen, J.; Liu, R.; Guo, Y.; Chen, L.; Gao, H. Selective Hydrogenation of Biomass-Based 5-Hydroxymethylfurfural over Catalyst of Palladium Immobilized on Amine-Functionalized Metal-Organic Frameworks. *ACS Catal.* **2015**, *5* (2), 722–733. https://doi.org/10.1021/cs5012926.

(27) Nakagawa, Y.; Takada, K.; Tamura, M.; Tomishige, K. Total Hydrogenation of Furfural and 5-Hydroxymethylfurfural over Supported Pd-Ir Alloy Catalyst. *ACS Catal.* **2014**, *4* (8), 2718–2726. https://doi.org/10.1021/cs500620b.

(28) Nakagawa, Y.; Tomishige, K. Total Hydrogenation of Furan Derivatives over Silica-Supported Ni-Pd Alloy Catalyst. *Catal. Commun.* **2010**, *12* (3), 154–156. https://doi.org/10.1016/j.catcom.2010.09.003.

(29) Yao, S.; Wang, X.; Jiang, Y.; Wu, F.; Chen, X.; Mu, X. One-Step Conversion of Biomass-Derived 5-Hydroxymethylfurfural to 1,2,6-Hexanetriol over Ni-Co-Al Mixed Oxide Catalysts under Mild Conditions. *ACS Sustain. Chem. Eng.* **2014**, *2* (2), 173–180. https://doi.org/10.1021/sc4003714.

(30) Buntara, T.; Melián-Cabrera, I.; Tan, Q.; Fierro, J. L. G.; Neurock, M.; De Vries, J. G.; Heeres, H. J. Catalyst Studies on the Ring Opening of Tetrahydrofuran-Dimethanol to 1,2,6-Hexanetriol. *Catal. Today* **2013**, *210*, 106–116.

https://doi.org/10.1016/j.cattod.2013.04.012.

(31) Gilkey, M. J.; Mironenko, A. V.; Yang, L.; Vlachos, D. G.; Xu, B. Insights into the Ring-Opening of Biomass-Derived Furanics over Carbon-Supported Ruthenium. *ChemSusChem* **2016**, *9* (21), 3113–3121. https://doi.org/10.1002/cssc.201600681.

(32) Pingen, D.; Schwaderer, J. B.; Walter, J.; Wen, J.; Murray, G.; Vogt, D.; Mecking, S. Diamines for Polymer Materials via Direct Amination of Lipid- and Lignocellulose-Based Alcohols with NH_3. *ChemCatChem* **2018**, *10* (14), 3027–3033. https://doi.org/10.1002/cctc.201800365.

(33) Xu, Y.; Jia, X.; Ma, J.; Gao, J.; Xia, F.; Li, X.; Xu, J. Selective Synthesis of 2,5-Bis(Aminomethyl)Furan: Via Enhancing the Catalytic Dehydration-Hydrogenation of 2,5-Diformylfuran Dioxime. *Green Chem.* **2018**, *20* (12), 2697–2701. https://doi.org/10.1039/c8gc00947c.

(34) Zhou, K.; Liu, H.; Shu, H.; Xiao, S.; Guo, D.; Liu, Y.; Wei, Z.; Li, X. A Comprehensive Study on the Reductive Amination of 5-Hydroxymethylfurfural into 2,5-Bisaminomethylfuran over Raney Ni Through DFT Calculations. *ChemCatChem* **2019**, *11* (11), 2649–2656. https://doi.org/10.1002/cctc.201900304.

(35) Liang, G.; Wang, A.; Li, L.; Xu, G.; Yan, N.; Zhang, T. Production of Primary Amines by Reductive Amination of Biomass-Derived Aldehydes/Ketones. *Angew. Chem. Int. Ed.* **2017**, *56* (11), 3050–3054. https://doi.org/10.1002/anie.201610964.

(36) Qi, H.; Liu, F.; Zhang, L.; Li, L.; Su, Y.; Yang, J.; Hao, R.; Wang, A.; Zhang, T. Modulating: Trans -Imination and Hydrogenation towards the Highly Selective Production of Primary Diamines from Dialdehydes. *Green Chem.* **2020**, *22* (20), 6897–6901. https://doi.org/10.1039/d0gc02280b.

(37) García, J. M.; García, F. C.; Serna, F.; de la Peña, J. L. High-Performance Aromatic Polyamides. *Prog. Polym. Sci.* **2010**, *35* (5), 623–686. https://doi.org/10.1016/J.PROGPOLYMSCI.2009.09.002.

(38) Winnacker, M.; Rieger, B. Biobased Polyamides: Recent Advances in Basic and Applied Research. *Macromol. Rapid Commun.* **2016**, *37* (17), 1391–1413. https://doi.org/10.1002/marc.201600181.

(39) Nie, J.; Xie, J.; Liu, H. Efficient Aerobic Oxidation of 5-Hydroxymethylfurfural to 2,5-Diformylfuran on Supported Ru Catalysts. *J. Catal.* **2013**, *301*, 83–91. https://doi.org/10.1016/j.jcat.2013.01.007.

(40) Davis, S. E.; Houk, L. R.; Tamargo, E. C.; Datye, A. K.; Davis, R. J. Oxidation of 5-Hydroxymethylfurfural over Supported Pt, Pd and Au Catalysts. *Catal. Today* **2011**, *160* (1), 55–60. https://doi.org/10.1016/j.cattod.2010.06.004.

(41) Zhu, Y.; Shen, M.; Xia, Y.; Lu, M. Au/MnO2 Nanostructured Catalysts and Their Catalytic Performance for the Oxidation of 5-(Hydroxymethyl)Furfural. *Catal. Commun.* **2015**, *64*, 37–43. https://doi.org/10.1016/j.catcom.2015.01.031.

(42) Zhang, Z.; Yuan, Z.; Tang, D.; Ren, Y.; Lv, K.; Liu, B. Iron Oxide Encapsulated by Ruthenium Hydroxyapatite as Heterogeneous Catalyst for the Synthesis of 2,5-Diformylfuran. *ChemSusChem* **2014**, *7* (12), 3496–3504.

https://doi.org/10.1002/cssc.201402402.

(43) Mishra, D. K.; Cho, J. K.; Kim, Y. J. Facile Production of 2,5-Diformylfuran from Base-Free Oxidation of 5-Hydroxymethyl Furfural over Manganese–Cobalt Spinels Supported Ruthenium Nanoparticles. *J. Ind. Eng. Chem.* **2018**, *60*, 513–519. https://doi.org/10.1016/j.jiec.2017.11.040.

(44) Takagaki, A.; Takahashi, M.; Nishimura, S.; Ebitani, K. One-Pot Synthesis of 2,5-Diformylfuran from Carbohydrate Derivatives by Sulfonated Resin and Hydrotalcite-Supported Ruthenium Catalysts. *ACS Catal.* **2011**, *1* (11), 1562–1565. https://doi.org/10.1021/cs200456t.

(45) Antonyraj, C. A.; Jeong, J.; Kim, B.; Shin, S.; Kim, S.; Lee, K. Y.; Cho, J. K. Selective Oxidation of HMF to DFF Using Ru/γ-Alumina Catalyst in Moderate Boiling Solvents toward Industrial Production. *J. Ind. Eng. Chem.* **2013**, *19* (3), 1056–1059. https://doi.org/10.1016/j.jiec.2012.12.002.

(46) Ghosh, K.; Molla, R. A.; Iqubal, M. A.; Islam, S. S.; Islam, S. M. Ruthenium Nanoparticles Supported on N-Containing Mesoporous Polymer Catalyzed Aerobic Oxidation of Biomass-Derived 5-Hydroxymethylfurfural (HMF) to 2,5-Diformylfuran (DFF). *Appl. Catal. A Gen.* **2016**, *520*, 44–52. https://doi.org/10.1016/j.apcata.2016.03.035.

(47) Chen, J.; Zhong, J.; Guo, Y.; Chen, L. Ruthenium Complex Immobilized on Poly(4-Vinylpyridine)-Functionalized Carbon-Nanotube for Selective Aerobic Oxidation of 5-Hydroxymethylfurfural to 2,5-Diformylfuran. *RSC Adv.* **2015**, *5* (8), 5933–5940. https://doi.org/10.1039/c4ra14592e.

(48) Liu, Y.; Gan, T.; He, Q.; Zhang, H.; He, X.; Ji, H. Catalytic Oxidation of 5-Hydroxymethylfurfural to 2,5-Diformylfuran over Atomically Dispersed Ruthenium Catalysts. *Ind. Eng. Chem. Res.* **2020**, *59* (10), 4333–4337. https://doi.org/10.1021/acs.iecr.9b06470.

(49) Yuan, Z.; Liu, B.; Zhou, P.; Zhang, Z.; Chi, Q. Aerobic Oxidation of Biomass-Derived 5-Hydroxymethylfurfural to 2,5-Diformylfuran with Cesium-Doped Manganese Dioxide. *Catal. Sci. Technol.* **2018**, *8* (17), 4430–4439. https://doi.org/10.1039/c8cy01246f.

(50) Fang, R.; Luque, R.; Li, Y. Selective Aerobic Oxidation of Biomass-Derived HMF to 2,5-Diformylfuran Using a MOF-Derived Magnetic Hollow Fe-Co Nanocatalyst. *Green Chem.* **2016**, *18* (10), 3152–3157. https://doi.org/10.1039/c5gc03051j.

(51) Wen, S.; Liu, K.; Tian, Y.; Xiang, Y.; Liu, X.; Yin, D. Phosphorus-Doped Carbon Supported Vanadium Phosphate Oxides for Catalytic Oxidation of 5-Hydroxymethylfurfural to 2,5-Diformylfuran. *Processes* **2020**, *8* (10), 1–8. https://doi.org/10.3390/pr8101273.

(52) Biswas, S.; Dutta, B.; Mannodi-Kanakkithodi, A.; Clarke, R.; Song, W.; Ramprasad, R.; Suib, S. L. Heterogeneous Mesoporous Manganese/Cobalt Oxide Catalysts for Selective Oxidation of 5-Hydroxymethylfurfural to 2,5-Diformylfuran. *Chem. Commun.* **2017**, *53* (86), 11751–11754. https://doi.org/10.1039/c7cc06097a.

(53) Nocito, F.; Ventura, M.; Aresta, M.; Dibenedetto, A. Selective Oxidation of 5-

(Hydroxymethyl)Furfural to DFF Using Water as Solvent and Oxygen as Oxidant with Earth-Crust-Abundant Mixed Oxides. *ACS Omega* **2018**, *3* (12), 18724–18729. https://doi.org/10.1021/acsomega.8b02839.

(54) Ren, Y.; Yuan, Z.; Lv, K.; Sun, J.; Zhang, Z.; Chi, Q. Selective and Metal-Free Oxidation of Biomass-Derived 5-Hydroxymethylfurfural to 2,5-Diformylfuran over Nitrogen-Doped Carbon Materials. *Green Chem.* **2018**, *20* (21), 4946–4956. https://doi.org/10.1039/c8gc02286k.

(55) Kim, M.; Su, Y.; Fukuoka, A.; Hensen, E. J. M.; Nakajima, K. Aerobic Oxidation of 5-(Hydroxymethyl)Furfural Cyclic Acetal Enables Selective Furan-2,5-Dicarboxylic Acid Formation with CeO_2-Supported Gold Catalyst. *Angew. Chem. Int. Ed.* **2018**, *57* (27), 8235–8239. https://doi.org/10.1002/anie.201805457.

(56) Kim, M.; Su, Y.; Aoshima, T.; Fukuoka, A.; Hensen, E. J. M.; Nakajima, K. Effective Strategy for High-Yield Furan Dicarboxylate Production for Biobased Polyester Applications. *ACS Catal.* **2019**, *9* (5), 4277–4285. https://doi.org/10.1021/acscatal.9b00450.

(57) Shuai, L.; Amiri, M. T.; Questell-Santiago, Y. M.; Héroguel, F.; Li, Y.; Kim, H.; Meilan, R.; Chapple, C.; Ralph, J.; Luterbacher, J. S. Formaldehyde Stabilization Facilitates Lignin Monomer Production during Biomass Depolymerization. *Science (80-.).* **2016**, *354* (6310), 329–333. https://doi.org/10.1126/science.aaf7810.

(58) Lan, W.; Amiri, M. T.; Hunston, C. M.; Luterbacher, J. S. Protection Group

Effects During α,γ-Diol Lignin Stabilization Promote High-Selectivity Monomer Production. *Angew. Chem. Int. Ed.* **2018**, *57* (5), 1356–1360. https://doi.org/10.1002/anie.201710838.

(59) Questell-Santiago, Y. M.; Zambrano-Varela, R.; Talebi Amiri, M.; Luterbacher, J. S. Carbohydrate Stabilization Extends the Kinetic Limits of Chemical Polysaccharide Depolymerization. *Nat. Chem.* **2018**, *10* (12), 1222–1228. https://doi.org/10.1038/s41557-018-0134-4.

(60) Questell-Santiago, Y. M.; Yeap, J. H.; Talebi Amiri, M.; Le Monnier, B. P.; Luterbacher, J. S. Catalyst Evolution Enhances Production of Xylitol from Acetal-Stabilized Xylose. *ACS Sustain. Chem. Eng.* **2020**, *8* (4), 1709–1714. https://doi.org/10.1021/acssuschemeng.9b06456.

(61) Luo, X.; Li, Y.; Gupta, N. K.; Sels, B.; Ralph, J.; Shuai, L. Protection Strategies Enable Selective Conversion of Biomass. *Angew. Chem. Int. Ed.* **2020**, *59* (29), 11704–11716. https://doi.org/10.1002/anie.201914703.

(62) Ebitani, K.; Motokura, K.; Mori, K.; Mizugaki, T.; Kaneda, K. Reconstructed Hydrotalcite as a Highly Active Heterogeneous Base Catalyst for Carbon-Carbon Bond Formations in the Presence of Water. *J. Org. Chem.* **2006**, *71* (15), 5440–5447. https://doi.org/10.1021/jo060345l.

(63) Davis, S. E.; Zope, B. N.; Davis, R. J. On the Mechanism of Selective Oxidation of 5-Hydroxymethylfurfural to 2,5-Furandicarboxylic Acid over Supported Pt and Au Catalysts. *Green Chem.* **2012**, *14* (1), 143–147. https://doi.org/10.1039/c1gc16074e.

(64) Krivtsov, I.; Ilkaeva, M.; García-López, E. I.; Marcì, G.; Palmisano, L.; Bartashevich, E.; Grigoreva, E.; Matveeva, K.; Díaz, E.; Ordóñez, S. Effect of Substituents on Partial Photocatalytic Oxidation of Aromatic Alcohols Assisted by Polymeric C_3N_4. *ChemCatChem* **2019**, *11* (11), 2713–2724. https://doi.org/10.1002/cctc.201900362.

(65) Ren, H. F.; Luo, X.; Zhang, K.; Cai, Q.; Liu, C. L.; Dong, W. S. Selective Aerobic Oxidation of 5-Hydroxymethylfurfural to 2,5-Dimethylfuran over Heteroatom-Doped Ordered Carbon Supported Ru Catalysts. *J. Porous Mater.* **2020**, *27* (4), 1003–1012. https://doi.org/10.1007/s10934-020-00872-6.

Chapter 3

Reductive amination of 5-Formyl-2-furancarboxylic Acid to 5-aminomethylfuran-2-carboxylic acid

Abstract

This study presents an efficient way for preparing 5-(aminomethyl)furan-2-carboxylic acid (AMFCA) from renewable biobased 5-formylfuran-2-carboxylic acid (FFCA) as a monomer for polyamides through reductive amination using catalytic single-crystal cobalt phosphide nanorods (Co_2P NRs). Strongly alkaline ammonia solutions, commonly used for reductive amination, caused severe degradation of FFCA, but no degradation occurred when using ammonium acetate (NH_4OAc) as a nitrogen source. Moreover, among binary water-organic solvent mixtures (Toluene, DMF, alcohol, etc.), AMFCA yield was the highest in water-methanol mixing solvent, due to in-situ acetal formation which provides protection of the labile aldehyde of FFCA and so suppresses degradation and other side reactions. Under optimized conditions, i.e., 0.5 mmol of substrate, 5 mmol of NH_4OAc, substrate to catalyst ratio of 10 mol/mol, under 0.5 MPa H_2 at 393 K for 3 hours in methanol/water 2:1 v/v, near-stoichiometric amounts of AMFCA (90 % yield) were formed at full conversion.

3.1 Introduction

Lignocellulosic biomass is widely regarded as an abundant and renewable carbon source for the replacement of diminishing fossil fuel resources.[1,2] Catalytic valorization of its constituents such as cellulose, hemicellulose, and lignin has been widely studied to develop biofuels and commodity chemicals.[3–7] A key compound synthesized from cellulose by acid-catalyzed hydrolysis and subsequent dehydration of glucose is 5-hydroxymethylfurfural (HMF),[8–14] which is a versatile intermediate for the production of valuable chemicals. Scheme 3.1 presents several reaction paths for the conversion of HMF to monomers for biomass-based polymers. The hydrogenation of HMF yields 2,5-bis(hydroxymethyl)furan (BHMF)[15–18] and 2,5-(bis(hydroxymethyl)tetrahydrofuran (BHMTHF).[19–23] BHMTHF can be further transformed to aliphatic alcohols such as 1,6-hexanediol and 1,2,6-hexanetriol.[19,24–26] Aerobic oxidation of HMF affords three important products, 2,5-diformylfuran (DFF), 5-formylfuran-2-carboxylic acid (FFCA), and 2,5-furandicarbocylic acid (FDCA).[27–31] Reductive amination converts FFCA to 5-(aminomethyl)furan-2-carboxylic acid (AMFCA), which is a biobased monomer for the production of a Nylon 6-type polyamide. AMFCA can be potentially utilized to synthesize another attractive polyamide, poly(iminomethylene(cis-tetrahydro-2,5-furandiyl)carbonyl) (PITC)[32] via the formation of 8-oxa-3-azabicyclo[3.2.1]octan-2-one.[33] Applications of AMFCA possibly extend in biochemical products, which include oligopeptides[34] such as G-quadruplex used for the development of anticancer drugs.[35] Despite the potential of AMFCA in polyamide applications, the synthetic procedures for AMFCA has not been established yet.

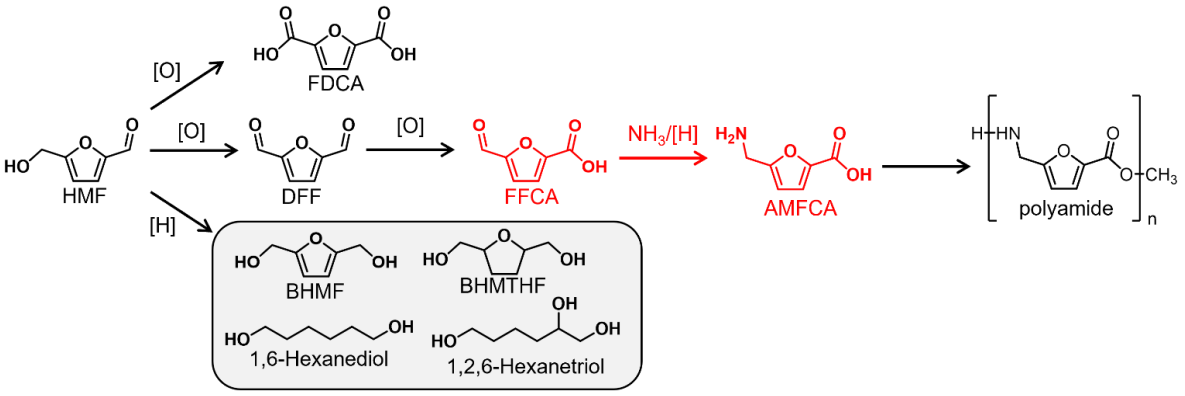

Scheme 3.1. Reaction pathways to several valuable monomers obtainable from HMF

Recently we have reported an acetal protection strategy to synthesize DFF,[36] FFCA,[37] and FDCA[37,38] in concentrated solutions (> 10 wt%). Introduction of a six-membered ring acetal through the acetalization of HMF with 1,3-propanediol (HMF-acetal) stabilized the highly reactive formyl group during the oxidation reactions even using concentrated solutions and suppressed complex side-reactions that mainly form polymerized species so-called humin. An acetal form of FFCA was obtained in 94% yield using a 20 wt% solution of the HMF-acetal and a hydroxyapatite-supported Au catalyst. FFCA and 1,3-propanediol was then recovered almost quantitatively from the reaction mixtures by a simple deprotection reaction using a homogeneous acid catalyst. In sharp contrast, previous reports on FFCA production by the oxidation of non-protected HMF limited the substrate concentration below 10 wt% and obtained FFCA in low yield (~15%) and obtained other products such as FDCA (4%) and HMFCA (35%) with other unknown products (40%) that mean non-selective oxidation from HMF. Efficient FFCA production using the HMF-acetal has prompted us to study reductive amination of FFCA to AMFCA using a heterogeneous catalyst.

Precious metal-based catalysts such as ruthenium, rhodium, and gold are active for

reductive amination to synthesize functional amines.[39–48] Liang et al. reported reductive amination of several important biomass-derived aldehydes or ketones to their primary amines in high selectivities (> 90%) by using Ru/ZrO_2.[46] In contrast, non-noble metal catalysts typically studied in the reductive amination are Raney Ni or Co catalysts.[49–51] Despite their high activities, the use of these Raney catalysts accompanies several drawbacks typically represented by pyrophoricity, which results in the difficulty of catalyst handling and its reuse.[52] Recently, several non-noble metal catalysts were developed through precise control of their physicochemical properties (particle size, crystal phase, additional dopants, etc.) and studied in the reductive amination of benzaldehyde and biomass-derived furanics such as glyceraldehyde, HMF, and DFF to their respective primary amines with high selectivities (>80%) as shown in Entry 3-14 of Table 1.2.[44,50,53–59] Yuan et al. synthesized primary amines in excellent yields, ranging from 82% to 100%, from several carbonyl compounds using a nitrogen-doped carbon-supported Co catalyst.[59] Mitsudome et al. devised a phosphor-alloying strategy to develop well-defined metal phosphides and their excellent applications in reductive transformation for a variety of organic compounds.[60] Cobalt phosphide nanorod (Co_2P NRs) exhibited high activities in the reductive amination of a variety of aldehydes and ketones with aqueous ammonia (NH_3) or ammonium acetate (NH_4OAc), yielding the primary or secondary amines in high yields.[57] Specific feature of the Co_2P NRs catalyst is explained not only by its high activities at low H_2 pressures and mild reaction temperatures, but also by its excellent stability. Furthermore, the coordination number (CN) ratio (1.6) of the Co_2P NRs is smaller than that of bulk Co_2P (2.0), with the ideal value (1.8) calculated from the crystal structure of orthorhombic Co_2P.[57] The small CN ratio of the Co_2P NRs indicates that a number of coordinatively unsaturated Co−Co sites

is present on the nanorod surfaces, which is induced by the formation of the rod-shape morphology with a high content of Co. Such undercoordinated metals are known for enhanced hydrogenation activity, as compared to their saturated counterparts.[61–65] Thus, I applied the Co_2P NRs catalyst in the reductive amination of FFCA in this study.

3.2 Experimental

3.2.1 Materials

Acetone, acetonitrile, chloroform, ammonium acetate, N,N-dimethlyformamide Super dehydrated (DMF), and ZrO_2 were purchased from FUJIFILM Wako Pure Chemical Corporation. HMF was procured from Sigma-Aldrich. AMFCA was purchased from Fluorochem Ltd. Hexadecylamine, Triphenyl phosphite, 1-octadecene, methanol-d_4, DFF, FFCA, and FDCA were obtained from Tokyo Chemical Industry (TCI). 5-Hydroxymethyl-2-furan carboxylic acid (HMFCA) was purchased from Combi-Blocks Inc. Aerosil-380 (SiO_2) was obtained from Evonic industries and Ajinomoto Fine-Techno Corporation, respectively. Cobalt(II) acetylacetonate dihydrate ($Co(acac)_2 \cdot 2H_2O$) was purchased from Mitsuwa pure chemicals. Deuterium oxide and dipotassium hydrogenphosphate were purchased from Kanto chemical corporation. Nb_2O_5 (JRC-NBO-1) and CeO_2 (JRC-CEO-5), are a reference catalyst supplied from the Catalyst Society of Japan. Co_2P commercial catalyst was procured from Santa Cruz Biotechnology, Inc.

3.2.2 Catalyst preparation

In a typical synthesis,[57] the mixture of $Co(acac)_2 \cdot 2H_2O$ (2 mmol), 1-octadecene (10

mL), and triphenylphosphine (5.4 mL) were heated stepwise at 150 °C for 1 h and at 300 °C for 3 h under a N_2 flow. After the heat treatment, the mixture was cooled down in air to room temperature and the resulting precipitate was washed with a chloroform-acetone mixture. The obtained powder was dried at room temperature in vacuo overnight. Synthesis of other Co support catalysts was followed along previous reports.[66] All catalysts were prepared by wetness impregnation. 244 mg of $Co(NO_3)_2 \cdot 6H_2O$ was added to 1.5 g water and sonicated for 10 min, followed by addition of 1 g of each support such as SiO_2, CeO_2, Nb_2O_5, and ZrO_2. Then the mixture was evaporated to dryness at 333 K. The obtained solid was ground to powder and then heated to 673 K in air at a ramp of 5 K/min and was held at that temperature for 2 h. After cooling to room temperature, the solids were subsequently reduced at 623 K in hydrogen flow at a ramp of 2 K /min and was held at that temperature for 2 h. After cooling to room temperature, the Co catalyst was stored under inert atmosphere.

3.2.3 Synthetic procedure for FFCA-acetal

FFCA (500 mg) was added to a mixture of trimethyl orthoformate (2 mL), and methanol (50 mL). After stirring at room temperature for 24 h, solvent was removed by vacuum evaporation to obtain FFCA-acetal. NMR assignment of 5-(1,1'-dimethoxymethyl) furan-2-yl methyl carboxylic acid (FFCA-acetal): ^{1}H NMR (400 MHz, Methanol-d_4): 7.11 (d, 1H), 6.55 (d, 1H), 5.42 (s, 1H), 4.83 (s, 2H), 3.77 (s, 6H).

3.2.4 Catalyst characterization

Powder X-ray diffraction (XRD) patterns were obtained from an X-ray diffractometer (Rigaku, Ultima IV) using Cu Kα radiation (40 kV, 20 mA) over the 2θ

range of 10°−90°. Adsorption isotherms were acquired from a micromeritics (3-FLEX). The BET equation was used on the linear part of the adsorption branch to estimate the specific surface areas (P/P_0 = 0.05−0.30).

3.2.5 Catalytic experiments

Catalytic activity was tested in a 10 mL SUS-316 stainless steel batch reactor equipped with a PTFE liner. Substrate (FFCA 0.5 mmol), methanol-d_4 (MeOD, 0-3 mL), deuterium oxide (D_2O, 0-3 mL), and Co_2P NRs catalyst (0.025 mmol, 10 mol% based on Co molar content) were charged into the reactor, which was subsequently pressurized with hydrogen to 0.5 MPa and heated in an oil bath at 393 K. After a specified reaction period, the reactor was cooled to room temperature, and products were analyzed by High-Performance Liquid Chromatography (HPLC). The quantification of HMF, DFF, FFCA, and FDCA was conducted by HPLC (SHIMADZU, Japan) consisting of a RID-10A detector, a UV-SPD-20A detector, and an Shodex ODP_2 HP-4E column (column temp., 313 K). A mixture of a diluted K_2HPO_4 aqueous solution (0.02 M, pH=9.5, 23 vol%) and acetonitrile (77 vol%) was used as the eluent at a flow rate of 0.4 mL min^{-1}. The retention time for FFCA-acetal, FFCA, HMFCA, and AMFCA was 5.3, 5.8, 6.5, and 7.5 min, respectively. Secondary imine was directly analyzed by ^1H NMR spectrometry (ECX 400, JEOL Ltd.).

3.3 Results and disscussion

3.3.1 Selecting nitrogen source for reductive amination

Table 3.1. Reductive amination of FFCA over Co_2P NRs catalyst in water with different concentration of NH_3 or NH_4OAc

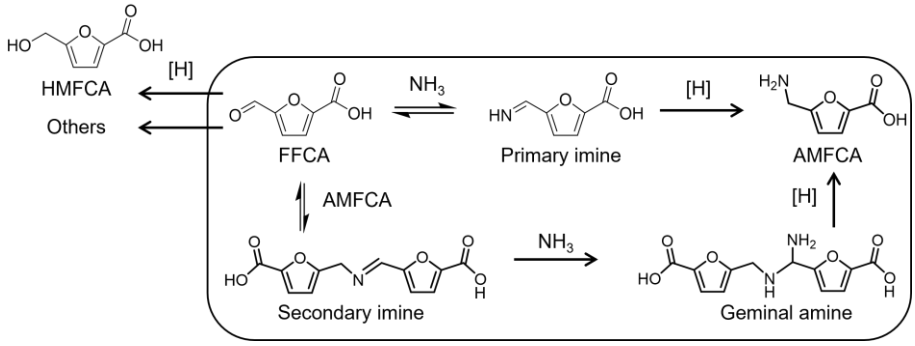

#	N source (mmol)		pH	FFCA conv. (%)	Product yield (selectivity) (%)			
	Type	Amount			AMFCA	HMFCA	Sec.-Imine	Others
1		0.5	8	63	13 (20)	2 (3)	18 (29)	30 (48)
2	NH_3	5	9-10	98	55 (56)	6 (6)	0	37 (38)
3		45	<12	96	0 (0)	29 (30)	0	67 (70)
4		3	6-7	35	15 (43)	9 (26)	0	11 (31)
5	NH_4OAc	5	6-7	59	35 (60)	12 (20)	0	12 (20)
6		8	6-7	57	27 (48)	7 (12)	0	23 (40)
7*		5	6-7	94	55 (59)	20 (21)	0	19 (20)

Conditions: substrate, FFCA 0.5 mmol; water 3 mL; catalyst, Co_2P NRs 0.025 mmol; hydrogen pressure, 0.5 MPa; temp., 393 K; time, 3 h. Entry 7* was conducted at 17 h.

FFCA can be reacted with ammonia and AMFCA to form undetectable primary imine and detectable secondary imine (Sec-imine), respectively. The primary imine is directly hydrogenated to AMFCA while the secondary imine is further reacted with ammonia to form undetectable germinal amine and its hydrogenation produces two

equivalents of AMFCA. FFCA is hydrogenated to HMFCA as the detectable byproduct and FFCA is degraded most likely through complex condensation reactions to undetectable byproducts shown as others in Table 3.1. The reductive amination of FFCA using Co_2P NRs catalyst was conducted at 393 K for 3 h in water using aqueous ammonia solution (NH_3) or ammonium acetate (NH_4OAc) under 0.5 MPa H_2. A mere 13% AMFCA and 18% secondary imine were obtained with a high level of others (30%) in the presence of equimolar amount of NH_3 to FFCA in entry 1. AMFCA yield was increasing to 50% with the increase in NH_3 loading to 5 mmol. Further increase in NH_3 loading to 45 mmol (entry 3) resulted in no AMFCA formation (0% yield) but accelerated side reactions to HMFCA (29% yield) and others (67%).

The increase in others is related to the stability of FFCA in the reaction media. The stability of FFCA, HMFCA, and AMFCA was investigated at 393 K for 2 h under an N_2 gas using different nitrogen sources and reaction media (Table 3.2). FFCA is stable in pure H_2O (entry 1). Despite the high stability of AMFCA and HMFCA (entries 3 and 4), FFCA was easily degraded to polymeric compounds such as humin in an aqueous NH_3 solution (5 mmol of NH_3, entry 2). FFCA was more stable than using NH_3 when changing nitrogen source to NH_4OAc (entries 2 and 5).

Table 3.2. Non-catalytic degradation of FFCA, AMFCA and HMFCA in innert gas system under the reaction conditions

Entry	Raw material	Solvent	Nitrogen source	FFCA conv. (%)	Others (%)
1	FFCA	Water	-	5	5
2	FFCA	Water	NH_3	90	90
3	AMFCA	Water	NH_3	0	0
4	HMFCA	Water	NH_3	0	0
5	FFCA	Water	NH_4OAc	65	65

Conditions: substrate, (FFCA, HMFCA or AMFCA) 0.5 mmol; solvent, (3 mL) NH_4OAc or NH_3 (5 mmol); catalyst, Co_2P NRs catalyst 0.05 mmol; temp., 393 K; time, 120 min, N_2 0.5 MPa.

The degradation behavior of FFCA in an NH_3 solution is different from that of benzaldehyde in the previous paper[57] and simply attributed to highly reactive formyl group of FFCA, which is also observed in HMF.[67] When the reaction was conducted with less basic NH_4OAc (5 mmol) under the identical reaction conditions to entry 2 of Table 3.2, AMFCA in 35 yield was obtained at 59% conversion (entry 5). These values are lower than those of entry 2 using the same amount of NH_3 but there is no difference in AMFCA selectivity in both reactions. FFCA conversion and AMFCA yield became comparable when prolonged the reaction time to 17 h (entry 7*). When the amount of NH_4OAc was changed from 3 mmol to 8 mmol (entries 4-6), both yield and selectivity for AMFCA are maximized at 5 mmol. There was no difference in the AMFCA selectivity at 5 mmol of NH_3 and NH_4OAc but the selectivity of others was low with NH_4OAc (entries 3 and 7). Therefore, I studied reductive amination of FFCA with 5 mmol of NH_4OAc to increase AMFCA productivity.

3.3.2 Reductive amination of FFCA in various mathanol-water ratio

Reductive amination of FFCA was further investigated at 393 K for 1 hour or 3 hours under 0.5 MPa H_2 atmosphere using Co_2P NRs with NH_4OAc in various methanol-water mixtures (Table 3.3). Methanol was used as a suitable solvent in the reductive amination of cyclohexanone, due to prefereable imine formation.[68] However, FFCA itself was unstable in pure mehanol using NH_3 and NH_4OAc (Table 3.3, entries 5,6). I used methanol-water mixing medium in this study. In pure water (entrie 1 and 7), FFCA was slowly converted to AMFCA with its yield of 35% after 3 hours, which is due to water inhibiting imine formation. Increasing methanol content led to the maximum AMFCA yield of 90% in the methanol:water ratio of 2:1 v/v as shown in entry 3. However, further increase in methanol content decreased AMFCA yield significantly (entries 4-5), which suggests that reductive amination of FFCA can be controlled by adjusting the methanol:water ratio. AMFCA was scarcely formed in in pure methanol and most of FFCA were converted to others (entries 5 an 9). There was no significant difference in conversion and AMFCA yield when the reaction was conducted using pure methanol and NH_3 instead of NH_4OAc (entry 6). These results mean that pure methanol is not appropriate for reductive amination of FFCA. Interestingly, FFCA-acetal was detected when the reaction of entry 5 was stopped at 1 hour (entry 8). FFCA-acetal was formed in 20% yield, which is significantly larger than other products.

Table 3.3 Reductive amination of FFCA over Co_2P NRs catalysts with different ratio of methanol

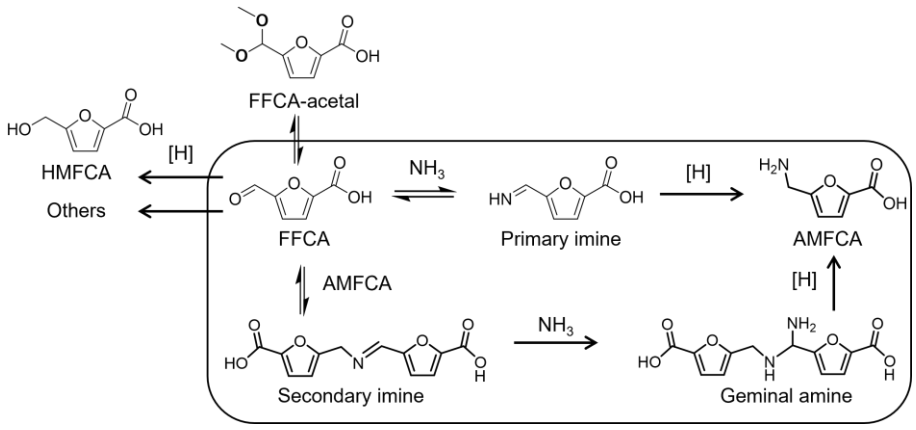

#	MeOH-H_2O mixture		conv.	t	Product yield (%)				
	MeOH (mL)	H_2O (mL)	(%)	(h)	Acetal	AMFCA	HMFCA	Imine	Others[1]
1	0	3	59	3	0	35	12	0	3
2	1	2	83		0	50	5	0	7
3	**2**	**1**	**95**		**0**	**90**	**3**	**0**	**2**
4	2.5	0.5	98		7	57	4	0	30
5	3	0	100		0	10	1	0	89
6*	3	0	100		0	20	1	0	79
7	0	3	8	1	0	6	0	0	2
8	**2**	**1**	**45**		**20**	**20**	**0**	**4**	**1**
9	3	0	100		0	8	0	0	92

Conditions: substrate, FFCA 0.5mmol; solvent, (3 mL) NH_4OAc (5 mmol); catalyst, Co_2P NRs catalyst 0.05 mmol; Hydrogen pressure, 0.5 MPa; temp., 393 K. * NH_3 (5 mmol) was used instead of

Table 3.4 Reductive amination of FFCA over Co_2P NRs catalysts in the mixture of water-organic solvent (=1:2 v/v)

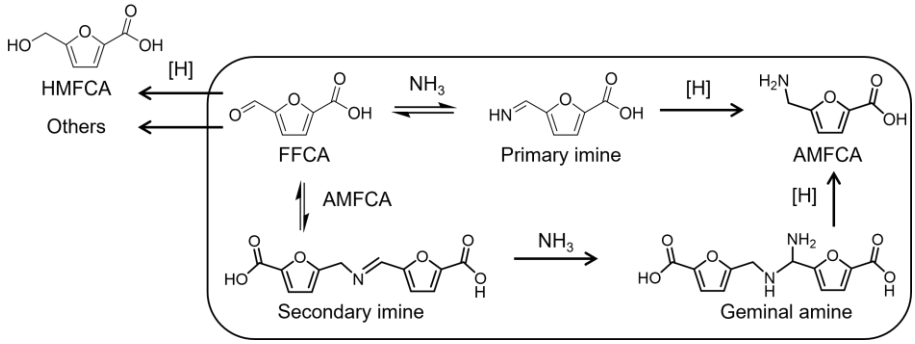

#	Organic solvent	FFCA conv. (%)	Product yield (%)			
			AMFCA	HMFCA	Imine	Others
1	MeOH	95	90	3	0	2
2	EtOH	89	46	6	0	37
3	Ethylene glycol	83	40	5	0	38
4	1,3-Propanediol	86	30	6	0	50
5	THF	98	52	6	0	40
6	DMF	95	4	32	16	43
7	Toluene	85	12	4	0	69

Conditions: substrate, FFCA 0.5mmol; solvent, (3 mL and for organic water mixing medium solvent ratio organic/water 2:1 v/v), NH_4OAc (5 mmol); catalyst, Co_2P NRs catalyst 0.05mmol; Hydrogen pressure, 0.5 MPa; temp., 393 K; time, 3 h.

Several solvents were studied in a 2/1 volume ratio with water for the reductive amination of FFCA (Table 3.4). All reactions were performed at 393 K for 3 h under pressurized 0.5 MPa H_2. AMFCA was obtained in 90% yield when methanol was used as a co-solvent. When using other alcohols such as ethanol, ethylene glycol and 1,3-propanediol, AMFCA yield was significantly low (entries 1-4). Low byproduct formation

in the methanol-water mixture was presumably due to acetal protection of aldehyde groups, inhibiting aldehyde hydrogenation and degradation of free FFCA. The formation of undetectable byproducts was predominant in other organic solvents (entries 5-7). Aprotic polar solvents such as THF and DMF have strong interactions with metal catalysts that inhibit the hydrogenation activity of primary and secondary imines.[68]

To confirm this speculation for the effect of acetal protection, I conducted the acetalization of FFCA in four alcohols (methanol, ethanol, ethylene glycol, 1,3-propanediol) at room temperature (Table 3.5) for 30 min and found that high acetal content is only obtained in methanol (50% yield). Thus, I selected methanol-water solvent for further studies. Effect of solvent in reductive amination of FFCA was similar results to previous study in reductive amination of cyclohexanone.[68]

Table 3.5. Acetal formation from FFCA with different type of alcohol

#	Solvent	FFCA conv. (%)	Product yield (%)	
			FFCA-acetal	others
1	MeOH	50	50	0
2	EtOH	20	20	0
3	Ethylene glycol	9	9	0
4	1,3-Propanediol	17	17	0

Condition: Substrate, FFCA 0.5 mmol; solvent, (3 mL and for alcohol solvent ratio alcohol/water 2:1 v/v), 10 min at room temperature. FFCA-acetal contents were measured by NMR.

3.3.3 Reductive amination of FFCA in water-methanol mixing solvent

Kinetic studies in the reductive amination of FFCA in methanol-water mixture (2:1 v/v) using NH_4OAc (5 mmol) were further investigated at 393 K under 0.5 MPa H_2 atmosphere. Time courses for substrate (FFCA) and products (AMFCA, FFCA-acetal, HMFCA, secondary-imine, and others) are shown in Figure 3.1, together with presumable reaction pathways in this reaction (Scheme 3.2). Half of FFCA was acetalized with methanol before the reaction, meaning the amounts of FFCA and FFCA-acetal are estimated as 0.25 mmol (50% yield). FFCA-acetal decreased constantly with time. In contrast, FFCA increased to 0.3 mmol at 30 min and then changed to decrease for 2.5 hours. This difference can be explained by the change in reaction equilibrium between bare FFCA and FFCA-acetal by changing reaction temperatures: a part of FFCA-acetal is going back to bare FFCA at reaction temperature (393 K). Two products were detected at 30 min: AMFCA and secondary imine. The amount of AMFCA increased during the reaction and reached 0.4 mmol at 3 hours, which corresponds to 90% yield. AMFCA is formed via undetectable primary imine predominantly in the initial 30 min. A part of AMFCA is comsumed for the formation of secondary imine, which is also an intermedate for AMFCA. The rate of AMFCA formation at 30 min (25 mmol g-cat^{-1} h^{-1}) is smaller than that at 1 hour (35 mmol g-cat^{-1} h^{-1}), mainly due to the formation of secondary imine from AMFCA and FFCA. The amount of secondary imine is always low (< 0.05 mmol) during the reaction. Side-reactions were largely suppressed under the reaction conditions and the amounts of HMFCA and others are negligibly small even after 3 hours (< 0.0015 mmol). According to the mechanism in Scheme 3.2, FFCA-acetal is likely a supply source of FFCA in this reaction. The increase in AMFCA yield is derived from high stability of dimethylacetal functionality against the side reactions, compared to a reactive formyl

group in bare FFCA that is easily susceptible to the formation of HMFCA and undetectable byproducts (others). However, the content of FFCA-acetal is not always high in the course of the reaction. If direct and highly efficient path from FFCA-acetal to AMFCA is available in this system, the situation changes completely: FFCA is a supply source of FFCA-acetal. Futher studies on the role of "FFCA-acetal" was described in Chapter 4.

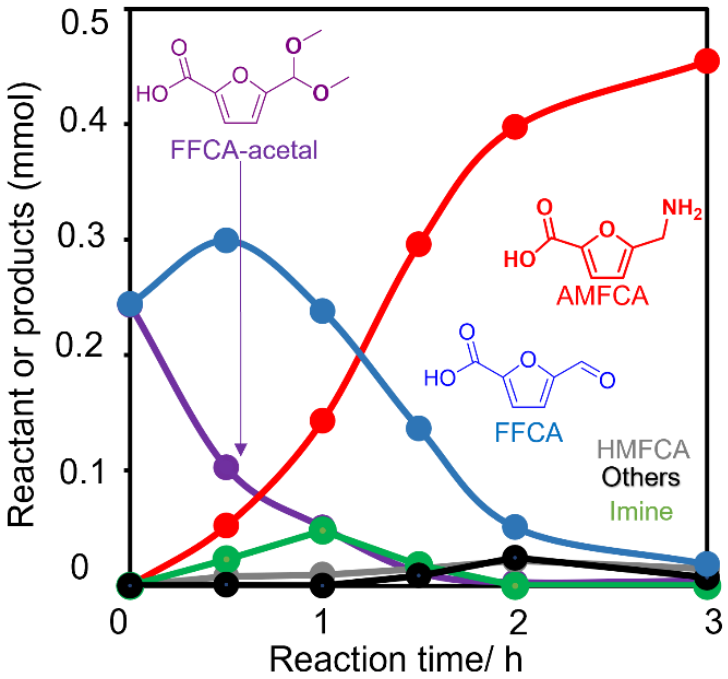

Figure 3.1 Reductive amination of FFCA in water-methanol mixing solvent: substrate 0.5 mmol; solvent, (3 mL), Ratio of methanol to water (2:1), NH_4OAc (5 mmol); catalyst, Co_2P NRs catalyst 0.05mmol; Hydrogen pressure, 0.5 MPa; temp., 393 K

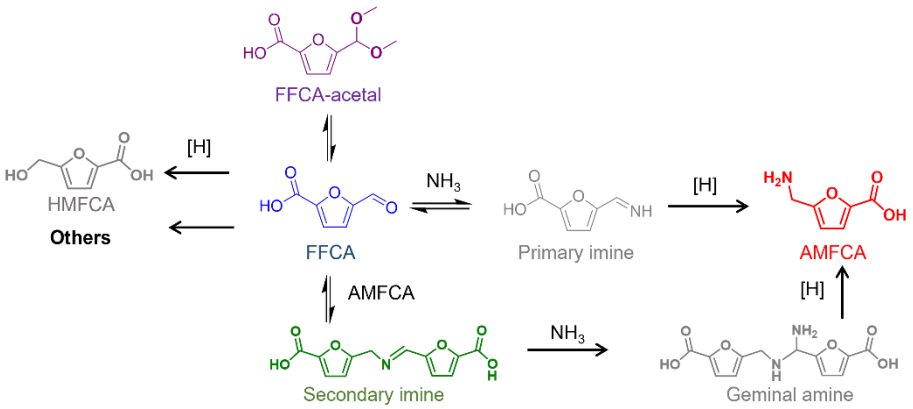

Scheme 3.2 Reaction pathways for the conversion of FFCA to AMFCA by reductive amination through primary imine and secondary imine.

3.3.4 Comparison with other Cobalt catalysts

The reductive amination of FFCA using different Co-based reference catalysts were investigated in the methanol-water mixture (2:1 v/v) using NH_4OAc at 0.5 MPa H_2 and 393 K for 3 h (Figure 3.2). Co_2P NRs produced AMFCA in 90% yield, which is much higher than that of other reference catalysts including commercially available Co_2P*. Supported Co catalysts and commercially available Co_2P* converted FFCA to undetectable byproducts predominantly under the reaction conditions, affording poor AMFCA yields (< 15%) and selectivities (< 25%). Co/ZrO_2 gave a moderate AMFCA yield (58%) but produced undetectable byproduct in 35% yield. I expect that the cobalt nanoparticles present on these supports are partially oxidized as they were handled in air after their reduction pretreatment. This has a detrimental effect on the hydrogenation activity of these materials. XRD patterns of three supported catalysts (Co/Nb_2O_5, Co/ZrO_2, and Co/CeO_2) in Figure 3.3 showed no diffractions assignable to metallic Co and Co oxides, which suggests that Co nanoparticles that cannot be detected by XRD are

present in the oxidized form. Co/SiO_2 has diffraction peaks for metallic Co (α-phase) with its average crystalline size of 4 nm estimated by using the Scherrer equation. Both metallic Co and CoO_x nanoparticles on SiO_2, Nb_2O_5, ZrO_2, and CeO_2 are not effective for the reductive amination of FFCA to AMFCA under the reaction conditions.

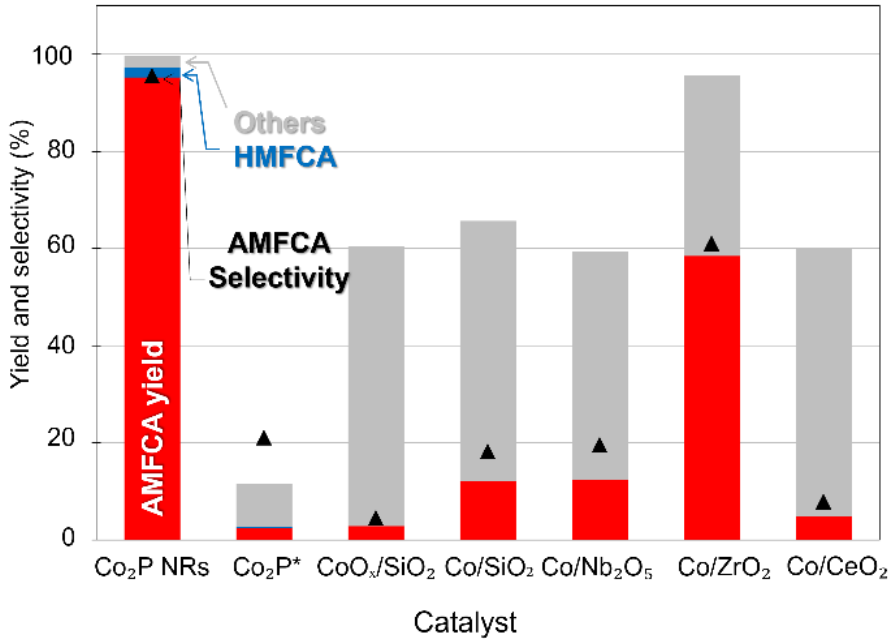

Figure 3.2. Reductive amination of FFCA with Co_2P NRs and reference catalysts. Conditions: FFCA, 0.5 mmol; solvent, (3 mL), Ratio of methanol to water (2:1), NH_4OAc (5 mmol); catalyst, Co catalyst 0.05 mmol; Hydrogen pressure, 0.5 MPa; temp., 393 K, 3 h.

Structural feature of Co_2P NRs is different from those of commercial Co_2P*. Highly active Co_2P NRs only contains β-Co_2P, while commercial Co_2P* is the mixture of β-Co_2P, α-Co_2P, and metallic Co (α-phase). Moreover, surface area of commercial Co_2P* was 0.51 m^2 g^{-1}, which was significantly smaller than that of Co_2P NRs (40 m^2 g^{-1}). Earlier

reports claim that Co sites in the Co_2P NRs are largely undercoordinated compared to those of commercial Co_2P*.[57] Due to a large number of coordinatively unsaturated Co−Co sites, Co_2P NRs is active compared to commercial Co_2P* and other supported Co Catalysts in mild conditions such as low H_2 pressures and low temperatures.

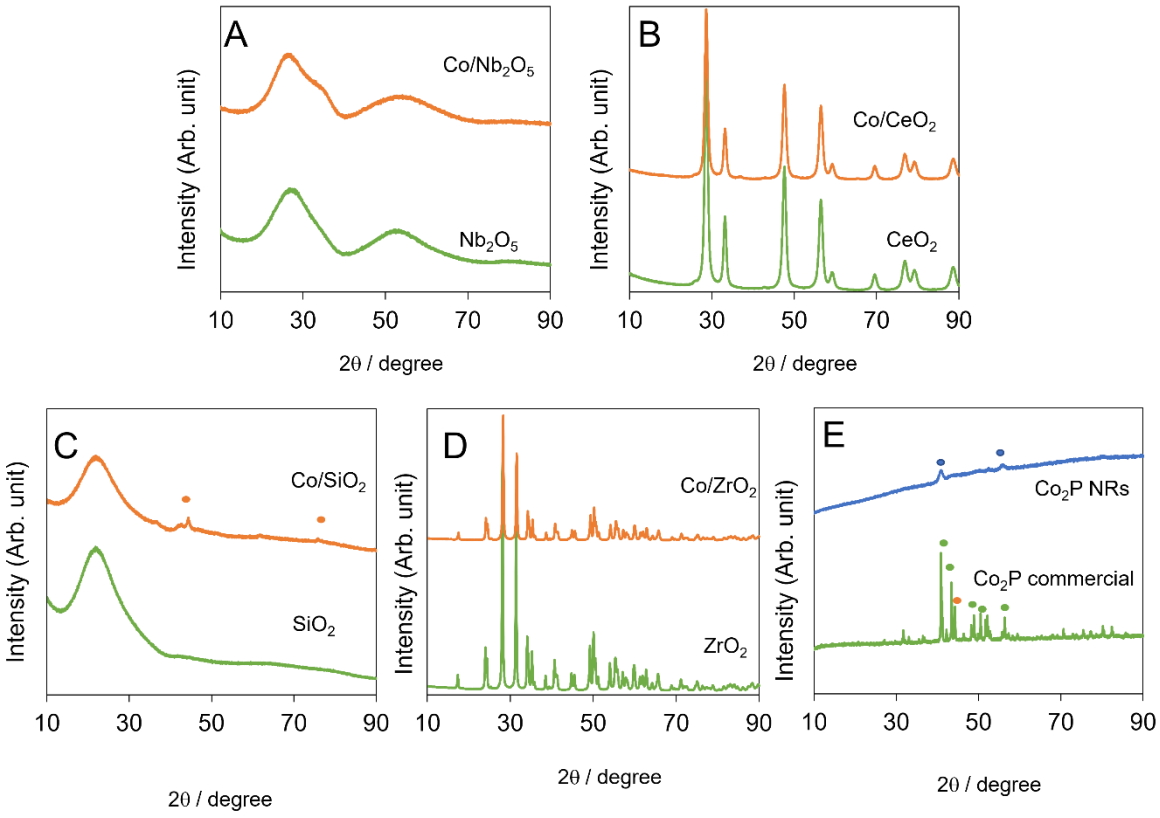

Figure 3.3. XRD pattern of supported Co catalysts and its support materials: (A) Co/Nb_2O_5, (B) Co/CeO_2, (C) Co/SiO_2, (D) Co/ZrO_2, and (E) Co_2P catalyst: α-Co metallic phase (dot orange), α-Co_2P phase (dot green), and β-Co_2P phase (dot blue).

3.3.5 Reusability of Co_2P NRs catalyst

Mitsudome et al. reported that Co_2P NRs are easily recovered in air and reused without loss of original activity, highlighting its high durability. Moreover, the used Co_2P NRs were fully characterized, which indicates no structural changes such as aggregation and sintring.[57]

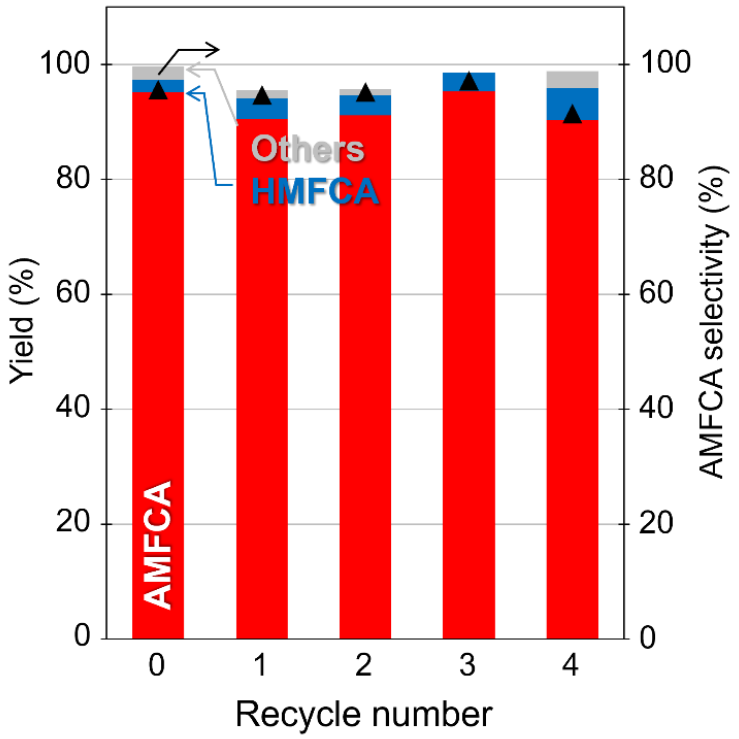

Figure 3.4 Reductive amination of FFCA: substrate, FFCA 0.5 mmol; solvent, (3 mL), Ratio of methanol to water (2:1), NH_4OAc (5 mmol); catalyst, Co_2P NRs catalyst 0.05 mmol; Hydrogen pressure, 0.5 MPa; temp., 393 K, 3 h.

The reusability of Co_2P NRs was investigated in the reductive amination of FFCA. Reactions were conducted at 393 K for 3 h under pressurized 0.5 MPa H_2. After the reaction, the catalyst was recovered by filtration, washed with water, dried at 373 K in air

overnight, and then used for the subsequent reaction (Figure 3.4). After the fourth cycle, AMFCA yield was still over 90% with small by-product formation including HMFCA (<10%). Therefore, Co_2P NRs can be identified as a durable and highly active catalyst in the reductive amination of FFCA in methanol-water mixture (2:1 v/v).

3.4 Conclusion

Reductive amination to AMFCA from FFCA was successfully performed using Co_2P NRs catalyst in methanol-water solutions, with NH_4OAc as a benign nitrogen source. Among organic-water solvents, methanol was the most optimal cosolvent due to its tendency to form suitable levels of protective acetal with the substrate. Acetal protection of the formyl group in FFCA prevents side reactions such as its premature hydrogenation to form HMFCA and its degradation to unknown byproducts. Under optimized conditions, i.e., 0.5 mmol of FFCA, 5 mmol of NH_4OAc, substrate to catalyst ratio of 10 mol/mol, under 0.5 MPa H_2 at 393 K for 3 hours in methanol/water 2:1 v/v, an AMFCA yield of 90% could be obtained from FFCA at full conversion. This insight can spark development of a methodology for the controlled synthesis of biomass-derived amines for a variety of biobased applications in the future.

3.5 References

(1) Chheda, J. N.; Huber, G. W.; Dumesic, J. A. Liquid-Phase Catalytic Processing of Biomass-Derived Oxygenated Hydrocarbons to Fuels and Chemicals. *Angew. Chem. Int. Ed.* **2007**, *46* (38), 7164–7183. https://doi.org/10.1002/anie.200604274.

(2) Bozell, J. J.; Petersen, G. R. Technology Development for the Production of Biobased Products from Biorefinery Carbohydrates—the US Department of Energy's "Top 10" Revisited. *Green Chem.* **2010**, *12* (4), 539–555. https://doi.org/10.1039/b922014c.

(3) Huber, G. W.; Iborra, S.; Corma, A. Synthesis of Transportation Fuels from Biomass: Chemistry, Catalysts, and Engineering. *Chem. Rev.* **2006**, *106* (9), 4044–4098. https://doi.org/10.1021/cr068360d.

(4) Corma Canos, A.; Iborra, S.; Velty, A. Chemical Routes for the Transformation of Biomass into Chemicals. *Chem. Rev.* **2007**, *107* (6), 2411–2502. https://doi.org/10.1021/cr050989d.

(5) Delidovich, I.; Hausoul, P. J. C.; Deng, L.; Pfützenreuter, R.; Rose, M.; Palkovits, R. Alternative Monomers Based on Lignocellulose and Their Use for Polymer Production. *Chem. Rev.* **2016**, *116* (3), 1540–1599. https://doi.org/10.1021/acs.chemrev.5b00354.

(6) Li, C.; Zhao, X.; Wang, A.; Huber, G. W.; Zhang, T. Catalytic Transformation of Lignin for the Production of Chemicals and Fuels. *Chem. Rev.* **2015**, *115* (21), 11559–11624. https://doi.org/10.1021/acs.chemrev.5b00155.

(7) Isikgor, F. H.; Becer, C. R. Lignocellulosic Biomass: A Sustainable Platform for the Production of Bio-Based Chemicals and Polymers. *Polym. Chem.* **2015**, *6* (25), 4497–4559. https://doi.org/10.1039/c5py00263j.

(8) Zhao, H.; Holladay, J. E.; Brown, H.; Zhang, Z. C. Metal Chlorides in Ionic Liquid Solvents Convert Sugars to 5-Hydroxymethylfurfural. *Science.* **2007**, *316* (5831), 1597–1600. https://doi.org/10.1126/science.1141199.

(9) Pidko, E. A.; Degirmenci, V.; Van Santen, R. A.; Hensen, E. J. M. Glucose Activation by Transient Cr2+ Dimers. *Angew. Chem. Int. Ed.* **2010**, *49* (14), 2530–2534. https://doi.org/10.1002/anie.201000250.

(10) Nikolla, E.; Román-Leshkov, Y.; Moliner, M.; Davis, M. E. "One-Pot" Synthesis of 5-(Hydroxymethyl)Furfural from Carbohydrates Using Tin-Beta Zeolite. *ACS Catal.* **2011**, *1* (4), 408–410. https://doi.org/10.1021/cs2000544.

(11) Nakajima, K.; Baba, Y.; Noma, R.; Kitano, M.; N. Kondo, J.; Hayashi, S.; Hara, M. Nb_2O_5•nH2O as a Heterogeneous Catalyst with Water-Tolerant Lewis Acid Sites. *J. Am. Chem. Soc.* **2011**, *133* (12), 4224–4227. https://doi.org/10.1021/ja110482r.

(12) Noma, R.; Nakajima, K.; Kamata, K.; Kitano, M.; Hayashi, S.; Hara, M. Formation of 5-(Hydroxymethyl)Furfural by Stepwise Dehydration over TiO_2 with Water-Tolerant Lewis Acid Sites. *J. Phys. Chem. C* **2015**, *119* (30), 17117–17125. https://doi.org/10.1021/acs.jpcc.5b03290.

(13) Yue, C.; Li, G.; Pidko, E. A.; Wiesfeld, J. J.; Rigutto, M.; Hensen, E. J. M. Dehydration of Glucose to 5-Hydroxymethylfurfural Using Nb-Doped Tungstite.

ChemSusChem **2016**, *9* (17), 2421–2429. https://doi.org/10.1002/cssc.201600649.

(14) Li, G.; Pidko, E. A.; Hensen, E. J. M.; Nakajima, K. A Density Functional Theory Study of the Mechanism of Direct Glucose Dehydration to 5-Hydroxymethylfurfural on Anatase Titania. *ChemCatChem* **2018**, *10* (18), 4084–4089. https://doi.org/10.1002/cctc.201800900.

(15) Takeda, Y.; Tamura, M.; Nakagawa, Y.; Okumura, K.; Tomishige, K. Hydrogenation of Dicarboxylic Acids to Diols over Re-Pd Catalysts. *Catal. Sci. Technol.* **2016**, *6* (14), 5668–5683. https://doi.org/10.1039/c6cy00335d.

(16) Tamura, M.; Tokonami, K.; Nakagawa, Y.; Tomishige, K. Rapid Synthesis of Unsaturated Alcohols under Mild Conditions by Highly Selective Hydrogenation. *Chem. Commun.* **2013**, *49* (63), 7034–7036. https://doi.org/10.1039/c3cc41526k.

(17) Thompson, S. T.; Lamb, H. H. Palladium-Rhenium Catalysts for Selective Hydrogenation of Furfural: Evidence for an Optimum Surface Composition. *ACS Catal.* **2016**, *6* (11), 7438–7447. https://doi.org/10.1021/acscatal.6b01398.

(18) Wiesfeld, J. J.; Kim, M.; Nakajima, K.; Hensen, E. J. M. Selective Hydrogenation of 5-Hydroxymethylfurfural and Its Acetal with 1,3-Propanediol to 2,5-Bis(Hydroxymethyl)Furan Using Supported Rhenium-Promoted Nickel Catalysts in Water. *Green Chem.* **2020**, *22* (4), 1229–1238. https://doi.org/10.1039/c9gc03856f.

(19) Buntara, T.; Noel, S.; Phua, P. H.; Melián-Cabrera, I.; De Vries, J. G.; Heeres, H. J. Caprolactam from Renewable Resources: Catalytic Conversion of 5-

Hydroxymethylfurfural into Caprolactone. *Angew. Chem. Int. Ed.* **2011**, *50* (31), 7083–7087. https://doi.org/10.1002/anie.201102156.

(20) Kong, X.; Zheng, R.; Zhu, Y.; Ding, G.; Zhu, Y.; Li, Y. W. Rational Design of Ni-Based Catalysts Derived from Hydrotalcite for Selective Hydrogenation of 5-Hydroxymethylfurfural. *Green Chem.* **2015**, *17* (4), 2504–2514. https://doi.org/10.1039/c5gc00062a.

(21) Chen, J.; Liu, R.; Guo, Y.; Chen, L.; Gao, H. Selective Hydrogenation of Biomass-Based 5-Hydroxymethylfurfural over Catalyst of Palladium Immobilized on Amine-Functionalized Metal-Organic Frameworks. *ACS Catal.* **2015**, *5* (2), 722–733. https://doi.org/10.1021/cs5012926.

(22) Nakagawa, Y.; Takada, K.; Tamura, M.; Tomishige, K. Total Hydrogenation of Furfural and 5-Hydroxymethylfurfural over Supported Pd-Ir Alloy Catalyst. *ACS Catal.* **2014**, *4* (8), 2718–2726. https://doi.org/10.1021/cs500620b.

(23) Nakagawa, Y.; Tomishige, K. Total Hydrogenation of Furan Derivatives over Silica-Supported Ni-Pd Alloy Catalyst. *Catal. Commun.* **2010**, *12* (3), 154–156. https://doi.org/10.1016/j.catcom.2010.09.003.

(24) Yao, S.; Wang, X.; Jiang, Y.; Wu, F.; Chen, X.; Mu, X. One-Step Conversion of Biomass-Derived 5-Hydroxymethylfurfural to 1,2,6-Hexanetriol over Ni-Co-Al Mixed Oxide Catalysts under Mild Conditions. *ACS Sustain. Chem. Eng.* **2014**, *2* (2), 173–180. https://doi.org/10.1021/sc4003714.

(25) Buntara, T.; Melián-Cabrera, I.; Tan, Q.; Fierro, J. L. G.; Neurock, M.; De Vries, J. G.; Heeres, H. J. Catalyst Studies on the Ring Opening of Tetrahydrofuran-

Dimethanol to 1,2,6-Hexanetriol. *Catal. Today* **2013**, *210*, 106–116. https://doi.org/10.1016/j.cattod.2013.04.012.

(26) Gilkey, M. J.; Mironenko, A. V.; Yang, L.; Vlachos, D. G.; Xu, B. Insights into the Ring-Opening of Biomass-Derived Furanics over Carbon-Supported Ruthenium. *ChemSusChem* **2016**, *9* (21), 3113–3121. https://doi.org/10.1002/cssc.201600681.

(27) Casanova, O.; Iborra, S.; Corma, A. Biomass into Chemicals: Aerobic Oxidation of 5-Hydroxymethyl-2-Furfural into 2,5-Furandicarboxylic Acid with Gold Nanoparticle Catalysts. *ChemSusChem* **2009**, *2* (12), 1138–1144. https://doi.org/10.1002/cssc.200900137.

(28) Casanova, O.; Iborra, S.; Corma, A. Biomass into Chemicals: One Pot-Base Free Oxidative Esterification of 5-Hydroxymethyl-2-Furfural into 2,5-Dimethylfuroate with Gold on Nanoparticulated Ceria. *J. Catal.* **2009**, *265* (1), 109–116. https://doi.org/10.1016/j.jcat.2009.04.019.

(29) Gupta, N. K.; Nishimura, S.; Takagaki, A.; Ebitani, K. Hydrotalcite-Supported Gold-Nanoparticle-Catalyzed Highly Efficient Base-Free Aqueous Oxidation of 5-Hydroxymethylfurfural into 2,5-Furandicarboxylic Acid under Atmospheric Oxygen Pressure. *Green Chem.* **2011**, *13* (4), 824–827. https://doi.org/10.1039/c0gc00911c.

(30) Sajid, M.; Zhao, X.; Liu, D. Production of 2,5-Furandicarboxylic Acid (FDCA) from 5-Hydroxymethylfurfural (HMF): Recent Progress Focusing on the Chemical-Catalytic Routes. *Green Chem.* **2018**, *20* (24), 5427–5453.

https://doi.org/10.1039/c8gc02680g.

(31) Hayashi, E.; Yamaguchi, Y.; Kamata, K.; Tsunoda, N.; Kumagai, Y.; Oba, F.; Hara, M. Effect of MnO_2 Crystal Structure on Aerobic Oxidation of 5-Hydroxymethylfurfural to 2,5-Furandicarboxylic Acid. *J. Am. Chem. Soc.* **2019**, *141* (2), 899–900. https://doi.org/10.1021/jacs.8b09917.

(32) Woroch, C. P.; Lankenau, A. W.; Kanan, M. W. A High-T g Polyamide Derived from Lignocellulose and CO_2. https://doi.org/10.1021/acs.macromol.1c01547.

(33) Lankenau, A. W.; Kanan, M. W. Polyamide Monomers via Carbonate-Promoted C–H Carboxylation of Furfurylamine. *Chem. Sci.* **2019**, *11* (1), 248–252. https://doi.org/10.1039/C9SC04460D.

(34) Singh, H.; Arora, K.; Tapadar, S.; Chakraborty, T. K. Preferential Polymerization of 5-(Aminomethyl)-2-Furancarboxylic Acid (AMFC) into a Cyclic Tripeptide. *J. Theor. Comput. Chem.* **2004**, *3* (4), 555–566. https://doi.org/10.1142/S0219633604001203.

(35) Chakraborty, T. K.; Arora, A.; Roy, S.; Kumar, N.; Maiti, S. Furan Based Cyclic Oligopeptides Selectively Target G-Quadruplex. *J. Med. Chem* **2007**, *50*, 5539–5542. https://doi.org/10.1021/jm070619c.

(36) Boonyakarn, T.; Wiesfeld, J. J.; Asakawa, M.; Chen, L.; Fukuoka, A.; Hensen, E. J. M.; Nakajima, K. Effective Oxidation of 5-Hydroxymethylfurfural to 2,5-Diformylfuran by an Acetal Protection Strategy. *ChemSusChem* **2022**, *15* (7), e202200059. https://doi.org/10.1002/CSSC.202200059.

(37) Wiesfeld, J. J.; Asakawa, M.; Aoshima, T.; Fukuoka, A.; Emiel,]; Hensen, J. M.;

Nakajima, K. A Catalytic Strategy for Selective Production of 5-Formylfuran-2-Carboxylic Acid and Furan-2,5-Dicarboxylic Acid. *ChemCatChem* **2022**, e202200191. https://doi.org/10.1002/CCTC.202200191.

(38) Kim, M.; Su, Y.; Fukuoka, A.; Hensen, E. J. M.; Nakajima, K. Aerobic Oxidation of 5-(Hydroxymethyl)Furfural Cyclic Acetal Enables Selective Furan-2,5-Dicarboxylic Acid Formation with CeO_2-Supported Gold Catalyst. *Angew. Chem. Int. Ed.* **2018**, *57* (27), 8235–8239. https://doi.org/10.1002/anie.201805457.

(39) Beydoun, K.; Ghattas, G.; Thenert, K.; Klankermayer, J.; Leitner, W. Ruthenium-Catalyzed Reductive Methylation of Imines Using Carbon Dioxide and Molecular Hydrogen. *Angew. Chem. Int. Ed. Engl.* **2014**, *53* (41), 11010–11014. https://doi.org/10.1002/ANIE.201403711.

(40) Zhu, S.; Lu, X.; Luo, Y.; Zhang, W.; Jiang, H.; Yan, M.; Zeng, W. Ruthenium(II)-Catalyzed Regioselective Reductive Coupling of α-Imino Esters with Dienes. *Org. Lett.* **2013**, *15* (7), 1440–1443. https://doi.org/10.1021/OL4006079.

(41) Zhu, M. Ruthenium-Catalyzed Direct Reductive Amination in HCOOH/NEt3 Mixture. *Catal. Lett. 2014 1449* **2014**, *144* (9), 1568–1572. https://doi.org/10.1007/S10562-014-1314-5.

(42) Chatterjee, M.; Ishizaka, T.; Kawanami, H. Reductive Amination of Furfural to Furfurylamine Using Aqueous Ammonia Solution and Molecular Hydrogen: An Environmentally Friendly Approach. *Green Chem.* **2016**, *18* (2), 487–496.

https://doi.org/10.1039/c5gc01352f.

(43) Kolobova, E.; Mäki-Arvela, P.; Pestryakov, A.; Pakrieva, E.; Pascual, L.; Smeds, A.; Rahkila, J.; Sandberg, T.; Peltonen, J.; Murzin, D. Y. Reductive Amination of Ketones with Benzylamine Over Gold Supported on Different Oxides. *Catal. Lett. 2019 14912* **2019**, *149* (12), 3432–3446. https://doi.org/10.1007/S10562-019-02917-1.

(44) Chen, W.; Sun, Y.; Du, J.; Si, Z.; Tang, X.; Zeng, X.; Lin, L.; Liu, S.; Lei, T. Preparation of 5-(Aminomethyl)-2-Furanmethanol by Direct Reductive Amination of 5-Hydroxymethylfurfural with Aqueous Ammonia over the Ni/SBA-15 Catalyst. *J. Chem. Technol. Biotechnol.* **2018**, *93* (10), 3028–3034. https://doi.org/10.1002/JCTB.5661.

(45) Bódis, J.; Lefferts, L.; Müller, T. E.; Pestman, R.; Lercher, J. A. Activity and Selectivity Control in Reductive Amination of Butyraldehyde over Noble Metal Catalysts. *Catal. Lett. 2005 1041* **2005**, *104* (1), 23–28. https://doi.org/10.1007/S10562-005-7431-4.

(46) Liang, G.; Wang, A.; Li, L.; Xu, G.; Yan, N.; Zhang, T. Production of Primary Amines by Reductive Amination of Biomass-Derived Aldehydes/Ketones. *Angew. Chem. Int. Ed.* **2017**, *56* (11), 3050–3054. https://doi.org/10.1002/anie.201610964.

(47) Sha, J.; Kusema, B. T.; Zhou, W.-J.; Yan, Z.; Streiff, S.; Pera-Titus, M. Single-Reactor Tandem Oxidation–Amination Process for the Synthesis of Furan Diamines from 5-Hydroxymethylfurfural. *Green Chem.* **2021**, *23* (18), 7093–

7099. https://doi.org/10.1039/D1GC01621K.

(48) Komanoya, T.; Kinemura, T.; Kita, Y.; Kamata, K.; Hara, M. Electronic Effect of Ruthenium Nanoparticles on Efficient Reductive Amination of Carbonyl Compounds. *J. Am. Chem. Soc.* **2017**, *139* (33), 11493–11499. https://doi.org/10.1021/JACS.7B04481.

(49) Nugent, T. C.; Wakchaure, V. N.; Ghosh, A. K.; Mohanty, R. R. Evolution of Titanium(IV) Alkoxides and Raney Nickel for Asymmetric Reductive Amination of Prochiral Aliphatic Ketones. *Org. Lett.* **2005**, *7* (22), 4967–4970. https://doi.org/10.1021/OL051909V.

(50) Wei, Z.; Cheng, Y.; Zhou, K.; Zeng, Y.; Yao, E.; Li, Q.; Liu, Y.; Sun, Y. One-Step Reductive Amination of 5-Hydroxymethylfurfural into 2,5-Bis(Aminomethyl)Furan over Raney Ni. *ChemSusChem* **2021**. https://doi.org/10.1002/cssc.202100564.

(51) Zhou, K.; Chen, B.; Zhou, X.; Kang, S.; Xu, Y.; Wei, J. Selective Synthesis of Furfurylamine by Reductive Amination of Furfural over Raney Cobalt. *ChemCatChem* **2019**, *11* (22), 5562–5569. https://doi.org/10.1002/CCTC.201901269.

(52) Ertl, G.; Knozinger, H.; Weitkamp, J. Preparation of Solid Catalysts. *Prep. Solid Catal.* **2008**, 1–622. https://doi.org/10.1002/9783527619528.

(53) Hangkong Yuan; T. Kusema, B.; Zhen Yan; Stéphane Streiff; Feng Shi. Highly Selective Synthesis of 2,5-Bis(Aminomethyl)Furan via Catalytic Amination of 5-(Hydroxymethyl)Furfural with NH 3 over a Bifunctional Catalyst. *RSC Adv.*

2019, *9* (66), 38877–38881. https://doi.org/10.1039/C9RA08560B.

(54) Chatterjee, M.; Ishizaka, T.; Kawanami, H. Reductive Amination of Furfural to Furfurylamine Using Aqueous Ammonia Solution and Molecular Hydrogen: An Environmentally Friendly Approach. *Green Chem.* **2016**, *18* (2), 487–496. https://doi.org/10.1039/C5GC01352F.

(55) Le, N.-T.; Byun, A.; Han, Y.; Lee, K.-I.; Kim, H. Preparation of 2,5-Bis(Aminomethyl)Furan by Direct Reductive Amination of 2,5-Diformylfuran over Nickel-Raney Catalysts. *Green Sustain. Chem.* **2015**, *05* (03), 115–127. https://doi.org/10.4236/gsc.2015.53015.

(56) Qi, H.; Liu, F.; Zhang, L.; Li, L.; Su, Y.; Yang, J.; Hao, R.; Wang, A.; Zhang, T. Modulating: Trans -Imination and Hydrogenation towards the Highly Selective Production of Primary Diamines from Dialdehydes. *Green Chem.* **2020**, *22* (20), 6897–6901. https://doi.org/10.1039/d0gc02280b.

(57) Sheng, M.; Fujita, S.; Yamaguchi, S.; Yamasaki, J.; Nakajima, K.; Yamazoe, S.; Mizugaki, T.; Mitsudome, T. Single-Crystal Cobalt Phosphide Nanorods as a High-Performance Catalyst for Reductive Amination of Carbonyl Compounds. *JACS Au* **2021**, *1* (4), 501–507. https://doi.org/10.1021/jacsau.1c00125.

(58) Mitsudome, T.; Sheng, M.; Nakata, A.; Yamasaki, J.; Mizugaki, T.; Jitsukawa, K. A Cobalt Phosphide Catalyst for the Hydrogenation of Nitriles. *Chem. Sci.* **2020**, *11* (26), 6682–6689. https://doi.org/10.1039/d0sc00247j.

(59) Yuan, Z.; Liu, B.; Zhou, P.; Zhang, Z.; Chi, Q. Preparation of Nitrogen-Doped Carbon Supported Cobalt Catalysts and Its Application in the Reductive

Amination. *J. Catal.* **2019**, *370*, 347–356. https://doi.org/10.1016/J.JCAT.2019.01.004.

(60) Sheng, M.; Fujita, S.; Yamaguchi, S.; Yamasaki, J.; Nakajima, K.; Yamazoe, S.; Mizugaki, T.; Mitsudome, T. Single-Crystal Cobalt Phosphide Nanorods as a High-Performance Catalyst for Reductive Amination of Carbonyl Compounds. *JACS Au* **2021**, *1* (4), 501–507. https://doi.org/10.1021/JACSAU.1C00125.

(61) Singh, J. A.; Yang, N.; Liu, X.; Tsai, C.; Stone, K. H.; Johnson, B.; Koh, A. L.; Bent, S. F. Understanding the Active Sites of CO Hydrogenation on Pt-Co Catalysts Prepared Using Atomic Layer Deposition. *J. Phys. Chem. C* **2018**, *122* (4), 2184–2194. https://doi.org/10.1021/ACS.JPCC.7B10541.

(62) Fujita, S.; Yamaguchi, S.; Yamasaki, J.; Nakajima, K.; Yamazoe, S.; Mizugaki, T.; Mitsudome, T. Ni_2P Nanoalloy as an Air-Stable and Versatile Hydrogenation Catalyst in Water: P-Alloying Strategy for Designing Smart Catalysts. *Chem. – A Eur. J.* **2021**, *27* (13), 4439–4446. https://doi.org/10.1002/CHEM.202005037.

(63) Wang, H.; Xu, K.; Yao, X.; Ye, D.; Pei, Y.; Hu, H.; Qiao, M.; Li, Z. H.; Zhang, X.; Zong, B. Undercoordinated Site-Abundant and Tensile-Strained Nickel for Low-Temperature CO_x Methanation. *ACS Catal.* **2018**, *8* (2), 1207–1211. https://doi.org/10.1021/ACSCATAL.7B02944.

(64) Hartfelder, U.; Kartusch, C.; Makosch, M.; Rovezzi, M.; Sá, J.; Van Bokhoven, J. A. Particle Size and Support Effects in Hydrogenation over Supported Gold Catalysts. *Catal. Sci. Technol.* **2013**, *3* (2), 454–461. https://doi.org/10.1039/C2CY20485A.

(65) Wang, M.; Feng, B.; Li, H.; Li, H. Controlled Assembly of Hierarchical Metal Catalysts with Enhanced Performances. *Chem* **2019**, *5* (4), 805–837. https://doi.org/10.1016/J.CHEMPR.2019.01.003.

(66) Qi, H.; Liu, F.; Zhang, L.; Li, L.; Su, Y.; Yang, J.; Hao, R.; Wang, A.; Zhang, T. Modulating: Trans -Imination and Hydrogenation towards the Highly Selective Production of Primary Diamines from Dialdehydes. *Green Chem.* **2020**, *22* (20), 6897–6901. https://doi.org/10.1039/d0gc02280b.

(67) Shen, H.; Shan, H.; Liu, L. Evolution Process and Controlled Synthesis of Humins with 5-Hydroxymethylfurfural (HMF) as Model Molecule. *ChemSusChem* **2020**, *13* (3), 513–519. https://doi.org/10.1002/CSSC.201902799.

(68) Song, S.; Wang, Y.; Yan, N. A Remarkable Solvent Effect on Reductive Amination of Ketones. *Mol. Catal.* **2018**, *454*, 87–93. https://doi.org/10.1016/J.MCAT.2018.05.017.

Chapter 4

Reductive amination of FFCA-acetal to 5-aminomethylfuran-2-carboxylic acid

Abstract

This study presents the role of FFCA-acetal (dimethyl acetal form of FFCA) in reductive amination using catalytic cobalt phosphide nanorods (Co_2P NRs). Strongly alkaline methanolic ammonia solutions, commonly used for reductive amination, caused severe degradation of FFCA, but no degradation occurred when using FFCA-acetal. AMFCA was directly produced in 97% selectivity from FFCA-acetal in methanolic ammonia solution without production of the free aldehyde (FFCA) as intermediate. The acetal protected the aldehyde from any side reactions, but the alkaline environment and absence of water retarded the reaction rate significantly. Reductive amination of FFCA-acetal using ammonium acetate (NH_4OAc) as an amphoteric nitrogen source in methanol:water mixtures was faster than when using ammonia in anhydrous conditions. In this case, FFCA was detected as the more acidic and aqueous conditions caused some hydrolysis of the dimethyl acetal. The rate for AMFCA formation was improved using an optimized ratio of methanol:water 2:1 v/v (80 mmol g-cat^{-1} h $^{-1}$) compared to pure methanol (30 mmol g-cat^{-1} h $^{-1}$). Under optimized conditions, i.e., 0.5 mmol of FFCA-acetal, 5 mmol of NH_4OAc, substrate to catalyst (Co_2P NRs) ratio of 10 mol/mol, under 0.5 MPa H_2 at 393 K for 3 hours in methanol/water 2:1 v/v, a 91% yield of AMFCA was

achieved at full conversion.

4.1 Introduction

Acetalization is a well-known protection strategy to shield aldehydes from side reactions.[1–3] Acetal protection strategy has recently been applied to the production of many valuable furanics from HMF-acetal such as 2,5-furandicarboxylic acid (FDCA), 2,5-furandimethylcarboxylate (2,5-FDMC), 2,5-furandi-2-hydroyethylcarboxylate (2,5 FDHEC) and 2,5-bishydroxymethylfuran (BHMF) in Scheme 4.1.[4–6]

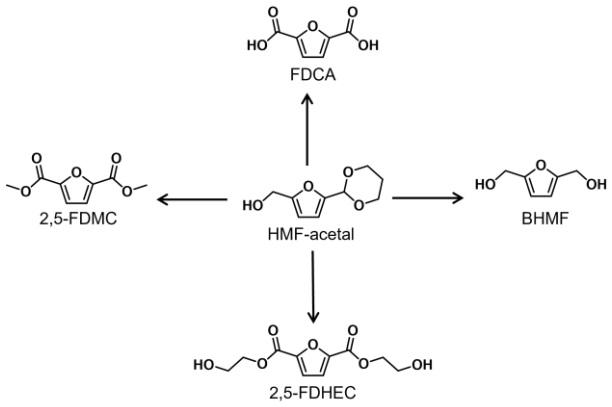

Scheme 4.1. Reaction pathways to several valuable compounds obtainable from HMF-acetal.

With regards to this thesis; I oxidized the acetal form of HMF with 1,3-propanediol (HMF-acetal) using Ru/γ-Al_2O_3- in DMF as a solvent and obtained high DFF-acetal yields (~80%) from 10-50 wt% HMF-acetal solutions.[1] Both HMF-acetal and DFF-acetal were more stable than HMF and DFF. In chapter 3, I focused on reductive amination of FFCA to AMFCA using Co_2P NRs catalyst and NH_4OAc. AMFCA could be obtained in 90% yield from FFCA in a methanol-water mixture. Interestingly, a

significant amount of FFCA was converted to FFCA-acetal prior to the reaction. We found that the increase in FFCA-acetal content results in high AMFCA yield and selectivity in methanol-water-mixture. Our assumption is that the acetal not only protects the aldehyde of FFCA from side reactions but could also be involved in the reductive amination mechanism. Thus, kinetic studies were used to evaluate the role of acetal functionality toward the reductive amination rate by comparison with FFCA to reveal the reaction mechanism in the reductive amination of FFCA-acetal.

4.2 Experimental

4.2.1 Materials

Acetone, acetonitrile, chloroform, ammonium acetate, N,N-dimethlyformamide Super dehydrated (DMF), and ZrO_2 were purchased from FUJIFILM Wako Pure Chemical Corporation. HMF was procured from Sigma-Aldrich. AMFCA was purchased from Fluorochem Ltd. Hexadecylamine, Triphenyl phosphite, 1-octadecene, methanol-d_4, and DFF, and FFCA were obtained from Tokyo Chemical Industry (TCI). 5-Hydroxymethyl-2-furan carboxylic acid (HMFCA) was purchased from Combi-Blocks Inc. Aerosil-380 (SiO_2) was obtained from Evonic industries and Ajinomoto Fine-Techno Corporation, respectively. Cobalt(II) acetylacetonate dihydrate ($Co(acac)_2 \cdot 2H_2O$) was purchased from Mitsuwa pure chemicals. Deuterium oxide and dipotassium hydrogenphosphate were purchased from Kanto chemical corporation. Nb_2O_5 (JRC-NBO-1) and CeO_2 (JRC-CEO-5), are a reference catalyst supplied from the Catalyst Society of Japan. Co_2P commercial catalyst was procured from Santa Cruz Biotechnology, Inc.

4.2.2 Catalyst preparation

In a typical synthesis, the mixture of $Co(acac)_2 \cdot 2H_2O$ (2 mmol), 1-octadecene (10 mL), and triphenylphosphine (5.4 mL) were heated stepwise at 150 °C for 1 h and at 300 °C for 3 h under a N_2 flow. After the heat treatment, the mixture was cooled down in air to room temperature and the resulting precipitate was washed with a chloroform-acetone mixture. The obtained powder was dried at room temperature in vacuo overnight.

4.2.3 Synthetic procedure for FFCA-acetal

FFCA (500 mg) was added to a mixture of trimethyl orthoformate (2 mL), and methanol (50 mL). After stirring at room temperature for 24 h, solvent was removed by vacuum evaporation to obtain FFCA-acetal. NMR assignment of 5-(1,1'-dimethoxymethyl) furan-2-yl methyl carboxylic acid (FFCA-acetal): 1H NMR (400 MHz, Methanol-d4): 7.11 (d, 1H), 6.55 (d, 1H), 5.42 (s, 1H), 4.83 (s, 2H), 3.77 (s, 6H). Materials, catalyst preparation, synthetic FFCA-acetal, and catalyst characterization were similar to previous chapter and was provided in experiment section of chapter 3.

4.2.4 Catalytic experiments

Catalytic activity was tested in 10 mL SUS-316 stainless steel batch reactors equipped with a PTFE liner. 0.5 mmol of FFCA-acetal, 0-3 mL of methanol-d_4 (MeOD) and/or deuterium oxide (D_2O), and (0.05 mmol)) of catalyst based on Co content were charged into the reactor, which was subsequently pressurized with hydrogen to 0.5 MPa and heated in an oil bath at 393 K. After a specified reaction period, the reactor was cooled to room temperature, and products were analyzed by High-Performance Liquid

Chromatography (HPLC). The quantification of HMFCA, AMFCA, FFCA-acetal, and FFCA was conducted by HPLC (SHIMADZU, Japan) consisting of a RID-10A detector, a UV-SPD-20A detector, and an Shodex ODP_2 HP-4E column (column temp., 313 K). A mixture of a diluted K_2HPO_4 aqueous solution (0.02 M, pH=9.5, 23 vol%) and acetonitrile (77 vol%) was used as the eluent at a flow rate of 0.4 mL min^{-1}. The retention time for FFCA-acetal, FFCA, HMFCA, and AMFCA was 5.3, 5.8, 6.5, and 7.5 min, respectively. Secondary imine was directly analyzed by ^1H NMR spectrometry (ECX 400, JEOL Ltd.).

4.3 Results and discussion

4.3.1 Reductive amiantion of FFCA-acetal in pure methnanol

Ammonium acetate (NH_4OAc) and ammonia (NH_3) were used as nitrogen sources to examine the reductive amination of FFCA-acetal using Co_2P NRs catalyst. The reactions were conducted at 393 K in methanol under 0.5 MPa H_2 pressure with a substrate to Co_2P NRs ratio of 10 mol/mol. Figure 4.1 shows time courses for FFCA-acetal conversion and product yields. AMFCA was obtained in 72% yield with 97% selectivity after 6 h, with negligible amount of bare FFCA by the hydrolysis of FFCA-acetal. The rate for AMFCA formation at 20% FFCA-acetal conversion is estimated as 25 mmol g-cat^{-1} h^{-1}. FFCA-acetal was stable under the reaction conditions and stayed intact as evidenced by the formation of no undetectable byproduct. The reaction mixture is a non-aqueous and basic solution that stabilizes acetal moiety against side reactions as well as the hydrolysis to formyl group. The formation of AMFCA from FFCA-acetal in a water-free solvent suggests that FFCA-acetal is not simply converted to AMFCA via non-protected FFCA and this route is highly selective (97% selectivity). One issue of this

system is the small reaction rate compared to those in Chapter 3. This is most likely due to high stability of acetal moiety in FFCA-acetal in a non-aqueous and highly basic solution.

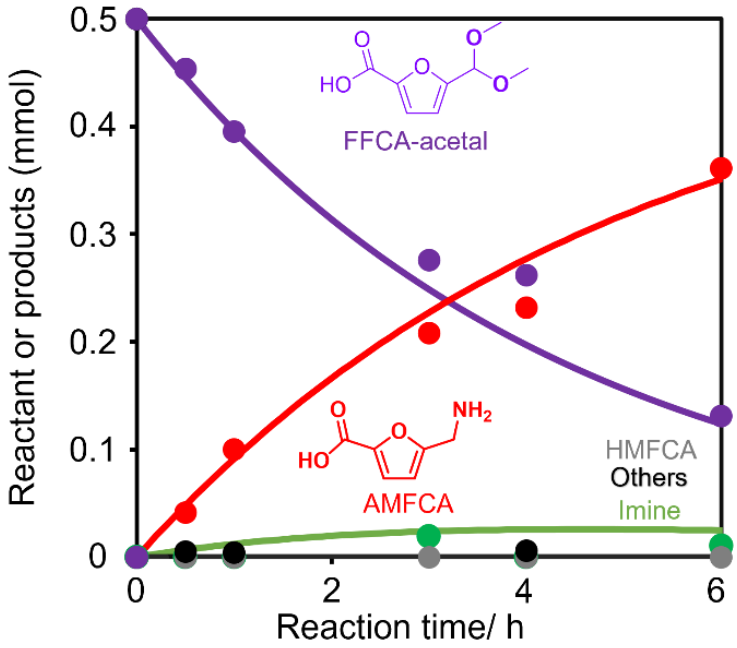

Figure 4.1. Reductive amination of FFCA-acetal in methanol: substrate 0.5 mmol; solvent, (3 mL), NH_3 (5 mmol); catalyst, Co_2P NRs catalyst (0.05 mmol); hydrogen pressure, 0.5 MPa; temperature, 393 K.

I speculated that hemiacetal form of FFCA-acetal plays a key role in this mechanism. Figures 4.2 and 4.3 shows presumable reaction path in the reductive amination of FFCA-acetal to AMFCA with NH_3. FFCA-acetal is first converted to its hemiacetal form with a tiny amount of water at a contamination level and the hemiacetal is directly converted to undetectable primary amine with NH_3 (monomolecular path, Figure 4.2) or detectable secondary amine with AMFCA (bimolecular path, Figure 4.3). The primary amine is hydrogenated with Co_2P NRs catalyst to AMFCA, while the secondary imine is reacted with NH_3 to form an intermediate **(g)** and its hydrogenation produces two molecules of AMFCA.

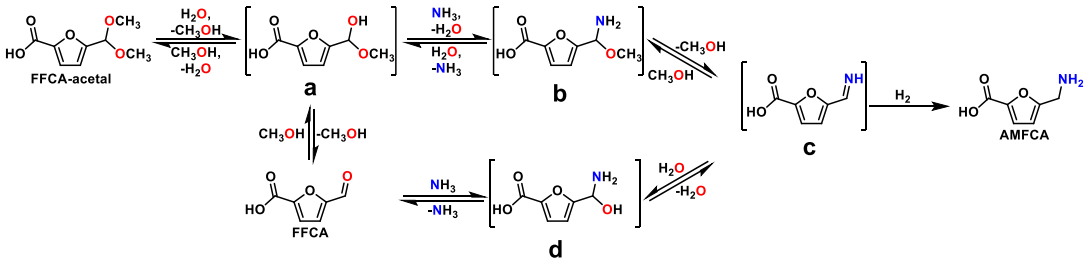

Figure 4.2. Mono-molecule pathway in the reductive amination of FFCA-acetal

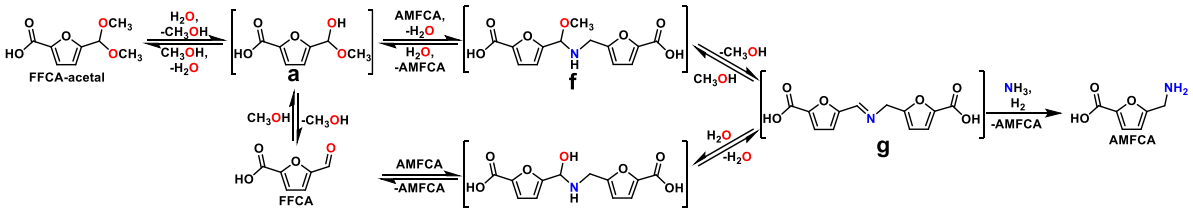

Figure 4.3. Bi-molecule pathway in the reductive amination of FFCA-acetal

Figure 4.4 shows time courses for FFCA-acetal conversion and product yields when the reactions were conducted with NH_4OAc instead of NH_3. FFCA-acetal was converted to AMFCA in 90% yield and 97% selectivity at 6 hours. The rate for AMFCA formation at 29% conversion is estimated as 30 mmol g-cat^{-1} h $^{-1}$, which is slightly larger than that with NH_3 (25 mmol g-cat^{-1} h $^{-1}$) as shown in Figure 4.1. This difference can be explained by two reasons. Acetal moiety in FFCA-acetal is reactive toward the reductive amination in methanol-NH_4OAc system due to less basicity compared to methanol-NH_3 system. The addition of NH_4OAc increase in water content in methanol, due to the physisorbed water of NH_4OAc. Water in the reaction mixture hydrolyzed a part of FFCA-acetal, giving bare FFCA during the reaction. However, the yields of non-protected FFCA were kept low (<5%) during the reaction. The formation of bare FFCA is less important for efficient AMFCA formation because free FFCA is involved in side-reactions forming undetectable byproducts under the reaction conditions (entries 5 and 9 of Table 3.3 in chapter 3). Therefore, mono-molecular and bi-molecular pathways via hemiacetal form of FFCA-acetal is also predominant in this reaction system.

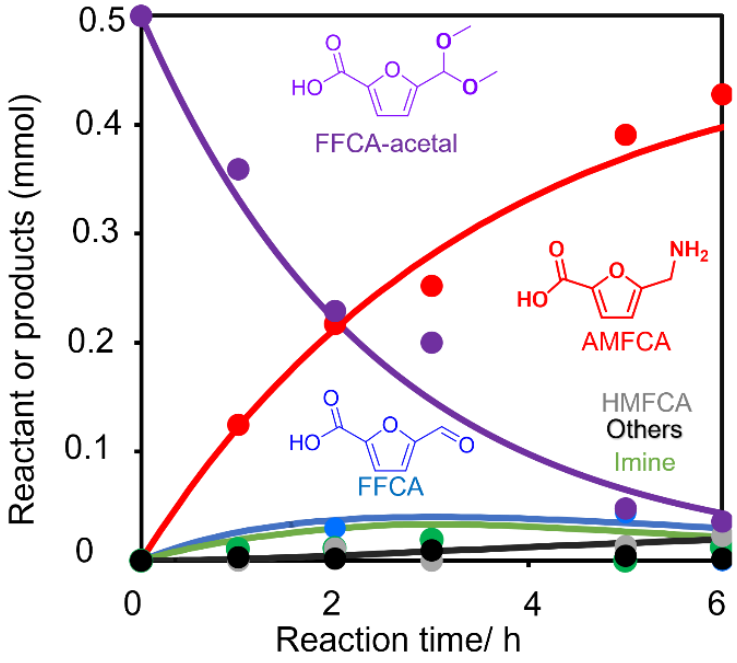

Figure 4.4. Reductive amination of FFCA-acetal in methanol: substrate 0.5 mmol; solvent, (3 mL), NH_4OAc (5 mmol); catalyst, Co_2P NRs catalyst (0.05 mmol); hydrogen pressure, 0.5 MPa; temperature, 393 K.

4.3.2 Effect of methanol:water on reductive amiantion of acetal

Focusing on the effect of water to accelerate AMFCA formation from FFCA-acetal, reductive amination of FFCA-acetal was further investigated at 393 K for 1 hour under 0.5 MPa H_2 atmosphere using Co_2P NRs with NH_4OAc in methanol-water mixture with varying ratios (Table 4.1). In pure water (entry 1), FFCA-acetal was quickly hydrolyzed to FFCA, which was obtained in 82% yield after 3 hours. Most of FFCA stayed unreacted and AMFCA was obtained in 15% yield. AMFCA yields increased with increasing methanol content, up to a maximum AMFCA yield of 65% in methanol:water ratio of 2:1 v/v as shown in Table 4.1, entry 3.

Table 4.1 Reductive amination of FFCA-acetal with different

#	MeOH-H_2O mixture			Product yield (%)				
	MeOH (mL)	H_2O (mL)	conv. (%)	FFCA	AMFCA	HMFCA	Imine	Others[1]
1	0	3	100	82	15	0	0	3
2	1.75	1.25	99	34	52	2	4	7
3	**2**	**1**	**95**	**22**	**65**	**2**	**4**	**2**
4	2.25	0.75	91	22	55	4	8	2
5	2.5	0.5	85	23	47	3	10	2
6	2.75	0.25	55	9	43	0	2	1
7	2.9	0.1	47	9	33	2	2	1
8	3	0	30	0	28	0	2	0

Conditions: FFCA-acetal 0.5 mmol; solvent, (3 mL) NH_4OAc (5 mmol); catalyst, Co_2P NRs catalyst (0.05 mmol); hydrogen pressure, 0.5 MPa; temperature, 393 K; time, 60 min.

However, FFCA-acetal conversion, FFCA yield, and AMFCA yield significantly decreased with methanol:water ratios greater than 2:1 v/v (entries 3-8). Low conversion and AMFCA yield at high methanol contents mean that FFCA-acetal is stable in methanol-rich solutions and converted to AMFCA at a small reaction rate. The rection in pure methanol (entry 8) afforded low conversion (30%) and low AMFCA yield (28%) but high AMFCA selectivity (93%). Any free FFCA cannot be detected in this system, which means that reductive amination of FFCA-acetal proceeds without the formation of free FFCA as shown in Figure 4.1. The presence of water accelerates reductive amination of FFCA-acetal. In terms of conversion and AMFCA yield, methanol/water 2:1 v/v was selected as solvent mixture for further study. The optimal methanol-water ratio identified

here is the same completely with that in the reductive amination of non-protected FFCA with NH_4OAc as shown in table 3.3 in chapter 3. Next, kinetic studies in the reductive amination of FFCA-acetal were conducted at the optimal methanol-water ratio.

4.1.1 Reductive amiantion of FFCA-acetal in methanol-water (2:1 v/v) mixture

Figure 4.5 (A) shows time courses in the reductive amination of FFCA-acetal at 393 K under 0.5 MPa H_2 atmosphere using Co_2P NRs in methanol:water ratio of 2:1 (v/v) using NH_4OAc. AMFCA was obtained in 0.46 mmol (~91% yield) for 3 h at full conversion. Due to the presence of water, FFCA-acetal was partially hydrolyzed to FFCA, which was maximized at 0.11 mmol (22% yield) at 30 min. Secondary imine as an intermediate was formed as an intermediate in around 0.03 mmol during the reaction. Moreover, low levels of undetectable byproducts and HMFCA were obtained in a combined amount of approximately 0.03 mmol (~5% yield).

These results are compared to those of FFCA under the same reaction conditions. Figure 4.5(B) shows the reductive amination of FFCA at 393 K under 0.5 MPa H_2 atmosphere using Co_2P NRs in methanol:water ratio of 2:1 (v/v) using NH_4OAc. FFCA-acetal was fully retained in its acetal form at 0 hours (Figure 4.5(A)), while the reaction mixture in Figure 4.5(B) contained equal amounts of FFCA and FFCA-acetal before the reaction. FFCA contents in Figure 4.5(A) was always low compared to those in Figure 4.5(B). Note that rates for AMFCA formation in Figures 4.5(A) and 4.5(B) are estimated as 80 mmol g-cat^{-1} h^{-1} and 35 mmol g-cat^{-1} h^{-1}, respectively at 1 h. This difference can be attributed to high content of FFCA-acetal in Figure 4.5(A). In both systems, the decrease in FFCA-acetal resulted in the increase in AMFCA and FFCA. FFCA-acetal can be

consumed for AMFCA formation in Figure 4.5(A) more efficiently than that in Figure 4.5(B), which gives a large reaction rate. This discussion is fully supported with the result in Chapter 3. Reductive amination of FFCA in pure H_2O and pure methanol with NH_4OAc exhibited poor activity and selectivity for AMFCA as shown in entries 1, 5, 6, 7, and 9 of Table 3.3.

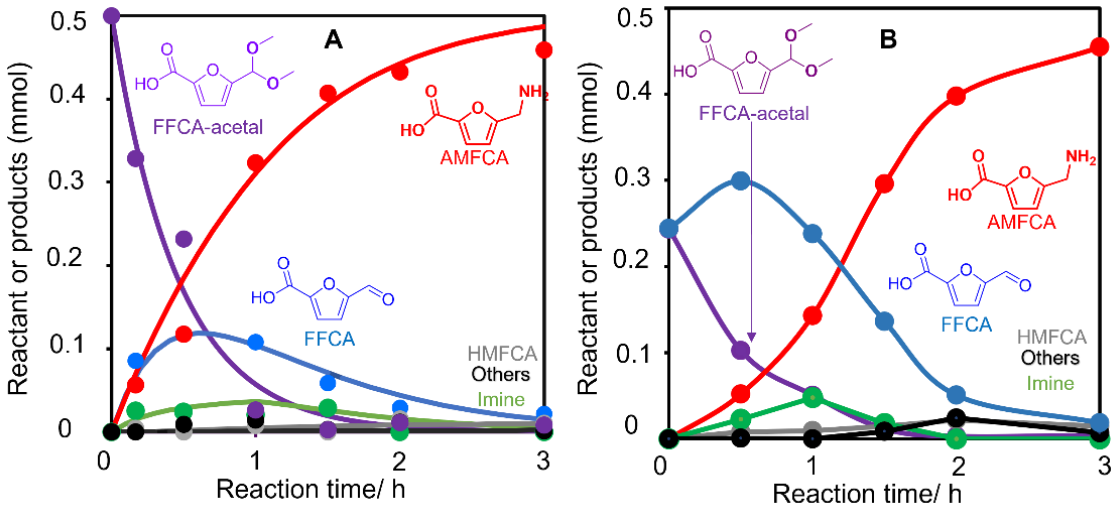

Figure 4.5. Reductive amination of FFCA-acetal (A) or FFCA (B) in methanol:water mixed solvent (2:1 v/v): substrate 0.5 mmol; solvent, (3 mL), NH_4OAc (5 mmol); catalyst, Co_2P NRs catalyst (0.05 mmol); hydrogen pressure, 0.5 MPa; temperature, 393 K.

4.3.3 Catalyst regeneration

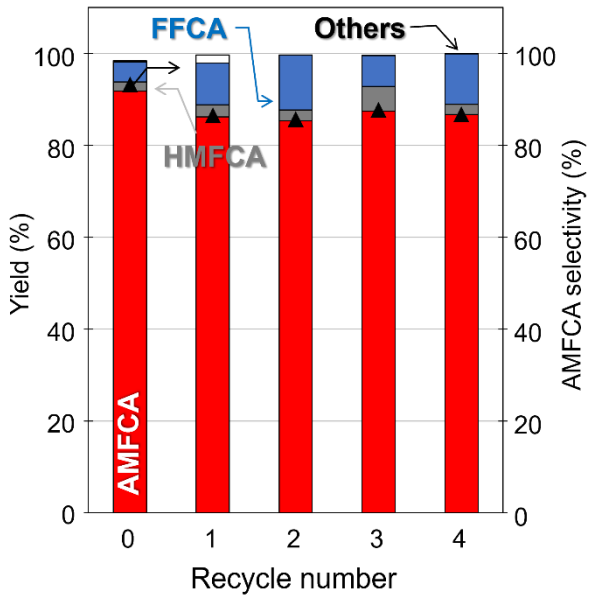

Figure 4.6. Reductive amination of FFCA-acetal 0.5 mmol; solvent, (3 mL), Ratio of methanol to water (2:1 v/v), NH_4OAc (5 mmol); catalyst, Co_2P NRs catalyst (0.05 mmol); hydrogen pressure, 0.5 MPa; temperature, 393 K, 3 h.

The reusability of Co_2P NRs was investigated in the reductive amination of FFCA-acetal. Reactions were conducted at 393 K for 3 h under pressurized 0.5 MPa H_2. After the reaction, the catalyst was recovered by filtration, washed with water, dried at 373 K in air overnight, and then used for subsequent reaction (Figure 4.6). After the first cycle, AMFCA yield was slightly decreased from 90% to 85% but the activity was maintained after the second run. Co_2P NRs were easily recovered by centrifugation under air and could be reused without deactivating the catalyst, highlighting its high durability.

4.4 Conclusion

Reductive amination of FFCA-acetal to AMFCA was successfully performed using Co_2P NRs catalyst in methanol-water solutions, with NH_3 and NH_4OAc. Acetal protection of the formyl group in FFCA prevents side reactions such as its premature hydrogenation to form HMFCA and limits its degradation to undetectable byproducts. FFCA-acetal can be directly converted to AMFCA without prior formation of the free aldehyde. The reductive amination rate of FFCA-acetal was faster than that of FFCA by approximately 2 times when using NH_4OAc in methanol:water ratio of 2:1 (v/v). Under optimized conditions, i.e., 0.5 mmol of FFCA-acetal, 5 mmol of NH_4OAc, substrate to catalyst ratio of 10 mol/mol, under 0.5 MPa H_2 at 393 K for 3 hours in methanol:water of 2:1 (v/v), an AMFCA yield of 91% could be obtained from FFCA-acetal at full conversion.

References

(1) Boonyakarn, T.; Wiesfeld, J. J.; Asakawa, M.; Chen, L.; Fukuoka, A.; Hensen, E. J. M.; Nakajima, K. Effective Oxidation of 5-Hydroxymethylfurfural to 2,5-Diformylfuran by an Acetal Protection Strategy. *ChemSusChem* **2022**, *15* (7), e202200059. https://doi.org/10.1002/CSSC.202200059.

(2) Wiesfeld, J. J.; Asakawa, M.; Aoshima, T.; Fukuoka, A.; Hensen, E. J. M.; Nakajima, K. A Catalytic Strategy for Selective Production of 5-Formylfuran-2-Carboxylic Acid and Furan-2,5-Dicarboxylic Acid. *ChemCatChem* **2022**, e202200191. https://doi.org/10.1002/CCTC.202200191.

(3) Chang, H.; Huber, G. W.; Dumesic, J. A. Chemical-Switching Strategy for

Synthesis and Controlled Release of Norcantharimides from a Biomass-Derived Chemical. *ChemSusChem* **2020**, *13* (19), 5213–5219. https://doi.org/10.1002/CSSC.202001471.

(4) Coumans, F. J. A. G.; Overchenko, Z.; Wiesfeld, J. J.; Kosinov, N.; Nakajima, K.; Hensen, E. J. M. Protection Strategies for the Conversion of Biobased Furanics to Chemical Building Blocks. *ACS Sustain. Chem. Eng.* **2022**, *10* (10), 3116–3130. https://doi.org/10.1021/ACSSUSCHEMENG.1C06723.

(5) Kim, M.; Su, Y.; Aoshima, T.; Fukuoka, A.; Hensen, E. J. M.; Nakajima, K. Effective Strategy for High-Yield Furan Dicarboxylate Production for Biobased Polyester Applications. *ACS Catal.* **2019**, *9* (5), 4277–4285. https://doi.org/10.1021/acscatal.9b00450.

(6) Kim, M.; Su, Y.; Fukuoka, A.; Hensen, E. J. M.; Nakajima, K. Aerobic Oxidation of 5-(Hydroxymethyl)Furfural Cyclic Acetal Enables Selective Furan-2,5-Dicarboxylic Acid Formation with CeO_2-Supported Gold Catalyst. *Angew. Chem. Int. Ed.* **2018**, *57* (27), 8235–8239. https://doi.org/10.1002/anie.201805457.

Chapter 5

Reductive amination of 2,5-diformylfuran to 2,5-bis(aminomethyl)furan

Abstract

Reductive amination of 2,5-diformylfuran (DFF) for the synthesis of 2,5-bis(aminomethyl)furan (AMF) was studied using cobalt phosphide nanorods (Co_2P NR) catalyst. Because of severe degradation of DFF, using acetalized DFF with 1,3-propanediol (DFF-acetal) was required. In the first step, the reductive amination of the DFF-acetal selectively converted the formyl group to amine with retaining the acetal moiety, yielding an intermediate in the maximum yield of 90% at full conversion of DFF-acetal. AMF can be produced from the intermediate in 65% yield when the intermediate was heated at 393 K for 3 hours in methanol-water 2:1 v/v-mixture with NH_3 and Co_2P NR catalyst.

5.1 Introduction

Recently, many researchers have focused on the synthesis of AMF from DFF by reductive amination. Partial oxidation of HMF can produce DFF, which can be further converted to AMF by reductive amination.[1–5] AMF has substantial potential as a building block for polyamides.[6,7] AMF was obtained in approximately 40% yield from DFF using Ni-Raney catalyst in THF-water mixture.[8] Reductive amination of DFF requires a delicate approach to prevent the generation of by-products such as humins, polyimines and polyamines, due to the condensation between a formyl group and an amine group and subsequent hydrogenation of imine moiety in Scheme 5.1.

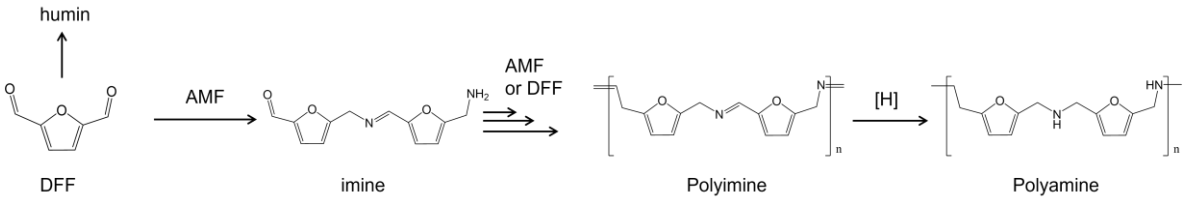

Scheme 5.1 Possible side reactions in the reductive amination of DFF to AMF.

Byproduct formation such as polyimine, polyamine or humin is a serious issue, which cannot be simply controlled by optimization of the reaction conditions. To suppress byproduct formation in concentrated solutions, we have developed a protection strategy of the highly reactive formyl group in HMF by the acetalization with 1,3-propanediol.[9,10] Acetalization of the formyl group with 1,3-propanediol forms a six-membered ring acetal, which shows high stability against side reactions during aerobic oxidation as demonstrated in the previous papers.[9,11] Such a protection strategy is regarded to be effective for biomass conversion as biomass-derived intermediates usually have highly

reactive functional groups that are easily involved in side reactions.[12–16] Herein, we employed the acetal protection strategy for the reductive amination of DFF-acetal or bis-dimethyl-DFF-acetal to selectively produce AMF using Co_2P NRs (Scheme 5.2).

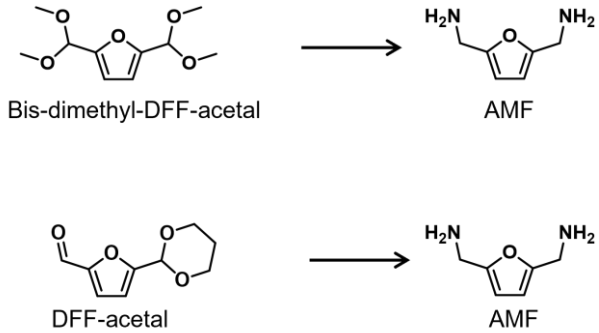

Scheme 5.2 Reductive amination of Bis-dimethyl-DFF-acetal and DFF-acetal to AMF

5.2 Experimental

5.2.1 Materials

Acetone, acetonitrile, chloroform, ammonium acetate, and N,N-dimethlyformamide Super dehydrated (DMF) were purchased from FUJIFILM Wako Pure Chemical Corporation. HMF was procured from Sigma-Aldrich. Hexadecylamine, Triphenyl phosphite, 1-octadecene, methanol-d_4, and DFF were obtained from Tokyo Chemical Industry (TCI). $Co(acac)_2 \cdot 2H_2O$ was purchased from Mitsuwa pure chemicals. Deuterium oxide and dipotassium hydrogenphosphate were purchased from Kanto chemical corporation. AMF was purchased from Santa Cruz Biotechnology. DFF was obtained from Tokyo Chemical Industry (TCI).

5.2.2 Catalyst preparation

In a typical synthesis, the mixture of $Co(acac)_2 \cdot 2H_2O$ (2 mmol), 1-octadecene (10 mL), and triphenylphosphine (5.4 mL) were heated stepwise at 150 °C for 1 h and at 300 °C for 3 h under a N_2 flow. After the heat treatment, the mixture was cooled down in

air to room temperature and the resulting precipitate was washed with a chloroform-acetone mixture. The obtained powder was dried at room temperature in vacuo overnight.

5.2.3 Preparation for DFF-acetal

Amberlyst-15 (250 mg) was added to a mixture of 2,5-diformylfuran (500 mg), 1,3-propanediol (350 μL), and dichloromethane (15 mL). After stirring the mixture at room temperature for 24 h, the solid catalyst and solvent were removed by suction filtration and vacuum evaporation, respectively. The crude product was purified by column chromatography to obtain DFF-acetal.1H NMR assignment of DFF-acetal: 1H NMR (400 MHz, CDCl3) 9.67 (s, 1H), 7.21 (d, 1H), 6.65 (d, 1H), 5.63 (s, 1H), 4.26 (m, 2H), 3.97 (m, 2H), 2.25 (m, 1H), 1.48 (m, 1H).

5.2.4 Catalytic experiments

Catalytic activity was tested in 10 ml SUS-316 stainless steel batch reactors equipped with a PTFE liner. 0.2 mmol of substrate (DFF or DFF-acetal), 0-3 ml of methanol-d_4 (MeOD) and/or deuterium oxide (D_2O), and 0.02 mmol of catalyst based on Co content were charged into the reactor, which was subsequently pressurized with hydrogen to 0.5 MPa and heated in an oil bath at 393 K. After a specified reaction period, the reactor was cooled to room temperature, and products were analyzed by High-Performance Liquid Chromatography (HPLC). The quantification of HMF-acetal, DFF, DFF-acetal, and AMF was conducted by HPLC (SHIMADZU, Japan) consisting of a RID-10A detector, a UV-SPD-20A detector, and an Shodex ODP_2 HP-4E column (column temp., 313 K). A diluted K_2HPO_4 aqueous solution (0.02 M and pH 9.5) 23% and acetonitrile 77% was used as the eluent at a flow rate of 0.4 mL min^{-1}. The retention

time for DFF, HMF-acetal, DFF-acetal, and AMF was 6.0, 6.5, 6.9, and 13.0 min, respectively. Analysis of secondary imine, Bis-Dimethyl-DFF-acetal, intermediate A, and intermediate B were conducted by NMR spectrometry (ECX 400, JEOL Ltd.).

5.3 Results and discussion

5.3.1 Reductive amiantion of DFF

Firstly, the reductive amination of DFF using Co_2P NRs was investigated in pure water using two types of nitrogen source (NH_3 and NH_4OAc) under 0.5 MPa H_2 at 393 K. DFF was quickly degraded to undetectable byproducts and AMF yield was always 0% (Table 5.1). When chaning the solvent from water to methanol, AMF was not formed as well (Table 5.1, entry 7). Due to highly reative aldehyde, DFF was easily degraded under the reaction conditions. Thus, an acetal protection strategy for DFF was required to ensure high AMF yields.

Table 5.1. Reductive amination of DFF over Co_2P NRS catalysts with NH_4OAc or NH_3

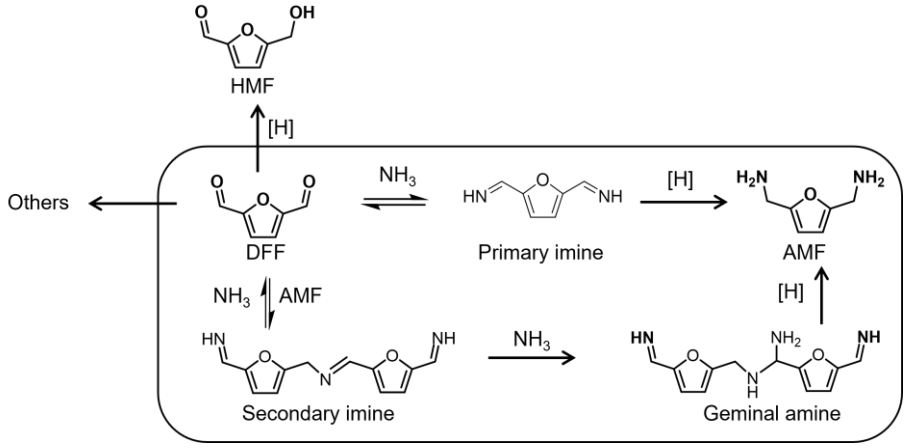

Entry	Nitrogen source	Time (h)	conv. (%)	Product yield (selectivity) (%)			
				AMF	HMF	Imine	Others
1	NH_4OAc	1	100	0	0	0	100
2		2	100	0	0	0	100
3		3	100	0	0	0	100
4	NH_3	1	100	0	0	0	100
5		2	100	0	0	0	100
6		3	100	0	0	0	100
7*		3	100	0	0	0	100

Conditions: substrate, (0.2 mmol); methanol:water ratio 2:1 v/v (3 ml); catalyst, Co_2P NRs catalyst (0.05 mmol); nitrogen source (5 mol), hydrogen pressure, 0.5 MPa; temperature, 393 K; Entry 7* was conducted in pure methanol.

5.3.2 Reductvie amiantion of Bis-dimethyl-DFF-acetal

The reductive amination of bis-dimethyl-DFF-acetal using Co_2P NRs was investigated in pure methanol using NH_3 or NH_4OAc under 0.5 MPa H_2 at 393 K. Working hypothesis to synthesize AMF in this system is that 1) dimethylacetal is expected to suppress side reactions observed in Table 5.2 and 2) two amine groups are formed stepwisely by reductive amination of hemiacetal intermediates as shown in

Scheme 5.3.

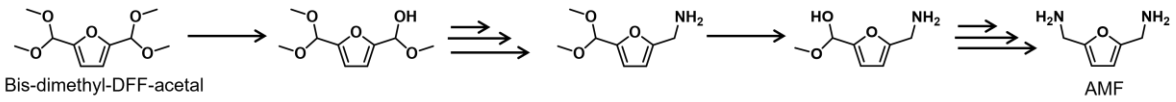

Scheme 5.3 Presubamle reaction paths in the reductive amination of bis-dimethyl-DFF acetal to AMF.

Table 5.2. Reductive amination of bis-dimethyl-DFF-acetal over Co_2P NRs catalysts with different concentration of NH_3

Entry	Nitrogen source	Time (h)	conv. (%)	Product yield (selectivity) (%)			
				AMF	HMF	Imine	Others
1	NH_3	1	8	0	0	0	8
2		2	15	0	0	0	15
3		3	20	0	0	0	20
4*	NH_4OAc	1	100	0	0	0	100
5*		2	100	0	0	0	100
6*		3	100	0	0	0	100
7*		3	100	0	0	0	100

Condition: substrate, DFF (0.2 mmol); methanol (3 ml); catalyst, Co_2P NRs catalyst (0.05 mmol); nitrogen source (5 mmol), hydrogen pressure, 0.5 MPa; temp., 393 K; Entries 4*-7* was conducted in the mixture of methanol (2 mL) and water (1 mL).

First, reductive amaintion of bis-dimethyl-DFF-acetal was conducted in pure methanol using NH_3. However, rates for the substrate conversion was quite slow as water-free and alkaline methanolic solution retarded hemiacetal formation. In addition, there was no detectable products in all runs (entries 1-3). When the reactions were conducted in 3 mL of aqueous methanol solution (methanol=2 mL, water=1 mL) using NH_4OAc to

enhance hemiacetal formation, rates for the substrate conversion were apparently increased. However, there were still no detectable products in all runs (entries 4-7). Acetalization with methanol to protect two formyl groups of DFF is not effective for AMF formation. I therefore changed acetal type from dimethyacetal to more stable six-membered ring acetal with 1,3-propanediol, which can be obtained directly from HMF-acetal as shown in chapter 2.

5.3.3 Reductvie amiantion of DFF-monoacetal with 1,3-propanediol

DFF-monoacetal (DFF-acetal) used as a substrate here has a formyl group and a six-membered ring acetal bonded to a furan ring (Scheme 5.4). The reductive amination of DFF-acetal using Co_2P NRs was investigated in pure methanol using NH_3 from 3 mmol to 21 mmol under 0.5 MPa H_2 at 393 K for 2 h. In this system, a formyl group in DFF-acetal is first converted to an amine group giving an intermediate (Intermediate A). In the second step, complete (or partial) deprotection with a catalytic amount of water and immediate reductive amination enables the formation of AMF.

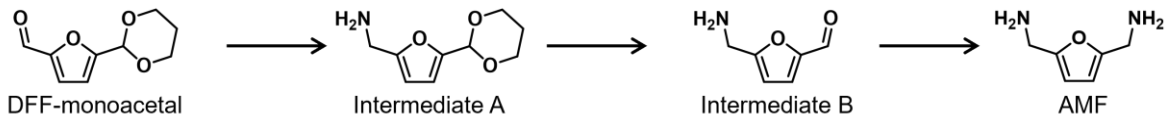

Scheme 5.4 Presumable reaction paths in the reductive amiantion of DFF-monoacetal

Table 5.3. Reductive amination of DFF-monoacetal with different NH_3 contents

#	NH_3 (mmol)	Conv. (%)	Product yield (%)					
			Intermediate A	AMF	HMF-acetal	DFF	Imine	Others
1	3	99	62	0	0	7	0	30
2	5	99	76	0	0	8	0	15
3	11	99	88	0	0	6	0	5
4	21	99	92	0	0	2	0	3

Condition: substrate, DFF-acetal (0.2 mmol); methanol (3 ml); catalyst, Co_2P NRs (0.05 mmol); hydrogen pressure, 0.5 MPa; temperature, 393 K for 2 h.

When increasing NH_3 from 3 mmol to 21 mmol (Table 5.3), the yield of intermediate A (Scheme 5.4) increased significantly along with the decrease in undetectable byproducts (others) and free DFF. The highly alkaline environment severely limited hydrolysis of DFF-acetal, which strongly repressed byproduct formation as a consequence. In terms of yield of intermediate A, 21 mmol of ammonia in methanol was selected for further study.

5.3.4 Time course for reductive amiantion of DFF-acetal.

Reaction pathways for the reductive amination of DFF-acetal were further investigated at 393 K under 0.5 MPa H_2 atmosphere using Co_2P NRs in methanol using NH_3 (21 mmol). Figure 5.1 shows time courses for the conversion of DFF-acetal and product yields. Imine formation is preferred in the absence of water. Secondary imine was formed in around 50% yield at 15 min and quickly dropped. Maximum AMFCA yield was 92% at full conversion of DFF-acetal confirmed by HPLC and NMR, together with minor by-products in only 10%, possibly resulting from hydrolysis of the acetal.

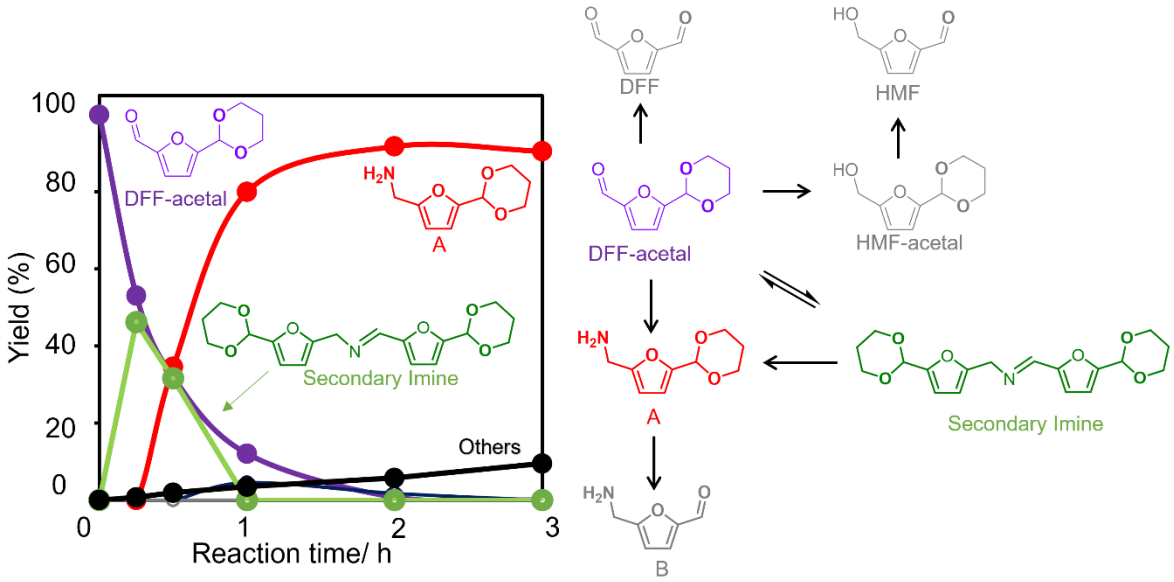

Figure 5.1. Reductive amianiton of DFF-acetal using Co_2P NRs.

5.3.5 Reductive amination of Intermediate A to AMF

Hydrolysis of intermediate A to intermediate B as shown in Scheme 5.4 was investigated by adding acetic acid (0.02 mol to reach pH 2-3) at room temperature or at 333 K, but most of Intermediate A are quickly converted to undetectable byproducts. This is due to polyimine formation as shown in Scheme 5.5. Intermediate B can react with intermediate A or another intermediate B to form two different imine compounds. Further reaction of these dimeric imines with intermediate B will result in the formation of oligomeric and polymeric imines. Secondary imine oligomers can possibly be converted to AMF by reductive amination, but polyimines are supposed not to be available for AMF formation.

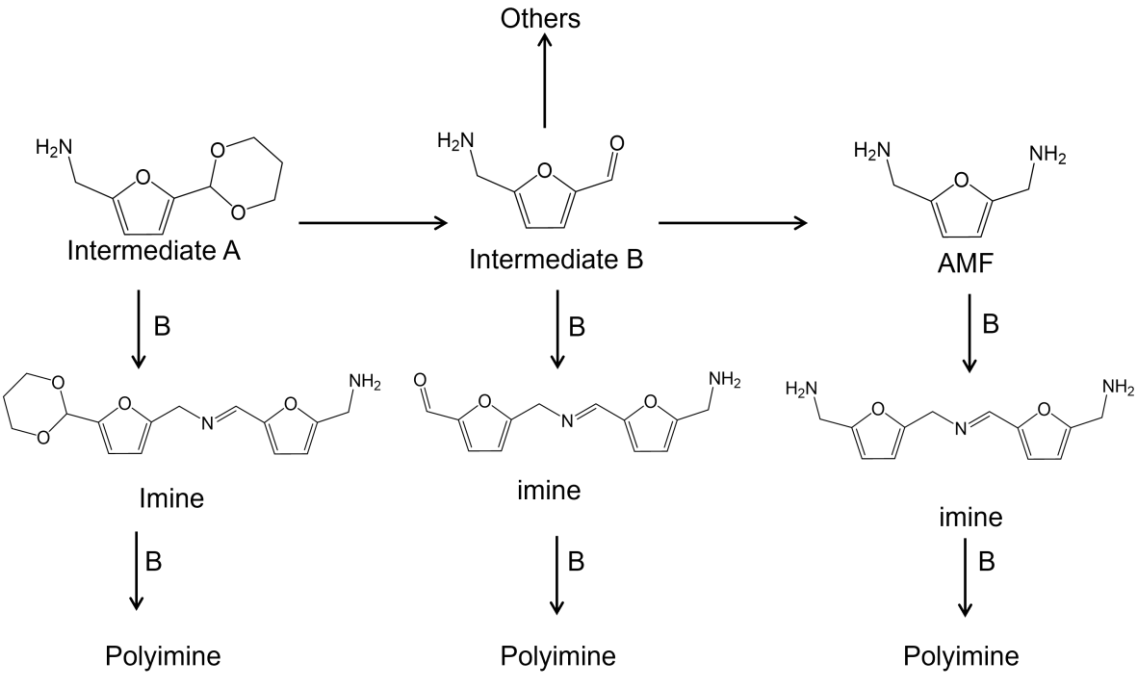

Scheme 5.5 Pathway of reductive amiantion and hydrolysis of intermediate A to AMF.

Table 5.4. Reductive amination of DFF-acetal over Co_2P NRs catalysts with different concentration of NH_3

#	NH_3 (mmol)	Acid (mmol)	pH	conv. (%)	Product yield (%)			
					B	AMF	Imine	Others
1	7	0	9	0	0	0	0	0
2	7	7	6	100	0	35	0	65
3	7	10	5	100	0	18	0	82
4	14	7	7	100	0	65	0	35

Condition: substrate, intermediate A (0.06 mmol); methanol:water ratio 2:1 v/v (3 ml); catalyst, Co_2P NRs (0.05 mmol), NH_3 (0-14 mmol), acetic acid (0-14 mmol), hydrogen pressure, 0.5 MPa; temperature, 393 K;

Reductive amination of intermediate A was investigated using the reaction mixture of entry 4 in Table 5.3. NH_3 contained in the host reaction mixture was partially

neutralized with acetic acid. The reactions were conducted at 393 K under 0.5 MPa H_2 atmosphere using Co_2P NRs after addition of water to prepare the reaction mixture containing 2 mL of methanol, 1 mL of water, 0.06 mmol of intermediate A, and 0.05 mmol of Co_2P NRs. Detail information for the contents of NH_3 and acetic acid is shown in Table 5.4.

Reductive amination of intermediate A did not proceed in the absence of acetic acid (entry 1) as a consequence of high basicity. AMF was obtained in 35% yield when adding 7 mmol acetic acid. Higher levels of acetic acid (10 mmol) while fixing the NH_3 amount at 7 mmol caused a decline in AMF yield to 18%, and higher byproduct formation as intermediate A was easily hydrolyzed to intermediate B (entries 2 and 3). On the other hand, AMF yield was increased to 65% when increasing the NH_3 content from 7 to 14 mmol with fixed amount of acetic acid (7 mmol, entries 2 and 4). Tuning pH is therefore a key parameter to control the reductive amination of intermediate A to AMF. At an optimized pH of 7 in entry 4, AMF yield of 65% was obtained as confirmed by both HPLC and ^1H NMR.

5.4 Conclusion

Reductive amination to AMF from DFF-acetal was successful, using Co_2P NRs catalyst in a two-step but one-pot reaction, with NH_3 in pure methanol. Under optimized conditions of the first step, i.e., 0.2 mmol of DFF-acetal, 21 mmol of NH_3, DFF to catalyst ratio of 4 mol/mol, under 0.5 MPa H_2 at 393 K for 2 hours in methanol, an intermediate A yield of 90% could be obtained from DFF-acetal at full conversion. Reductive amination to form AMF was performed using intermediate A. Controlled amounts of acetic acid were added to perform and tune the required in-situ hydrogenation in the

second step. Under optimized conditions (0.06 mmol of intermediate A, 14 mmol of NH_3, acetic acid 7 mmol, substrate to catalyst ratio of 1 mol/mol, under 0.5 MPa H_2 at 393 K for 3 hours in methanol:water 2:1 v/v), an AMF yield of 65% could be obtained at full conversion.

References

(1) Pingen, D.; Schwaderer, J. B.; Walter, J.; Wen, J.; Murray, G.; Vogt, D.; Mecking, S. Diamines for Polymer Materials via Direct Amination of Lipid- and Lignocellulose-Based Alcohols with NH_3. *ChemCatChem* **2018**, *10* (14), 3027–3033. https://doi.org/10.1002/cctc.201800365.

(2) Xu, Y.; Jia, X.; Ma, J.; Gao, J.; Xia, F.; Li, X.; Xu, J. Selective Synthesis of 2,5-Bis(Aminomethyl)Furan: Via Enhancing the Catalytic Dehydration-Hydrogenation of 2,5-Diformylfuran Dioxime. *Green Chem.* **2018**, *20* (12), 2697–2701. https://doi.org/10.1039/c8gc00947c.

(3) Zhou, K.; Liu, H.; Shu, H.; Xiao, S.; Guo, D.; Liu, Y.; Wei, Z.; Li, X. A Comprehensive Study on the Reductive Amination of 5-Hydroxymethylfurfural into 2,5-Bisaminomethylfuran over Raney Ni Through DFT Calculations. *ChemCatChem* **2019**, *11* (11), 2649–2656. https://doi.org/10.1002/cctc.201900304.

(4) Liang, G.; Wang, A.; Li, L.; Xu, G.; Yan, N.; Zhang, T. Production of Primary Amines by Reductive Amination of Biomass-Derived Aldehydes/Ketones. *Angew. Chem. Int. Ed.* **2017**, *56* (11), 3050–3054. https://doi.org/10.1002/anie.201610964.

(5) Qi, H.; Liu, F.; Zhang, L.; Li, L.; Su, Y.; Yang, J.; Hao, R.; Wang, A.; Zhang, T. Modulating: Trans -Imination and Hydrogenation towards the Highly Selective Production of Primary Diamines from Dialdehydes. *Green Chem.* **2020**, *22* (20), 6897–6901. https://doi.org/10.1039/d0gc02280b.

(6) García, J. M.; García, F. C.; Serna, F.; de la Peña, J. L. High-Performance Aromatic Polyamides. *Prog. Polym. Sci.* **2010**, *35* (5), 623–686. https://doi.org/10.1016/J.PROGPOLYMSCI.2009.09.002.

(7) Winnacker, M.; Rieger, B. Biobased Polyamides: Recent Advances in Basic and Applied Research. *Macromol. Rapid Commun.* **2016**, *37* (17), 1391–1413. https://doi.org/10.1002/marc.201600181.

(8) Le, N.-T.; Byun, A.; Han, Y.; Lee, K.-I.; Kim, H. Preparation of 2,5-Bis(Aminomethyl)Furan by Direct Reductive Amination of 2,5-Diformylfuran over Nickel-Raney Catalysts. *Green Sustain. Chem.* **2015**, *05* (03), 115–127. https://doi.org/10.4236/gsc.2015.53015.

(9) Kim, M.; Su, Y.; Fukuoka, A.; Hensen, E. J. M.; Nakajima, K. Aerobic Oxidation of 5-(Hydroxymethyl)Furfural Cyclic Acetal Enables Selective Furan-2,5-Dicarboxylic Acid Formation with CeO_2-Supported Gold Catalyst. *Angew. Chem. Int. Ed.* **2018**, *57* (27), 8235–8239. https://doi.org/10.1002/anie.201805457.

(10) Kim, M.; Su, Y.; Aoshima, T.; Fukuoka, A.; Hensen, E. J. M.; Nakajima, K. Effective Strategy for High-Yield Furan Dicarboxylate Production for Biobased Polyester Applications. *ACS Catal.* **2019**, *9* (5), 4277–4285.

https://doi.org/10.1021/acscatal.9b00450.

(11) Wiesfeld, J. J.; Asakawa, M.; Aoshima, T.; Fukuoka, A.; Hensen, E. J. M.; Nakajima, K. A Catalytic Strategy for Selective Production of 5-Formylfuran-2-Carboxylic Acid and Furan-2,5-Dicarboxylic Acid. *ChemCatChem* **2022**, e202200191. https://doi.org/10.1002/CCTC.202200191.

(12) Shuai, L.; Amiri, M. T.; Questell-Santiago, Y. M.; Héroguel, F.; Li, Y.; Kim, H.; Meilan, R.; Chapple, C.; Ralph, J.; Luterbacher, J. S. Formaldehyde Stabilization Facilitates Lignin Monomer Production during Biomass Depolymerization. *Science (80-.).* **2016**, *354* (6310), 329–333. https://doi.org/10.1126/science.aaf7810.

(13) Lan, W.; Amiri, M. T.; Hunston, C. M.; Luterbacher, J. S. Protection Group Effects During α,γ-Diol Lignin Stabilization Promote High-Selectivity Monomer Production. *Angew. Chem. Int. Ed.* **2018**, *57* (5), 1356–1360. https://doi.org/10.1002/anie.201710838.

(14) Questell-Santiago, Y. M.; Zambrano-Varela, R.; Talebi Amiri, M.; Luterbacher, J. S. Carbohydrate Stabilization Extends the Kinetic Limits of Chemical Polysaccharide Depolymerization. *Nat. Chem.* **2018**, *10* (12), 1222–1228. https://doi.org/10.1038/s41557-018-0134-4.

(15) Questell-Santiago, Y. M.; Yeap, J. H.; Talebi Amiri, M.; Le Monnier, B. P.; Luterbacher, J. S. Catalyst Evolution Enhances Production of Xylitol from Acetal-Stabilized Xylose. *ACS Sustain. Chem. Eng.* **2020**, *8* (4), 1709–1714. https://doi.org/10.1021/acssuschemeng.9b06456.

(16) Luo, X.; Li, Y.; Gupta, N. K.; Sels, B.; Ralph, J.; Shuai, L. Protection Strategies Enable Selective Conversion of Biomass. *Angew. Chem. Int. Ed.* **2020**, *59* (29), 11704–11716. https://doi.org/10.1002/anie.201914703.

Chapter 6

Conclusion

Lignocellulosic biomass is widely regarded as an abundant, easily accessible, and renewable carbon resource that can replace fossil fuels. Catalytic valorization of its main constituents (cellulose, hemicellulose, and lignin) into platform molecules has been extensively studied to realize sustainable production of fuels and commodity chemicals. Hydrolysis of cellulose into glucose and its subsequent dehydration yields HMF. Oxidation of HMF produces 2,5-diformylfuran (DFF) or 5-formylfuran-2-carboxylic acid (FFCA). DFF and FFCA can be further converted to 2,5-bis(aminomethyl)furan (AMF) and 5-(aminomethyl)furan-2-carboxylic acid (AMFCA) respectively, which is a biobased monomer for the polyamide production.

In Chapter 2, a facile reaction system to produce DFF from HMF was developed using concentrated HMF-acetal solutions and a Ru/γ-Al_2O_3 catalyst. Acetal protection of the formyl group in HMF prevents side reactions in concentrated solutions during aerobic oxidation. Under optimized conditions, HMF-acetal was oxidized at a concentration of 50 wt%, and a high DFF yield of 84% was obtained while only 21% of DFF could be obtained from unprotected HMF under the same conditions. Deposition of humin-type organic compounds during the reactions resulted in a substantial decrease of the original activity of Ru/γ-Al_2O_3 in reuse experiments. Sonication of the used catalyst in NaOH solution removed the deposits and fully recovered the activity, allowing efficient regeneration for at least 4 times without significant loss of activity.

Chapter 3 deals with reductive amination of FFCA, which is obtained from partial oxidation of HMF or DFF. Reductive amination to AMFCA from FFCA was successfully performed using Co_2P NRs catalyst in methanol-water solutions, with NH_4OAc as a benign nitrogen source. FFCA acetalized easily under these conditions, and the so-provided protection of the formyl group prevented side reactions such as its hydrogenation to form HMFCA and its degradation to unknown compounds during reductive amination. Under optimized conditions, an AMFCA yield of 90% could be obtained from FFCA at full conversion.

The in-situ acetalization of FFCA and its benefits was further explored in Chapter 4. In this chapter, FFCA-acetal was reductively aminated in different methanol to water ratios as reaction solvent to clarify the effect of the acetal functionality and aldehyde from acetal hydrolysis on the product distribution. Acetal protection of the formyl group in FFCA not only prevents side reactions but could also be directly converted to AMFCA without prior formation of the free aldehyde. The reductive amination rate of FFCA-acetal was faster than that of FFCA by approximately 2 times. Under optimized conditions, an AMFCA yield of 91% could be obtained from FFCA-acetal which is not significantly different from FFCA (90%) at full conversion. However, AMFCA could be obtained in 72% yield (97% selectivity) in absence of water after 6 hours.

Chapter 5 covers reductive amination of DFF-acetal, which is obtained from oxidation from HMF-acetal as shown in Chapter 2. In this chapter, the insights obtained from Chapters 3 and 4 were used to optimize the selectivity towards AMF in a 2-step reaction. Reductive amination to AMF directly from DFF was unsuccessful due to the instability of DFF. However, reductive amination to AMF from DFF-acetal was successful, using Co_2P NRs catalyst in a two-step one-pot reaction, with NH_3 as a nitrogen

source in pure methanol. Under optimized conditions of the first step (reductive amination of DFF-acetal to intermediate A), an intermediate A yield of 90% could be obtained from DFF-acetal at full conversion. Controlled amounts of acetic acid were added to perform and tune the required in-situ hydrogenation in the second step. Under optimized conditions an AMF yield of 65% could be obtained at full conversion.

This thesis is focused on creating chemical pathways for synthesis of biobased monomers for polyamide production in high concentration starting from HMF by using acetal protection strategy. Future works in this direction requires development of economically viable catalytic routes for polymerization of AMFCA or AMF as biobased chemicals and their transformation to value-added chemical industries such as polyamides.

Synopsis

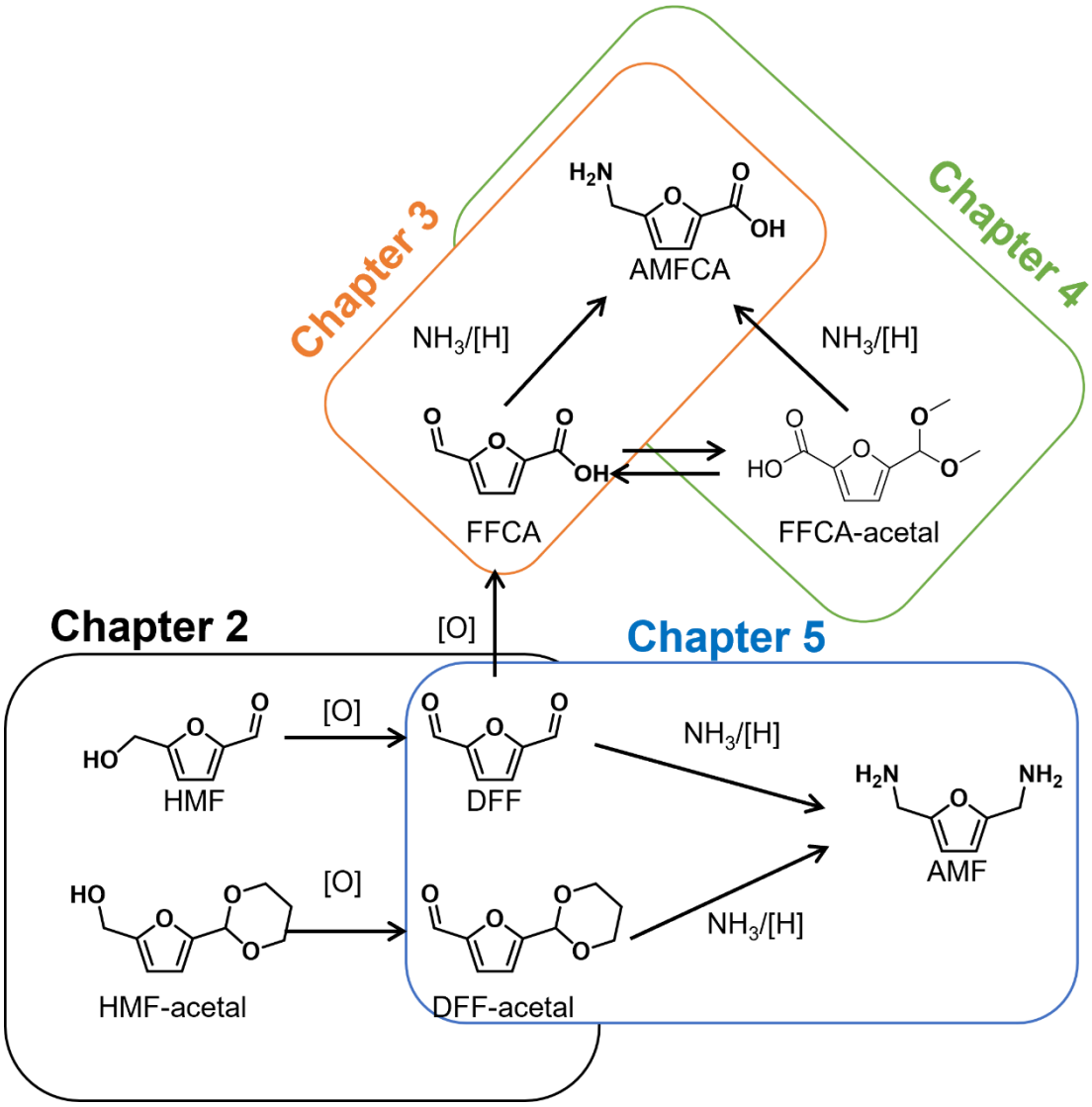
Chapter 3
Chapter 4
AMFCA
NH3/[H]
NH3/[H]
FFCA
FFCA-acetal
Chapter 2
[O]
Chapter 5
HMF
[O]
DFF
NH3/[H]
AMF
HMF-acetal
[O]
DFF-acetal
NH3/[H]

List of Publications

Journal publications

Tat Boonyakarn, Dr. Jan J. Wiesfeld, Miyuki Asakawa, Lulu Chen, Prof. Dr. Atsushi Fukuoka, Prof. Dr. Emiel J. M. Hensen, Prof. Dr. Kiyotaka Nakajima. Effective Oxidation of 5-Hydroxymethylfurfural to 2,5-Diformylfuran by an Acetal Protection Strategy, *Chemsuschem*, **2022**, 15 (7), e202200059

Journal publications (not related to this thesis)

Tat Boonyakarn, Dr. Piyaporn Wataniyakul, Dr. Panatpong Boonnoun, Prof. Dr. Armando T. Quitain, Prof. Dr. Tetsuya Kida, Prof. Dr. Mitsuru Sasaki, Prof. Dr. Navadol Laosiripojana, Prof. Dr. Bunjerd Jongsomjit, Prof. Dr. Artiwan Shotipruk, "Enhanced Levulinic Acid Production from Cellulose by Combined Brønsted Hydrothermal Carbon and Lewis Acid Catalysts", *Industrial Engineering Chemical Research*, Vol. 58, Issue 8, pp. 2697-2703 (2019)

Conference contributions

Tat Boonyakarn, Jan J Wiesfeld, Atsushi Fukuoka, Takato Mitsudome, Kiyotaka Nakajima, Reductive Amination of 5-Formyl-2-furancarboxylic Acid to 5-(Aminomethyl)furan-2-Carboxylic Acid over a Cobalt Phosphide Catalyst, *The 9th Tokyo conference on advanced catalytic science and technology*, On-site, July 24-29, **2022** (Poster)

Tat Boonyakarn, Jan J Wiesfeld, Atsushi Fukuoka, Takato Mitsudome, Kiyotaka

Nakajima, Reductive Amination of 5-Formyl-2-furancarboxylic Acid and its Dimethylacetal Form to 5-(Aminomethyl)furan-2-carboxylic Acid over a Cobalt Phosphide Nanorod Catalyst, *The Japan Petroleum Institute Tokyo Conv. of JPI*, On-site, May 31, **2022**, (Oral)

Tat Boonyakarn, Jan J Wiesfeld, Atsushi Fukuoka, Takato Mitsudome, Kiyotaka Nakajima, Reductive Amination of 5-Formyl-2-furancarboxylic Acid to 5-(Aminomethyl)furan-2-carboxylic Acid, *The Japan Petroleum Institute Hakodate Conv. of JPI* (51st Petroleum Petrochemical Symposium of JPI), On-site, November 12, **2021** (Oral)

Tat Boonyakarn, Jan J Wiesfeld, Atsushi Fukuoka, Kiyotaka Nakajima, Selective Oxidation of 5-Hydroxymethylfurfural-acetal to 2,5-Diformylfuran in Concentrated Solutions, *26th catalysis society of Japan meeting*, Online, September 17, **2020** (Oral)

Acknowledgement

I would like to take this opportunity to thank the people I am grateful to, throughout my doctoral degree. I have had a wonderful time during my doctoral research

At first, I would like to thank Professor Dr. Atsushi Fukuoka, my supervisor, for accepting me a as doctoral student in his group. You have been helpful to me during my doctoral research. Your suggestion has been helpful for me during the research of doctoral degree. Thank you for making me prepared for the thesis presentation.

Professor Dr. Kiyotaka Nakajima, thank you for the valuable suggestions and questions you have asked me in many times, and teach me many things to be good scientist. I have enjoyed working with you. Thank you for making me prepared for the thesis presentation. Thank you for correcting a lot of typing mistakes in my papers and thesis. I have learnt a lot about scholarly writing from you. Apart from this thank you for encouraging me to attend conferences, reviewing my papers.

Dr. Abhijit Shrotri, thank you for the valuable suggestions and questions you have asked me throughout the group meetings and teach me to use many lab equipment's such as TGA.

I would like to thank all the group members for being so helpful to me. Dr. Jan J. Wiesfeld, thank you for making me prepared for the thesis presentation. Thank you for correcting a lot of typing mistakes in my papers and thesis. Many your ideas are helpful in my research. Hiromi Matsushima, thank you for making all CSE documents and suggestion for me. Dr. Shazia Sharmin Satter, Dr. Takuya Sagawa, Dr. Eunhyeok Yang, Dr. Etty Nurlia Kusumawati, Dr. Li Lingcong and Dr. Pengru Chen, Dr. Shaikh Nazmul

Hasan Mohammad Dostagir, Dr. Palai, Yayati Naresh, Dr. Cheng Yang, we have Dr. Daniele Padovan, Kazuya Kato, Koichiro Endo, Yusuke Suzuki, Miyuki Asakawa, and Natsumi Shibayama, thank you for good friends and good environment.